

# Bioinspired and Biomimetic Delivery Platforms for Cancer Vaccines

Jing Liu, Si Si Liew, Jun Wang,\* and Kanyi Pu\*

Cancer vaccines aim at eliciting tumor-specific responses for the immune system to identify and eradicate malignant tumor cells while sparing the normal tissues. Furthermore, cancer vaccines can potentially induce long-term immunological memory for antitumor responses, preventing metastasis and cancer recurrence, thus presenting an attractive treatment option in cancer immunotherapy. However, clinical efficacy of cancer vaccines has remained low due to longstanding challenges, such as poor immunogenicity, immunosuppressive tumor microenvironment, tumor heterogeneity, inappropriate immune tolerance, and systemic toxicity. Recently, bioinspired materials and biomimetic technologies have emerged to play a part in reshaping the field of cancer nanomedicine. By mimicking desirable chemical and biological properties in nature, bioinspired engineering of cancer vaccine delivery platforms can effectively transport therapeutic cargos to tumor sites, amplify antigen and adjuvant bioactivities, and enable spatiotemporal control and on-demand immunoactivation. As such, integration of biomimetic designs into delivery platforms for cancer vaccines can enhance efficacy while retaining good safety profiles, which contributes to expediting the clinical translation of cancer vaccines. Recent advances in bioinspired delivery platforms for cancer vaccines, existing obstacles faced, as well as insights and future directions for the field are discussed here.

(CAR-T) cells and cancer vaccines can now be found.<sup>[3]</sup> However, despite the recent success of ICB and CAR-T therapies in cancer clinical trials, these approaches still face limitations as only a small fraction of patients derive clinical benefit.<sup>[4]</sup> ICB therapy cannot prime the immune system to specifically recognize or target tumor cells. This approach only works on related inhibitory signaling pathways, such as cytotoxic T-lymphocyte-associated protein 4 (CTLA-4) and programmed cell death protein 1 (PD-1), and exerts therapeutic efficacy when antigen-specific cytotoxic T lymphocytes (CTLs) are already present.<sup>[5]</sup> Successful treatment outcomes will therefore require the identification of predictive biomarkers to ascertain if the host tumor will respond to ICB therapeutics administered.<sup>[6]</sup> Although CAR-T has seen remarkable success in hematological malignancies, response rates of patients with solid tumors remain low.<sup>[7]</sup> Clinical applications of CAR-T therapies are limited due to on-target/off-tumor toxicities

## 1. Introduction


Cancer immunotherapy harnesses the capability of the immune system to combat cancer. In contrast with conventional treatment options such as chemotherapy, radiotherapy, targeted therapy and surgery that directly act on cancer cells, immunotherapeutic agents aim to improve antitumor responses with fewer off-target toxic side effects.<sup>[1]</sup> The past decade has witnessed breakthroughs in the field of cancer immunotherapy.<sup>[2]</sup> In drug discovery pipelines, immune-checkpoint blockade (ICB) inhibitors, chimeric antigen receptor-engineered T

and the need for predefined tumor antigen (Ag).<sup>[8]</sup> Notwithstanding, the marked progress of immunotherapy using ICB and CAR-T has seen a surge of reinvigorated interest in cancer vaccine development.<sup>[9]</sup>

Cancer vaccines involve the administration of tumor Ags and/or adjuvants to train the immune system to recognize and attack tumor cells.<sup>[10]</sup> Although vaccines against infectious diseases have been one of the greatest medical accomplishments of modern medicine, the application of vaccines in cancer treatment has seen far lesser success, and, till date only few cancer vaccines have received approval for clinical use.<sup>[11]</sup> Given their

J. Liu, J. Wang  
School of Biomedical Sciences and Engineering  
Guangzhou International Campus  
South China University of Technology  
Guangzhou 510006, P. R. China  
E-mail: mcjwang@scut.edu.cn

J. Liu, J. Wang  
National Engineering Research Center for Tissue Restoration  
and Reconstruction  
South China University of Technology  
Guangzhou 510006, P. R. China

 The ORCID identification number(s) for the author(s) of this article can be found under <https://doi.org/10.1002/adma.202103790>.

DOI: 10.1002/adma.202103790

J. Liu, J. Wang  
Key Laboratory of Biomedical Engineering of Guangdong Province  
and Innovation Center for Tissue Restoration and Reconstruction  
South China University of Technology  
Guangzhou 510006, P. R. China

J. Liu, J. Wang  
Key Laboratory of Biomedical Materials and Engineering of the Ministry  
of Education  
South China University of Technology  
Guangzhou 510006, P. R. China

S. S. Liew, K. Pu  
School of Chemical and Biomedical Engineering  
Nanyang Technological University  
70 Nanyang Drive, Singapore 637457, Singapore  
E-mail: kypu@ntu.edu.sg

potential to induce and direct a potent and Ag-specific immune response, cancer vaccines offer an attractive combinatorial approach with ICB or other treatment modalities to maximize therapeutic effectiveness.<sup>[12]</sup> Till date, multiple cancer vaccine strategies have been proposed using Ags such as whole tumor cells, DCs or Ags in the form of proteins, peptides, DNA or mRNA.<sup>[13]</sup> Different vaccine formulations, together with a variety of immunoadjuvants, employing varied delivery approaches have also been utilized.<sup>[14]</sup> The development of safe and effective cancer vaccines still faces a number of challenges. Due to preexisting immune tolerance, low tumor Ag immunogenicity may be present in tumor environments.<sup>[15]</sup> During disease progression, potent immunosuppressive mechanisms may be activated, enabling tumor cells to escape immune attack, resulting in a highly immunosuppressive tumor microenvironment (TME).<sup>[16]</sup> Furthermore, upon in vivo administration, biological barriers that hinder vaccine components delivery to desired therapeutic sites are also present.<sup>[17]</sup>

In view of the above challenges, novel strategies for delivering cancer immunotherapy in a safer and more efficient way could expand the therapeutic potential of these immunological cargos to a broader range of patients and at the same time, minimize immunotoxicities.<sup>[18]</sup> Nature inspires researchers to devise cutting-edge solutions by emulating and replicating the processes in living systems.<sup>[19]</sup> Through rational design, bioinspired delivery systems can mimic the natural, physical and chemical properties of biological systems or recapitulate biological processes.<sup>[20]</sup> More recently, these strategies have been increasingly utilized to enhance therapeutic efficacy, showing great promise for generating highly potent antitumor vaccines.<sup>[21]</sup> Engineering cancer vaccines with bioinspired and biomimetic delivery platforms enable amplified activities of Ag and adjuvant, good spatiotemporal controllability and on-demand immunoactivation, thereby offering great potential to address key limitations and expediting the clinical translation of promising cancer vaccines from laboratory bench to bedside.

In this review, we will discuss recent advances in bioinspired and biomimetic delivery technologies toward rational vaccine design as cancer therapeutics, with focus on synthetic, semi-synthetic/nature-derived delivery systems, along with biomaterial scaffolds (**Figure 1**). Such bioinspired and biomimetic cancer vaccines enable the potentiation of immunogenicity and adjuvanticity, while minimizing undesired immune responses by recapitulating or directly harnessing fascinating traits of biological systems. We aim to discuss strategies and provide insights for engineering delivery systems to boost the potency and safety of cancer vaccines, thereby realizing the potential of this class of therapeutics for benefiting cancer patients in the future.

## 2. Bioinspired and Biomimetic Delivery Platforms for Cancer Vaccines

In the development of drug delivery platforms, bioinspired and biomimetic approaches incorporate features of living processes or materials derived from nature into synthetic or semisynthetic nanosystems (**Figure 1a**). In the bioinspired (bottom-

up) approach, synthetic nanosystems are integrated with ideas derived from nature, endowing these delivery platforms with useful features that can address biological problems (**Table 1**).<sup>[22]</sup> As for the biomimetic (top-down) approach, existing or off-the-shelf natural materials are modified and improvised into semi-synthetic nanosystems closely mimicking nature's materials (**Table 2**).<sup>[23]</sup>

### 2.1. Bioinspired (Bottom-Up Approach)

Through the bioinspired approach, synthetic delivery systems that employ synthetic inorganic, polymeric, and lipid-based materials can be tailor-made to meet specific needs. Physicochemical properties from living systems can be adapted into the design of synthetic delivery systems to simulate naturally occurring traits and characteristics (**Figure 1a**).<sup>[24]</sup> Synthetic systems can also be engineered to model after biological entities, such as well-defined vesicles, artificial cells and extracellular matrices.<sup>[25]</sup> Biochemical ligands or chemical functionalities can be integrated into synthetic nanosystems to improve sensitivity and selectivity during targeted delivery.<sup>[26]</sup> By studying key signal transduction pathways in living systems, stimuli-responsive building blocks can also be incorporated into synthetic delivery platforms to achieve on-demand release of cargoes in the presence of endogenous triggers.<sup>[27]</sup>

### 2.2. Biomimetic (Top-Down Approach)

Although bioinspired synthetic delivery systems are being actively developed, they may still be insufficient to completely recapitulate the complexities of living biological systems. Natural particulates, ranging from pathogens to mammalian cells, organelles to intracellular vesicles, possess their own distinctive properties, unique delivery mechanisms and specific interactions with the body and cellular system.<sup>[28]</sup> Therefore, the biomimetic top-down approach directly leverages naturally occurring biological materials. They are usually nature-derived or semisynthetic/semibiological delivery systems that comprise one or more natural materials, functioning as biomimicry to their counterparts. By augmenting natural materials, semisynthetic nanosystems can be fabricated to closely mimic key interactions, such as cell-to-cell signaling, cell-based information exchange with extracellular matrices and systemic immune responses (**Figure 1a**).<sup>[29]</sup>

## 3. Bioinspired Synthetic Nanosystems for Vaccine Delivery

### 3.1. Endogenous Stimuli

Cancer cells are distinctly different from normal cells. They are characterized by hallmarks essential for supporting the acquisition and maintenance of malignant properties, e.g., reprogrammed energy metabolism, angiogenesis, activation of invasion and metastasis, resisting cell death, sustaining proliferative signaling and replicative immortality.<sup>[30]</sup> Therefore, TME

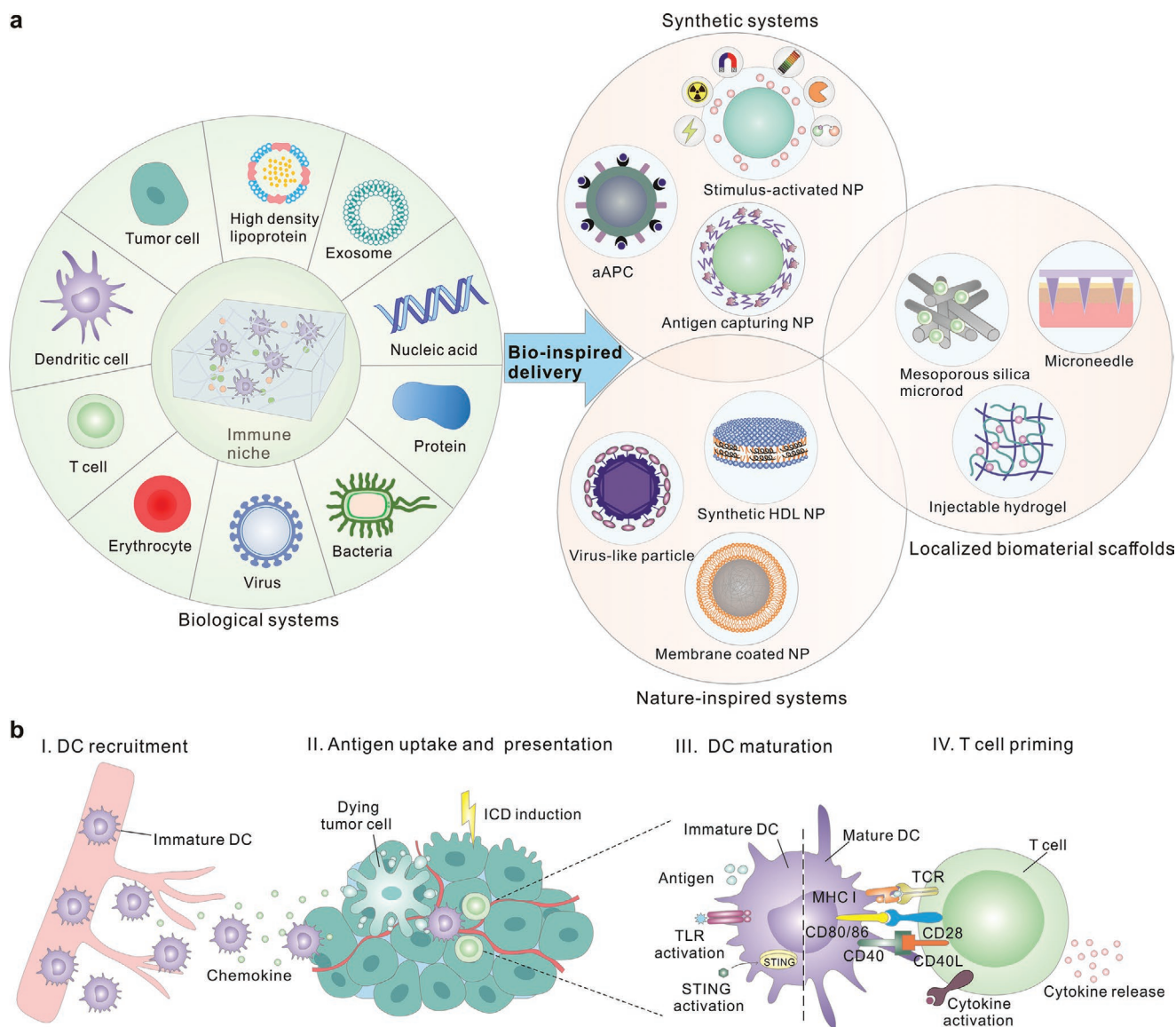


**Figure 1.** a) Schematic illustration of developing bioinspired and biomimetic delivery systems for cancer vaccines based on synthetic and nature-derived/semisynthetic systems; NP, nanoparticle; HDL, high-density lipoprotein; aAPC, artificial antigen-presenting cell (APC); DC, dendritic cell. b) The mechanisms of bioinspired cancer vaccines in eliciting tumor-specific immune response via I) regulating DC recruitment, II) enhancing Ag uptake and presentation, III) amplifying the activity of Ag and adjuvant, and IV) priming naïve CD8<sup>+</sup> T cells; TLR, Toll-like receptor; ICD, immunogenic cell death; STING, stimulator of interferon gene; MHC I, major histocompatibility complex I.

is often characterized by overexpression of various enzymes, as well as dysregulation of small molecules, such as pH, H<sub>2</sub>O<sub>2</sub>, glutathione (GSH), reactive oxygen species (ROS), hypoxia and high reduction–oxidation (redox) potential.<sup>[31]</sup> Capitalizing on these naturally occurring stimuli in diseased environments, synthetic nanosystems can be engineered with stimuli-responsive moieties to sense and respond to these endogenous triggers, enabling on-demand release of cargo at precise destination at tumor sites for enhanced therapeutic activity with reduced side effects.<sup>[32]</sup> This section highlights recent research employing the use of endogenous triggers for designing stimuli-responsive nanosystems to achieve activatable and precise antitumor immune responses as novel vaccination and immunotherapy modalities.

### 3.1.1. Small Molecules

Many small molecule-based stimuli exist intrinsically in TME and intracellular spaces of cancer cells.<sup>[33]</sup> In TME, the pH value (6.5–6.8) is much lower than that in blood or normal tissues (7.2–7.4).<sup>[34]</sup> As for GSH, higher levels are found in the cytosol of tumor cells compared to normal cells. Furthermore, intracellular GSH level in cancer cells ( $2\text{--}10 \times 10^{-3} \text{ M}$ ) is about 100 to 1000 times higher than that in extracellular space.<sup>[35]</sup> In the lysosomes of nearly all mammalian cells (except for mature erythrocytes), the pH is  $\sim 4\text{--}6$  while cytosolic pH is  $7\text{--}7.5$ .<sup>[36]</sup> Based on these gradients, a series of stimuli-responsive systems have been designed to regulate the spatiotemporal release of Ags or adjuvants at desired sites for inducing specific antitumor immune responses.

**Table 1.** Advances in bioinspired synthetic nanosystems for vaccine delivery.

Bioinspired approach		Major materials	Vaccine components	Mechanisms	Refs.
Endogenous stimuli-triggered nanosystems	pH	PEG- <i>b</i> -PDPA polymers	Ovalbumin (OVA) epitope, DMXAA adjuvant	pH-triggered Ag release	[40]
		Polyamidoamine (PAMAM) dendrimers	CpG	pH- and redox-triggered adjuvant release	[41]
		STING-activating polymers	OVA epitope, cGAMP	pH-triggered Ag release	[42,43]
	Redox	Polycondensate neoepitopes	OVA epitope, TLR1/2 agonist (Pam3CSK4)	Redox-triggered release of Ag or adjuvant	[46]
		Mesoporous silica NPs	CpG, neoantigen peptides (Adpgk, M27, and M30)	Redox-triggered Ag release	[47]
	Hypoxia	Mesoporous silica NPs	CpG	Hypoxia-triggered release of CpG/polymer complex	[50]
	Enzyme	Multilamellar lipid vesicles	OVA protein, monophosphoryl lipid A (MPLA)	Enzyme-triggered release of Ag and adjuvant	[54]
Poly(ethylene glycol) (PEG) pro-drug conjugates		TLR7/8 agonist (imidazoquinoline, IMDQ)	Enzyme-triggered release of adjuvant	[55]	
Exogenous stimuli-triggered nanosystems	Light	Upconversion NPs (UCNPs)	CpG	Ultraviolet (UV) light-activated release of adjuvant	[63]
		Organic semiconducting polymer NPs	NLG919, tumor-associated Ags (TAAs)	Near-infrared (NIR)-triggered release of adjuvant and TAAs	[64]
	Temperature	Organic semiconducting polymer NPs	TLR7/8 agonist (R848), TAAs	Photothermal heat activated release of adjuvant and TAAs	[68,69]
		Poly(lactic-co-glycolic acid) (PLGA) NPs	TLR7/8 agonist (R837), TAAs	X-ray radiation induced release of TAAs	[72]
	Radiation	Metal-organic frameworks (MOFs)	TAAs	X-ray radiation induced release of TAAs	[73]
		Ultrasound	Liposome-based nanosensitizers	R837, TAAs	Ultrasound irradiation induced release of TAAs
Antigen-capturing NPs		Functionalized PLGA NPs	TAAs	Presentation of TAAs released after radiotherapy	[78]
		Maleimide-functionalized UCNPs	TAAs	Capturing and retention of TAAs after phototherapy	[79]
Nanoscale aAPCs (nano-aAPCs)		Superparamagnetic iron oxide NPs (SPIOs)	Peptide loaded MHC (pMHC), anti-CD28	Providing two stimulatory signals for T cell activation	[81,82]

**pH:** Acidic extracellular pH is a major feature in tumor tissues due to excessive production of lactic acid from anaerobic glycolysis.<sup>[37]</sup> As such, the acidic extracellular environment of tumor tissues, as well as acidic intracellular endolysosomal environment in all cells, can be harnessed for pH-responsive immunotherapy.<sup>[38]</sup> Inspired by the degradation of endocytosed macromolecules in lysosomes, a series of pH-activated nanosystems which responds to extracellular tumor acidity and intracellular endolysosomal acidity, have been proposed for cancer vaccine delivery. pH-responsive systems can be employed to elicit specific immunoactivation of vaccine components at the tumor site. In addition, Ags and adjuvants need to be liberated in the cytosol to achieve cross-presentation and stimulating innate immune responses.<sup>[39]</sup> Therefore, pH-responsive nanovaccines can regulate the controllable release of Ags and adjuvants at the desired locations to exert their therapeutic effects efficaciously.

Li and co-workers developed an acid-responsive nanovaccine formed by amphiphilic polymers conjugated with neoantigens and STING agonist for enhanced vaccination immunotherapy of cancer (Figure 2a,b).<sup>[40]</sup> These nanovaccines collapsed in the

weakly acidic condition of the early endosomes due to pH-responsive protonation of tertiary amines, enabling cytosolic release of neoantigens. The polymer NPs displayed superior pH-responsive hemolytic property under acidic pH for endosomal escape (Figure 2c). After targeted accumulation at lymph node (LN) and cellular internalization by DCs, the nanovaccines induced efficient Ag presentation due to the release of neoantigens in the cytosol via intrinsic endosomal escape (Figure 2d,e). In the meantime, the released STING agonist stimulated the STING pathway to elicit DC maturation and boosted T cell activation with the neoantigen (Figure 2f,g). Combined with programmed death-ligand 1 (PD-L1) blockade, this pH-responsive nanovaccine overcame PD-L1 resistance and substantially enhanced antitumor efficacy. Additionally, Wang's group designed a dual-responsive nanoadjuvant based on dendrimer cluster for the delivery of CpG adjuvant.<sup>[41]</sup> PAMAM dendrimers were attached to a self-assembly nanocarrier through a tumor-pH labile amide bond to create a pH-responsive PAMAM cluster. Following which, CpG was conjugated onto the surface of PAMAM through a disulfide exchange reaction. The weakly acidic pH environment in tumor triggered the hydrolysis of amide bond and the rapid liberation

**Table 2.** Advances in biomimetic/nature-derived semisynthetic systems for vaccine delivery.

Bioinspired approach		Delivery systems	Vaccine components	Mechanisms	Refs.
Biomacromolecules- inspired nanosystems	Albumin	Vaccine-Evans blue (EB) conjugates	CpG, Ag peptides	Binding endogenous albumin for LN targeting	[86]
		Albumin fusion proteins	TAAAs	Tumor-targeted drug delivery	[87]
	Lipoprotein	Synthetic HDL (sHDL) nanodiscs	CpG, Ag peptides, TAAAs, ALDH peptides	Efficient LN- or tumor-targeted vaccine delivery	[90,91,93]
	Nucleic acid	DNA origami	Ag peptides, CpG motif, dsRNA	Ag/adjuvant incorporation through DNA hybridization	[95]
Single-stranded (ss) RNA origami		Itself as TLR3 agonist adjuvant	TLR3 pathway activation	[96]	
Cell-inspired nanosystems	Cytomembrane	Tumor cell membranes	Tumor cell membrane-derived Ags, MPLA	Homotypic targeting, insertion capacity for lipid-like adjuvant	[102,103]
		PLGA cores, Tumor cell membranes	Tumor cell membrane-derived Ags, CpG	Tumor targeting, incorporation of adjuvant in PLGA cores	[107,108]
	Red blood cell (RBC) membrane coating	PLGA cores, RBC membranes	Ag peptide hgp100, MPLA	Prolonged drug circulation time, surface modification via lipid anchoring	[110]
	Hybrid cell membrane coating	DC-tumor fusion cell membranes, NPs cores	Tumor Ags, costimulatory molecules, R848	Functioning like APCs for T cell activation	[111,112]
		RBC-tumor cell fusion membranes	Tumor cell membrane-derived Ags	Splenic APC targeting capacity for T cell activation	[113]
	Exosome	Fusogenic exosomes	Itself as TLR4 agonist adjuvant	Induced tumor cell xenogenization as non-self	[115]
		DC-derived exosomes	$\alpha$ -fetoprotein	Functioning as stronger APCs for T cell activation	[116]
	Bacteria	Attenuated Salmonella bacteria	Intrinsic immunostimulatory effect, TAAAs	Bacteria-triggered tumor-specific thrombosis for photothermal therapy (PTT)	[118]
		Bacterial membrane, PC7A/CpG polyplex cores	CpG, PC7A, TAAAs	pH-activated release of CpG and Ags	[119]
	Virus	Virus-like particles (VLPs)	Inherent immunogenicity, OVA peptides, HER2	Self-assembly into nanocage, ease of genetic modification	[121,122,123]
Artificially cloaked viral nanovaccines		Tumor cell membrane-derived Ags, viral CpG	Bypassing specific receptor-mediated uptake of oncolytic virus	[124]	
Microsphere scaffolds		Poly(lactic acid) (PLA) microspheres	MPLA, Ag proteins or peptides	Self-healing nature for Ag microencapsulation	[127,128]
		PLGA microparticles	Two stimulatory molecules	Function as aAPCs for T cell activation	[129]
Implantable scaffold	Hyaluronic acid/collagen scaffolds	Tumor lysates, poly(I:C), R848	Sustained release of the vaccine components	[132,133]	
		PLGA scaffolds	GM-CSF, CpG, CCL20, Flt3L, tumor lysates	Cytokine presentation for DC recruitment and activation	[134,135]
	Polysaccharide scaffolds	CAR T cells, STING agonist, cdGAMP	Converting the tumor bed into a self-vaccine site	[136]	
Injectable hydrogel	Peptide hydrogels	Tumor cells, DCs, OVA proteins, self-adjuvant	Serving as extracellular matrix	[142,141,143]	
	Synthetic polymer hydrogels	OVA proteins, OVA mRNA, Poly(I:C), R848	Hydrophobic/hydrophilic property for agonist adjuvant and Ag loading	[144,145]	
Mesoporous silica microrod (MSR)	High aspect ratio MSRs/MSR-PEI	GM-CSF, CpG, OVA protein, E7 peptide, DNA Ags	Generating of interparticle macropores for immune cell infiltration	[147, [148,149]	
Microneedle patch	Light-activated microneedle patches	Tumor lysates containing melanin, GM-CSF	Melanin as photosensitizer mediated PTT	[152]	
	Dissolving microneedle patches	OVA proteins, R848	Rapid generation of nanovaccine in situ	[153]	
	Coated microneedle patches	OVA proteins, poly(I:C)	pH-responsive generation of film for Ag transport	[154]	

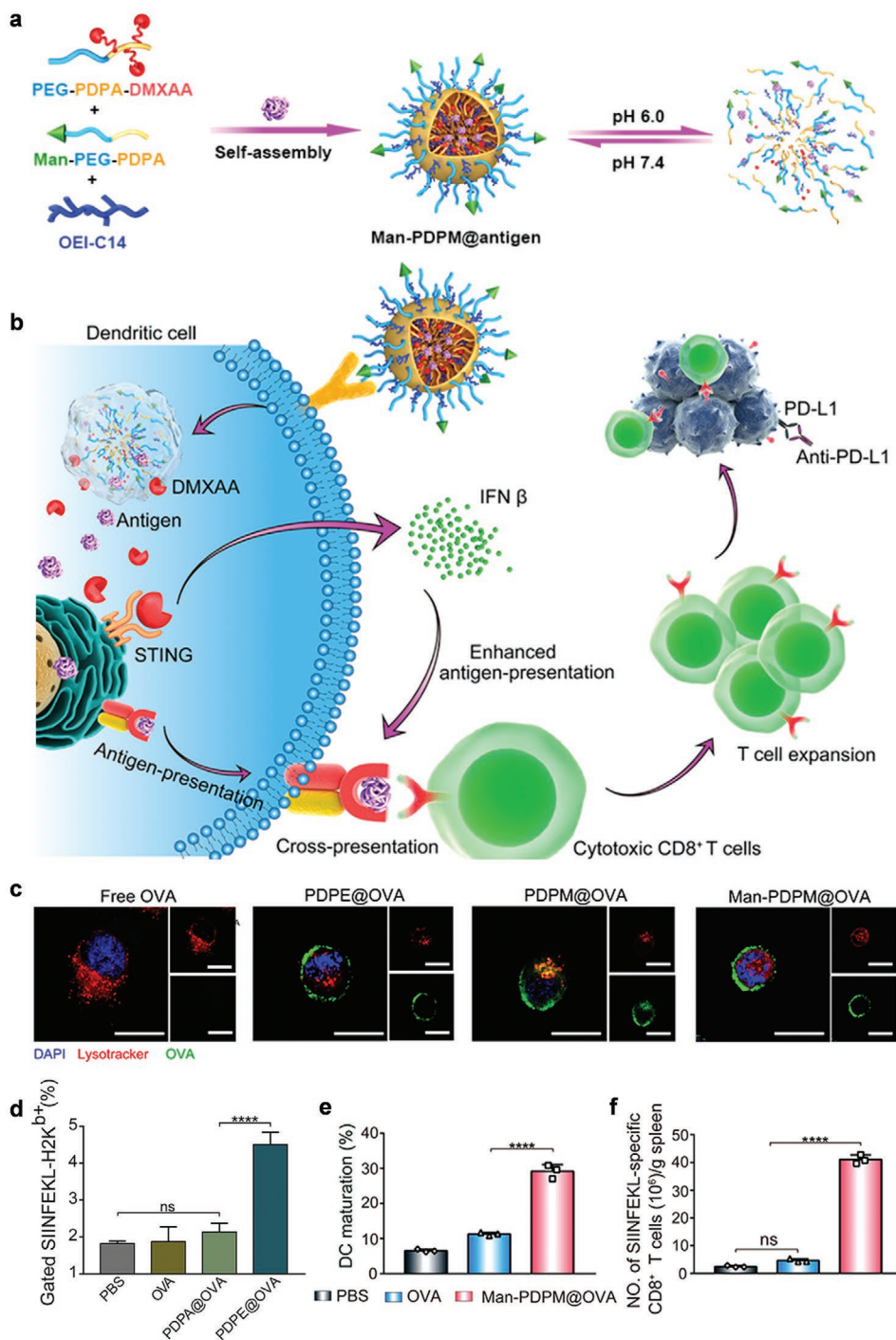


**Figure 2.** a) The fabrication of acid-responsive nanovaccine (Man-PDPM@OVA). b) Mechanism of the nanovaccine stimulating the STING pathway and boosting T cell priming for enhanced antitumor immune responses. c) Confocal microscopy imaging of OVA Ag presentation (green) and Lysotracker staining (red) at 24 h of incubation, scale bar = 20  $\mu$ m. d) Flow cytometric analysis of Ag presentation on the surface of bone marrow DCs 24 h after different treatment in vitro. Flow cytometric analysis of e) matured DC (CD11c<sup>+</sup>CD80<sup>+</sup>CD86<sup>+</sup>) in the tumor-draining LNs (TdLNs) and f) the SIINFEKL-specific CD8<sup>+</sup> T cells in the spleen on day 7 after the first vaccination. Reproduced with permission.<sup>[40]</sup> Copyright 2020, American Chemical Society.

of CpG-conjugated PAMAM, enabling their deep tumor penetration and increased DC phagocytosis. Afterward, the redox condition in endolysosomal compartment caused further release of free CpG, thus promoting DC activation and enhancing anti-tumor immunotherapies.

In addition to harnessing NPs as vehicles for delivering tumor Ag or adjuvant to APCs to provoke antitumor immunity, some nanomaterials possess intrinsic immunostimulatory activities without the participation of conventional immune adjuvants. For example, Gao and co-workers reported an

ultrasensitive pH polymer PC7A, comprising tertiary amines with cyclic side chains to deliver Ags to APCs.<sup>[42]</sup> Upon the protonation of tertiary amine residues in PC7A by early endosomal pH condition, this nanovaccine dissociated and enhanced cytosolic delivery of tumor Ags in APCs, resulting in increased cross-presentation while simultaneously activating the STING pathway to boost antitumor immunity. Following which, similar STING-activating NP (STING-NP) was utilized for cytosolic delivery of the endogenous STING ligand, 2'3' cyclic guanosine monophosphate–adenosine monophosphate (cGAMP).<sup>[43]</sup> This STING-NP promoted the cytosolic delivery of cGAMP via an endosomal escape mechanism, activating STING pathway in APCs within the TME and sentinel LN, converting immunosuppressive tumors to immunogenic microenvironments for enhanced antitumor immunity.

**Redox:** To prevent oxidative damage, cells maintain redox homeostasis. In cancer cells, a state of redox imbalance exists due to the accumulation of reducing molecules or reactive oxygen species.<sup>[44]</sup> Compared to normal cells, higher levels of GSH are usually found in the cytosol of tumors cells. Significant differences in GSH concentrations also exist between the extracellular ( $2\text{--}20 \times 10^{-6}$  M) and intracellular ( $2\text{--}10 \times 10^{-3}$  M) tumor environments.<sup>[45]</sup> Similar to the pH gradient that exists between endolysosomes and the cytosol, GSH has been extensively utilized as an endogenous trigger to achieve the cytosolic delivery and release of Ags or adjuvants in a controlled manner. As such, disulfide moieties are commonly employed in the design of GSH-responsive nanosystems.

Tang and co-workers designed a redox-sensitive polycondensate neoepitope (PNE) through copolymerization of peptide neoantigens and adjuvants together via a responsive linker-monomer containing disulfide bonds.<sup>[46]</sup> In intracellular environments, higher GSH levels facilitated the release of neoepitope from PNE. This GSH-responsive PNE with suitable size could efficiently accumulate in draining LNs (dLNs), significantly promoting Ag capture. Upon internalization by APCs, PNE degraded rapidly under the action of endogenous GSH, improving endosomal escape and cytosolic delivery of neoantigens, resulting in better cross-presentation. This intracellular GSH-responsive PNE vaccine successfully induced potent Ag-specific CTL responses for enhanced antitumor efficacy. In another work, Moon's group reported the use of biodegradable mesoporous silica NP (bMSN) for incorporating neoantigen peptide, CpG oligodeoxynucleotide (ODN) adjuvants and photosensitizer chlorin e6 (Ce6) for combined cancer immunotherapy.<sup>[47]</sup> Notably, neoantigen peptides were attached to bMSNs via disulfide bonds, which could be cleaved in response to higher GSH concentrations in tumor intracellular environment, facilitating cytosolic delivery of tumor Ags. bMSN vaccination combined with photodynamic therapy (PDT) induced DC recruitment and elicited robust neoantigen-specific T cell immunity for activatable cancer immunotherapy.

**Hypoxia:** Hypoxia, the reduced availability of oxygen compared with its demand in tissues, is considered a common feature in various solid tumors. It is largely associated with abnormal vascularization, resulting in insufficient supply of oxygen.<sup>[48]</sup> Hypoxia can be identified as a tumor-specific stimulus since normal tissues barely contain hypoxic regions. As such, hypoxia-responsive materials have been widely utilized for molecular imaging in cancer diagnosis and therapy.<sup>[49]</sup>

Moreover, hypoxia-responsive nanosystems have also recently been used in the targeted delivery of cancer vaccines to tumors.

Kim and co-workers developed a hypoxia-sensitive mesoporous silica NP (CAGE) carrying a photosensitizer (Ce6) for PDT, and an immune adjuvant (CpG) to enhance cancer immunotherapy.<sup>[50]</sup> CAGE was constructed by decorating glycol chitosan (GC) and PEG onto the surface of Ce6-laden CAGE using a hypoxia-sensitive azobenzene linker. Next, CpG was loaded via electrostatic interactions with GC. Hypoxia-stimulated release of CpG/GC facilitated the uptake by DCs, while photodynamic effects of Ce6 led to the generation of TAAs, recruitment of DCs and enhanced Ag presentation. This hypoxia-responsive vaccination combined with PDT induced the activation and maturation of DCs for enhanced cancer immunotherapy.

### 3.1.2. Enzymes

In tumor tissues, dysregulation of extracellular (e.g., matrix metalloproteinase, proteinase, hyaluronidase) and intracellular (cathepsin B) enzymatic activity frequently occurs.<sup>[51]</sup> Since enzymes catalyze chemical reactions with high specificity and efficiency under mild conditions, utilizing enzymatic activity as a biological stimulus for controlled payload release can provide new strategies for the design of delivery systems.<sup>[52]</sup> Several digestive enzymes such as esterase,  $\beta$ -glucuronidase and lipase are highly expressed in lysosomes of nearly all eukaryotic cells.<sup>[53]</sup> These enzymes have also been adapted in the design of enzyme-responsive biomaterials to achieve efficient cytosolic delivery and release of vaccine components with good bioavailability, thus boosting antitumor immune responses.

Irvine and co-workers designed interbilayer-crosslinked multilamellar vesicles (ICMVs) containing protein Ags encapsulated in the core and lipid-based adjuvants entrapped in the vesicle walls for lipase-sensitive payload activation and improved vaccination (Figure 3a).<sup>[54]</sup> This NPs were formed by crosslinking lipid headgroups across adjacent bilayers within the vesicle walls, while the phospholipid base of the particles rendered them inherently biodegradable by endolysosomal lipase. ICMVs loaded and retained high contents of protein Ags within the vesicles when exposed to serum (Figure 3b). In the presence of lipases usually found at high levels within endolysosome, these vesicles were quickly degraded (Figure 3c). After vaccination with ICMVs carrying OVA and MPLA, endolysosomal lipases induced the activation of OVA and MPLA for enhanced vaccine responses, thus achieving strong humoral and Ag-specific CTL responses following repeated immunization (Figure 3d,e). This lipase-sensitive vesicle formed a safe and highly potent subunit vaccine for boosting humoral and cell-mediated immunity. Furthermore, Shi and co-workers reported an enzyme-responsive amphiphilic polymer prodrug of TLR7/8 agonists for designing activatable cancer vaccines.<sup>[55]</sup> This amphiphile prodrug was formed by conjugating TLR7/8 agonist IMDQ to PEG chain via an enzyme-responsive linker, containing  $\beta$ -glucuronidase ( $\beta$ -GUS) sensitive glucuronide and ester bond. They could self-assemble into vesicular NPs and were trafficked to LNs after intratumoral injection. Upon endocytosis by APCs, these vesicular NPs collapsed in response to endosomal enzymes (esterase and  $\beta$ -GUS), leading to the liberation of native IMDQ and provoking robust immune activation in vivo.

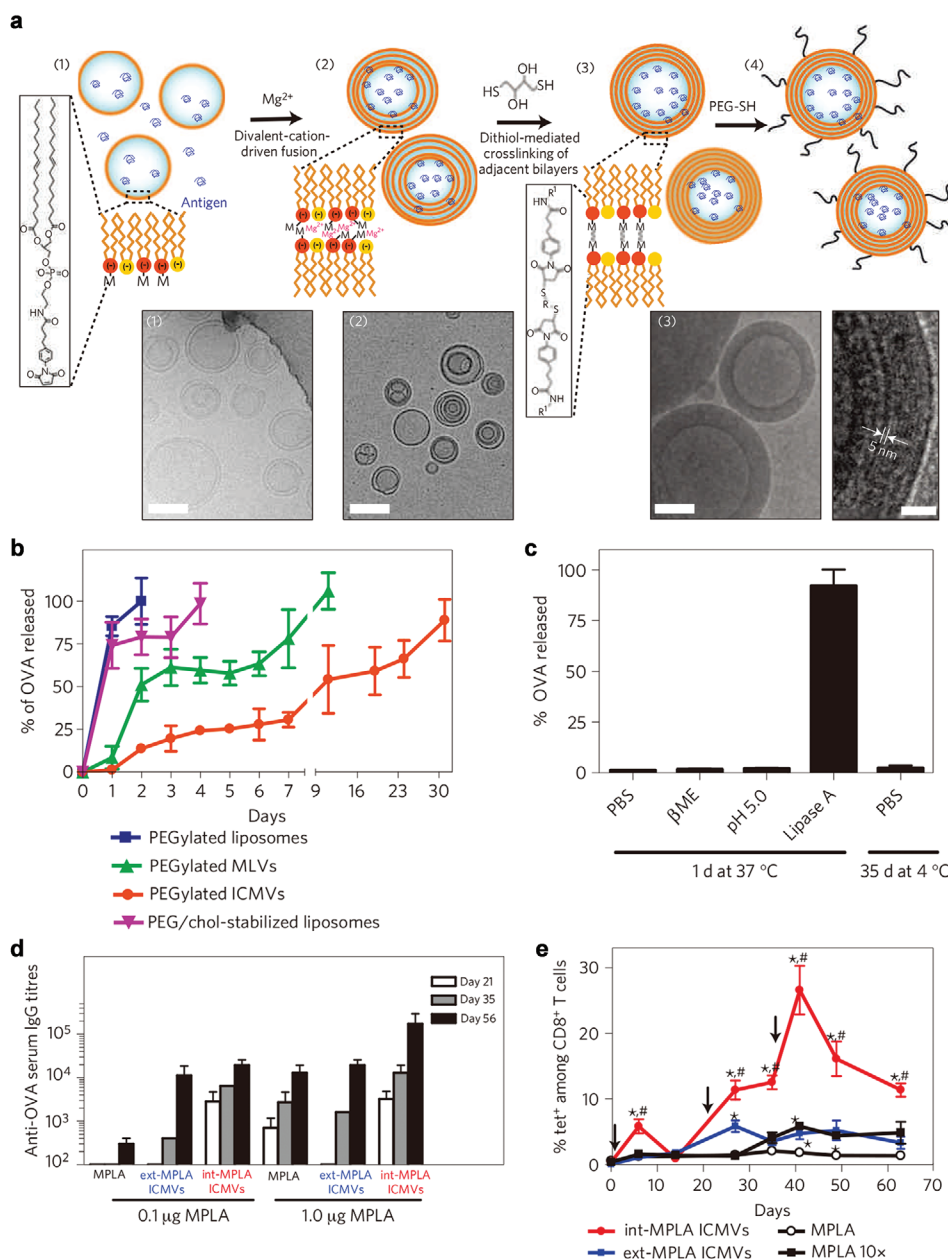


**Figure 3.** a) The synthesis process of enzyme-responsive ICMVs and cryo-electron microscope imaging. b) Kinetics of OVA release from ICMVs at 37 °C in complete media examined over 30 day in vitro. c) OVA release from ICMVs in buffers mimicking the endolysosomal conditions ( $100 \times 10^{-3}$  M  $\beta$ -mercaptoethanol,  $50 \times 10^{-3}$  M sodium citrate pH 5.0,  $500 \text{ ng mL}^{-1}$  lipase A). d) Total OVA-specific serum IgG measured by enzyme-linked immunosorbent assay on day 21, 35, and 56 after subcutaneous vaccination of C57BL/6 mice. e) Quantitative analysis of Ag-specific T cells in peripheral blood by tetramer staining among CD8<sup>+</sup> T cells after different immunizations versus time. Reproduced with permission.<sup>[54]</sup> Copyright 2011, Springer Nature.

### 3.2. Exogenous Stimuli

In addition to utilizing naturally occurring endogenous stimuli, considerable effort has been made to develop approaches that employ exogenous stimuli (e.g., light, radiation, ultrasound, electromagnetic radiation). Since endogenous stimuli may vary depending on tumor types, disease progression and pathological characteristics, exogenous stimuli present a more universal option for the manipulation

of the local host environment, allowing triggered cargo release in a remote and spatiotemporally controlled manner at the desired sites.<sup>[56]</sup>

#### 3.2.1. Light

Light, ranging from UV, visible to NIR irradiation, is one of the more biocompatible exogenous stimuli because they are



noninvasive, easy to control and possess high spatiotemporal precision.<sup>[57]</sup> Using light, a wide variety of photoresponsive systems have been engineered for spatiotemporal control of cell function, gene regulation, as well as protein interaction.<sup>[58]</sup> Photoresponsive activation modalities can be utilized for activation of vaccine components, involving photoresponsive activation by direct or indirect action. Photoresponsive activation by direct action is based on photocleavable/photolabile chemical groups in response to UV/visible or NIR light, which can be taken advantage for the construction of photoresponsive systems for drug release and activation.<sup>[59]</sup> Photoresponsive activation by indirect action is mediated by the production of ROS after exposure to NIR light. ROS-responsive delivery systems can be incorporated into design strategies for activatable cancer therapy.<sup>[60]</sup> Photochemical internalization is a highly specific and efficient approach for cytosolic delivery based on the co-delivery of photosensitizers and Ag into endolysosomes of APCs. Upon light exposure, the photosensitizer is activated and ROS is generated, rupturing the endolysosomal membrane, achieving cytosolic release of Ags and facilitating MHC I Ag cross-presentation and induction of Ag-specific CD8 T cell responses.<sup>[61]</sup> Additionally, photodynamic systems depend on the activation of photosensitizer to produce ROS for drug release and ICD induction, thus stimulating antitumor immune responses.<sup>[62]</sup>

Li and co-workers developed a NIR light-activated immunodevice based on direct activation for selective spatial control over antitumor immunity (Figure 4a,b).<sup>[63]</sup> This photoactivatable immunodevice was formed by integrating a UV light-activatable CpG adjuvant (PCpG) with UCNPs. UCNPs act as transducers for upconverting NIR light into UV light locally, resulting in the cleavage of photocleavable (PC) bonds and the following liberation of CpG oligonucleotides (ONDs) from PCpG. The light-activatable property of PCpG could be determined by Förster resonance energy transfer (FRET). FRET pair-labeled PCpG was created by the hybridization of Cy3-labeled CpG to Black Hole Quencher 2 (BHQ2)-labeled PcDNA. The significant decrease in fluorescence intensity of Cy3 verified the formation of the double-stranded PCpG (Figure 4c). Upon irradiation of the formed structure with UV light, the fluorescence intensity was substantially enhanced, demonstrating the liberation of Cy3–CpG from the hybrid because of the photolysis of PC group (Figure 4d). In vivo antitumor results showed that NIR irradiation-activated PCpG resulted in a substantial increased proportion of tumor-infiltrating T cells for improved antitumor efficacy (Figure 4e,f). Pu's group designed an organic semiconducting pro-nanostimulant (OSPS) based on indirect activation for NIR-photoactivatable cancer immunotherapy.<sup>[64]</sup> OSPS consisted of a semiconducting polymer NP core and an immunostimulator attached via a singlet oxygen (<sup>1</sup>O<sub>2</sub>)-responsive cleavable linker. Upon NIR laser irradiation, OSPS enabled the generation of heat and <sup>1</sup>O<sub>2</sub>, resulting in tumor ablation and subsequent release of TAAs. Additionally, NIR irradiation triggered the controlled release and activation of immunostimulants from OSPS to revert the immunosuppressive TME. Following which, the released TAAs along with activated immunostimulants induced a combined antitumor immunity.

### 3.2.2. Temperature

Apart from the above exogenous stimuli, temperature alteration is another important strategy for the activation of drug delivery systems. Moderate hyperthermia can be achieved by microwave, ultrasound, radiofrequency, infrared irradiation or magnetic hyperthermia.<sup>[65]</sup> Thermoresponsive drug delivery systems are stable at body temperature (37 °C). Under the stimuli of moderate hyperthermia, controlled release of therapeutic agents is achieved, thereby improving antitumor efficacy and decreasing side effects. A myriad of thermoresponsive system has been developed for diagnostics and therapy applications.<sup>[66]</sup> Liposome and lipid-based NP represent typical thermoresponsive systems with a phase transition temperature (T<sub>m</sub>) between 40 and 45 °C. They undergo lipid membrane rupture and subsequent release of entrapped cargos upon heating above T<sub>m</sub>.<sup>[67]</sup> In addition to achieving thermoresponsiveness by lipid-based phase transition, thermolabile cleavable bonds have also been incorporated in the design of nanocarriers to construct thermoresponsive drug delivery systems. Recently, temperature-sensitive systems have also been employed as vaccine delivery platforms for activatable cancer immunotherapy.

Pu's group reported a photothermal activatable polymer nanoagonist (APNA) using second near-infrared (NIR-II) light for combined photothermal immunotherapy (Figure 5a,b).<sup>[68]</sup> This APNA was comprised of a NIR-II semiconducting polymer as photothermal transducer and immunoadjuvant R848 through a thermoresponsive linker (2,2'-azobis[2-(2-imidazolin-2-yl)propane]). Photothermal heating of semiconducting backbone selectively activated R848 release from APNA (Figure 5c). After NIR-II light exposure, APNA took advantage of photothermal effects to direct tumor ablation and ICD induction, while elevated temperatures triggered the cleavage of thermoresponsive linker to liberate the immunoadjuvant R848 for DC activation. In vivo antitumor study indicated that NIR-II irradiation activated APNA induced stronger DC maturation in TdLNs and higher proportion of tumor-infiltrating CD4<sup>+</sup> and CD8<sup>+</sup> T cells to reinforce antitumor efficacy (Figure 5d,e). Moreover, they developed another semiconducting polymer nanoagonist SPN<sub>II</sub>R with a photothermally triggered TLR agonist release for NIR-II photothermal immunotherapy.<sup>[69]</sup> SPN<sub>II</sub>R was comprised of a semiconducting polymer core as NIR-II photothermal converter, TLR agonist R848, enveloped with a thermoresponsive lipid shell. This temperature-sensitive delivery system provided an alternative approach for bioinspired delivery of vaccine components for amplified cancer immunotherapy.

### 3.2.3. Radiation

Radiotherapy involves using ionizing radiation including X-rays,  $\gamma$ -rays, or electron beams to destroy tumor cells. It is commonly used as a treatment option in over half of all cancer patients.<sup>[70]</sup> Radiation is also considered a promising modality for promoting immunotherapy through initiating in situ vaccination by inducing ICD of tumor cells, facilitating DC maturation and subsequent T cell priming.<sup>[71]</sup> Radiation-triggered immunotherapy can further be synergized with other complementary immunotherapies to improve antitumor efficacy.

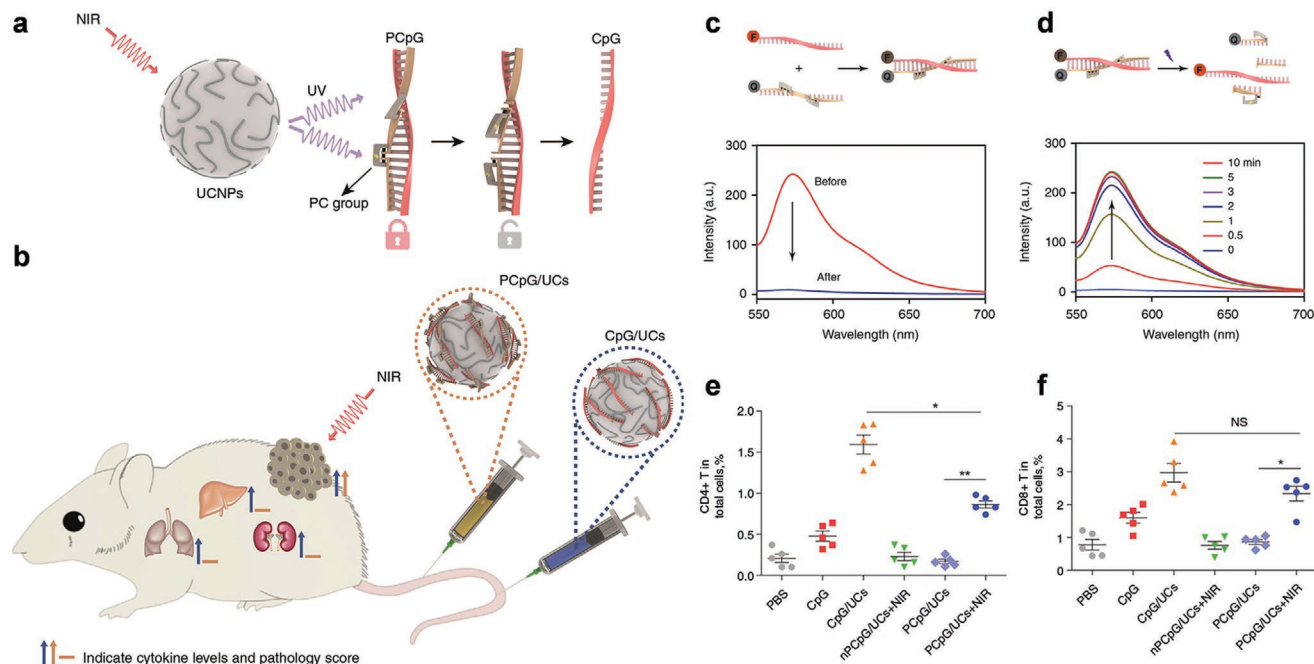


**Figure 4.** a) The design of photoactivatable immunodevice (PCpG/UCs) based on UCNP through the integration with a UV light-responsive CpG (PCpG) containing photocleavable group. b) Schematic of the photoactivatable immunodevice for remotely control of antitumor immunity mediated by NIR laser irradiation. c) Fluorescence spectroscopy of Cy3–CpG before and after double strand formation in PCpG. d) Fluorescence spectroscopy of FRET pair-labeled PCpG (BHQ2–PcDNA hybridized to Cy3–CpG) with elevated irradiation dose of 365 nm laser. Flow cytometric analysis of e) CD4<sup>+</sup>T and f) CD8<sup>+</sup>T cell subset in 4T1 tumor tissues from various treatment groups with or without NIR irradiation. Reproduced under terms of the CC-BY license.<sup>[63]</sup> Copyright 2019, The Authors, published by Springer Nature.

Liu's group designed a multifunctional core–shell PLGA NP for radiotherapy-triggered cancer immunotherapy (Figure 6a).<sup>[72]</sup> This NP was fabricated by encapsulating water-soluble catalase (Cat) inside the core and loading imiquimod (R837) adjuvant within the PLGA shell. PLGA-R837@Cat NPs under X-ray radiation can significantly improve radiotherapy efficacy by relieving Cat-triggered tumor hypoxia and reverting the immunosuppressive TME. Radiotherapy with PLGA-R837@Cat triggered ICD, induced high expression of surface calreticulin (CRT) on dying tumor cells (Figure 6b). The generated TAAs, in addition to R837-loading PLGA-R837@Cat NPs as immune adjuvants, significantly promoted DC maturation (Figure 6c). PLGA-R837@Cat-based radiotherapy together with CTLA-4 checkpoint blockade enhanced CD4<sup>+</sup> and CD8<sup>+</sup> T infiltration while reducing the proportion of regulatory T cells (Tregs) at tumor tissues (Figure 6d,e). Recently, Lin and co-workers presented a radiation-triggered nanoscale MOF (nMOF) to mediate radiotherapy for combined checkpoint blockade immunotherapy.<sup>[73]</sup> nMOF was constructed from two HF-based nMOFs as radioenhancers to produce ROS. By combining the advantages of local radiotherapy induced in situ vaccination and PD-L1 checkpoint blockade, these radiation-activated nMOFs could achieve systemic antitumor immunity to efficiently eradicate primary and distant tumors.

### 3.2.4. Ultrasound

As one of the most common nonionizing physical irradiation sources, ultrasound has been widely used for diagnostics

and therapeutic applications. Ultrasound-based therapeutic modality for noninvasive cancer treatment has shown great potential due to its deep-tissue penetration, noninvasiveness, high controllability and low expense.<sup>[74]</sup> In addition, ultrasound can also be utilized for sonodynamic therapy (SDT) by activating sonosensitizers to generate ROS for inducing ICD, eliciting host antitumor immunological effects.<sup>[75]</sup>

Chen and co-workers developed an ultrasound-activated nanosonosensitizer (HMME/R837@Lip) for noninvasive control of cancer immunotherapy (Figure 7a).<sup>[76]</sup> This HMME/R837@Lip nanosonosensitizer used liposomes for co-encapsulating sonosensitizers (hematoporphyrin monomethyl ether (HMME)) and R837 adjuvant. Upon repeated noninvasive ultrasound irradiations, HMME/R837@Lip effectively induced ICD and released TAAs. 4T1 tumor-cell debris after HMME/R837@Lip-augmented SDT greatly activated DC maturation by upregulation of costimulatory molecules CD80/CD86 (Figure 7b). Accompanied by DC maturation, high levels of proinflammatory cytokines IL-6 and TNF- $\alpha$  were increased to elicit specific immune response (Figure 7c,d). After intravenous injection, HMME/R837@Lip nanosonosensitizers acquired high accumulation and long-term retention in tumor tissues. HMME/R837@Lip-augmented SDT together with anti-PD-L1 checkpoint blockade have been demonstrated to increase the antitumor immune responses, including the upregulated levels of cytokines IFN- $\gamma$  and TNF- $\alpha$  in serum (Figure 7e), along with an obvious transition of naïve and central memory T cells toward effector memory phenotype (Figure 7f,g).

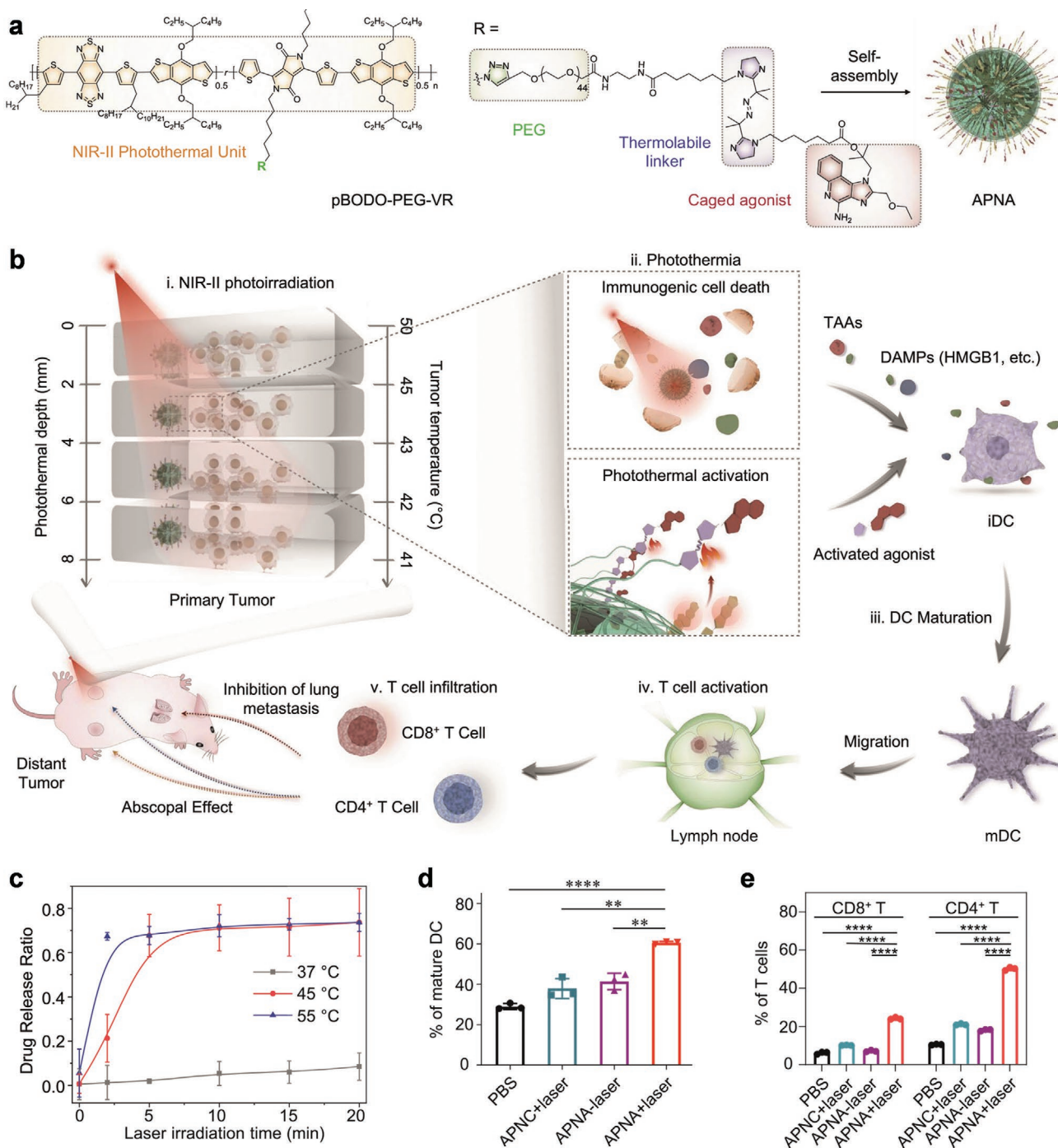


**Figure 5.** a) Scheme of the chemical structure and preparation of photoresponsive APNA. b) Working mechanism of temperature-triggered photothermal immunotherapy mediated by APNA nanoagony for the potentiation of antitumor responses. c) Release ratio of R848 from APNA at different temperature (37, 45, and 55 °C) controlled by changing power density of 1064 nm laser. d) Flow cytometric analysis of mature DC (CD80<sup>+</sup>CD86<sup>+</sup>) in TdLNs after various treatments. e) Quantification of percentages of CD8<sup>+</sup> and CD4<sup>+</sup> T cells in primary tumor after different treatments. APNC: the control NP without R848 agonist. Reproduced under terms of the CC-BY license.<sup>[68]</sup> Copyright 2021, The Authors, published by Springer Nature.

### 3.3. Antigen-Capturing Nanoparticles

Conventional cancer vaccines employ ex situ Ag loading during vaccine fabrication.<sup>[77]</sup> Nanocarriers can be tailored for in situ Ag capturing to improve their presentation without the

need for in vitro Ag loading. The aforementioned exogenous stimuli-based approaches and specific chemotherapies can induce tumor to undergo ICD through releasing TAAs and damage-associated molecular pattern proteins (DAMPs). By incorporating functional handles or specific microdomains on

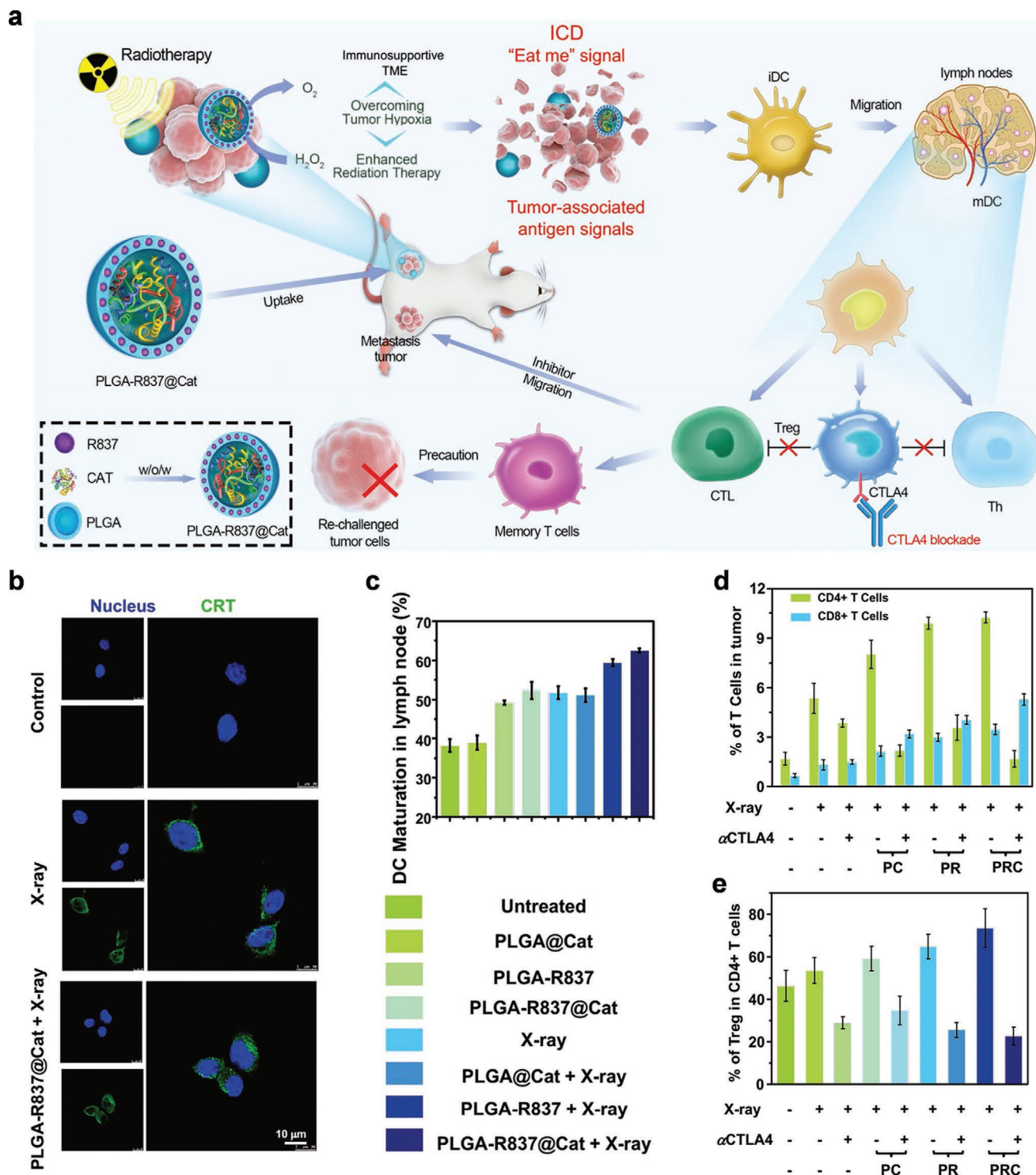


**Figure 6.** a) Mechanism of PLGA-R837@Cat-mediated radiotherapy to induce robust antitumor immune responses. b) Confocal imaging of the ICD marker CRT (green) on the surface of CT26 cells after X-ray irradiation. c) Flow cytometric analysis of in vivo DC maturation ( $CD80^+CD86^+$ ) in the TdLNs from CT26 tumor-bearing mice. Frequency of d) tumor-infiltrating  $CD8^+$  and  $CD4^+$  T cells, and e)  $FoxP3^+$  Tregs among  $CD4^+$  T cells in distant tumor tissues after different treatments in mice bearing CT26 tumors on two sides. PC: PLGA@Cat; PR: PLGA-R837; PRC: PLGA-R837@Cat. Reproduced with permission.<sup>[72]</sup> Copyright 2019, John Wiley and Sons.

the surface of nanocarriers, Ag-capturing nanovaccines can preferentially acquire tumor Ags in a manner that mimics how APCs capture Ags, thus facilitating further internalization by

professional APCs. Traditional strategies by delivering one or several “chosen” Ags fail to account for tumor heterogeneity. On the contrary, Ag capturing approach exposes the immune

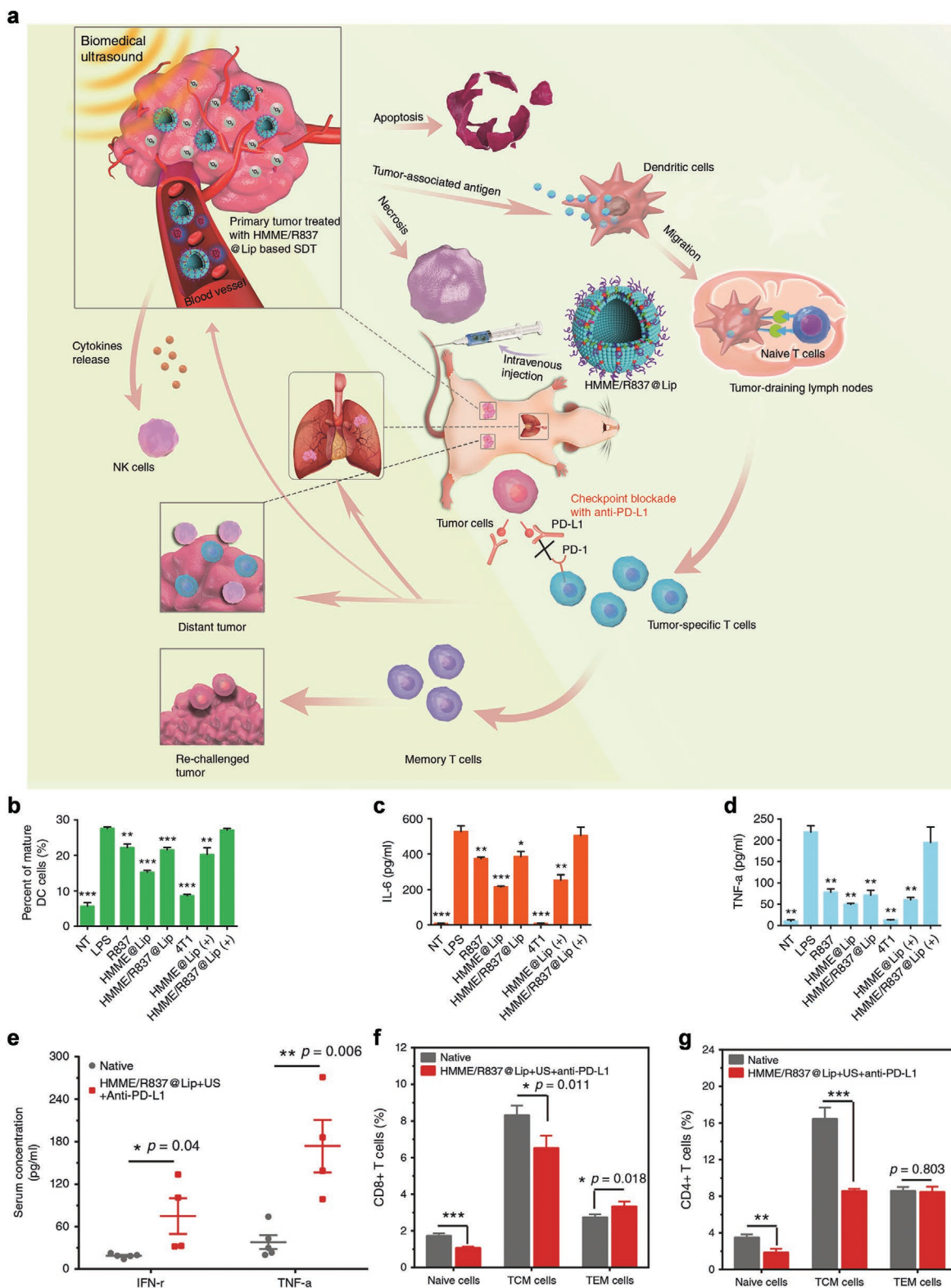


**Figure 7.** a) Schematic of ultrasound-activated cancer immunotherapy based on HMME/R837@Lip nanosensitizers combined with PD-L1 checkpoint blockade. b) Flow cytometric analysis of the matured DCs ( $CD86^+CD80^+$ ) after co-culture of pretreated 4T1 cells with BMDCs in a Transwell system for 20 h. The level of c) IL-6 and d) TNF- $\alpha$  in co-culture supernatant. e) The amount of serum TNF- $\alpha$  and IFN- $\gamma$  from different treatment group of mice 7 days after the second tumor was implanted. Quantification of naive, central memory (TCM), and effector memory (TEM) T cells among f)  $CD8^+$  T population and g)  $CD4^+$  population in the spleens of mice with combined treatments. Reproduced under terms of the CC-BY license.<sup>[76]</sup> Copyright 2019, The Authors, published by Springer Nature.

system to a wide range of TAAs in a patient-specific manner, thus carrying significant implications for the improvement of precision medicine through bioinspired design.

Wang and co-workers presented bioinspired antigen-capturing NPs (AC-NPs) that can induce abscopal effect and improve cancer immunotherapy (Figure 8a).<sup>[78]</sup> AC-NPs were formed using PLGA polymer with different modified surfaces to enable capturing of tumor-derived protein antigens (TDPAs) by chemical or physical interactions. AC-NP formulations successfully captured the neoantigens and DAMPs (Figure 8b). After radiotherapy, AC-NPs bound to TDPAs and transported them to APCs in TdLNs, thereby improving Ag uptake and presentation. In vivo results indicated that the addition of AC-NPs to PD-1 blockade greatly improved the ratio of CD8<sup>+</sup> T/Treg (Figure 8c) and CD4<sup>+</sup> T/Treg (Figure 8d). Furthermore, Chen and co-workers also designed a NIR-triggered Ag-capturing nanoplatform for photoimmunotherapy.<sup>[79]</sup> This nanoplatform was formed by self-assembly of DSPE-PEG-maleimide and indocyanine green (ICG, a light absorber) on oleate-capped UCNPs, followed by subsequent encapsulation of rose bengal (RB, a photosensitizer). Upon NIR light activation, TDPAs generated by phototherapy could be captured and retained in situ, hence increasing Ag uptake by APCs to elicit Ag-specific immune responses. As such, these AC-NPs not only eliminated primary tumors but also efficiently activated systemic antitumor immune response to inhibit untreated distant tumors.

### 3.4. Nano-Artificial Antigen Presenting Cells

Most cancer vaccines involve the regulation of APCs, which further stimulates tumor Ag-specific naïve T cells.<sup>[80]</sup> Recently, synthetic NPs have been engineered as alternative vaccine platforms by recapitulating signals necessary for direct T cell activation. Nano-APCs closely mimic natural APCs by co-coupling two essential signals (peptide-MHC complex and costimulatory molecules) onto their surface for T cell stimulation. The size, shape, surface ligand distribution and mobility of the nano-aAPCs are key parameters that can be modified to mimic different aspects of natural APCs, crucial for efficient signal presentation and efficacious T cell stimulation. For instance, the shape of the NPs can be optimized to facilitate increased interaction with T cells. Biodegradable particles can also be used for in vivo T cell modulation. NPs with in-built sustained release properties can be used to incorporate other soluble factors such as cytokines. Tumor immunotherapy with autologous APCs is an expensive and time-consuming process that limits its translation in clinical trials. Artificial signal presentation by nano-aAPCs offers well-defined systems with precise control over the signals presented. Thus, this approach has attracted significant interest as a strategy for improving cancer immunotherapy.

Schneck's group reported a reductionist approach for modulating T cell activation in T cell immunotherapy.<sup>[81]</sup> This nanoplatform was composed of SPIONs conjugated with two stimulatory signals for T cell activation (Figure 9a). The particle size, concentration, and stimulatory ligand density of

nano-aAPCs can be engineered to mimic endogenous APCs for improved T cell activation (Figure 9b). Quantitative analysis of CD8<sup>+</sup> T cell expansion suggested that nano-aAPCs with size more than 300 nm activated T cells more effectively than 50 nm nano-aAPCs (Figure 9c). A significant T cell receptor (TCR) downregulation was observed for cells stimulated with aAPCs larger than 300 nm, but this was not observed for 50 nm aAPCs when compared to noncognate aAPCs involved in inefficient TCR engagement and T cell stimulation (Figure 9d). In addition, they developed another reductionist T cell activation platform to simplify and streamline the customization of costimulatory conditions.<sup>[82]</sup> This platform was constructed by using paramagnetic NPs decorated with signal 1 Ag or signal 2 co-stimulus, instead of traditional methods with two signals conjugated together. CD8<sup>+</sup> T cells were significantly stimulated by NPs separately decorating signal 1 and signal 2 when particles were clustered together on the cell surface within a magnetic field, resulting in improved T cell activation for immunotherapy.

## 4. Biomimetic/Nature-Derived Semisynthetic Nanosystems for Vaccine Delivery

### 4.1. Biomacromolecule-Inspired Nanosystems

Biomacromolecules, such as proteins, lipids and nucleic acids, are essential for biological processes within living organisms. Their chemical composition and highly organized architecture provide clues and inspiration for designing functional biomaterials. Natural biomacromolecules have gained considerable interest as drug delivery systems owing to desirable intrinsic properties, including excellent biocompatibility, biodegradability, safety and long blood circulation time. As such, biomacromolecule-based carriers using albumin, lipoproteins, and nucleic acids, have been widely employed to improve cancer vaccine delivery.

#### 4.1.1. Albumin

With the FDA approval of Abraxane in 2004, albumin has since attracted significant attention for its potential use as drug carriers in cancer treatment.<sup>[83]</sup> Abraxane is an albumin-bound formulation of the anticancer drug paclitaxel, approved as indications for metastatic breast cancer, nonsmall cell lung cancer and pancreatic cancer patients. As a major component of plasma protein, albumin shows no immunogenicity and can be rescued from systemic degradation and clearance via inherent physiological mechanisms.<sup>[84]</sup> Albumin protein comprises a variety of reactive functional groups for chemical modifications. In addition, its hydrophobic domain can be employed as a binding pocket for the delivery of small drugs or photosensitizers.<sup>[85]</sup> An alternative strategy for the development of cancer vaccines is to leverage the natural LN trafficking properties of serum albumin for effective delivery of vaccine contents to LN. These intrinsic properties of albumin present albumin-based biomaterials as promising platforms for cancer vaccine delivery.

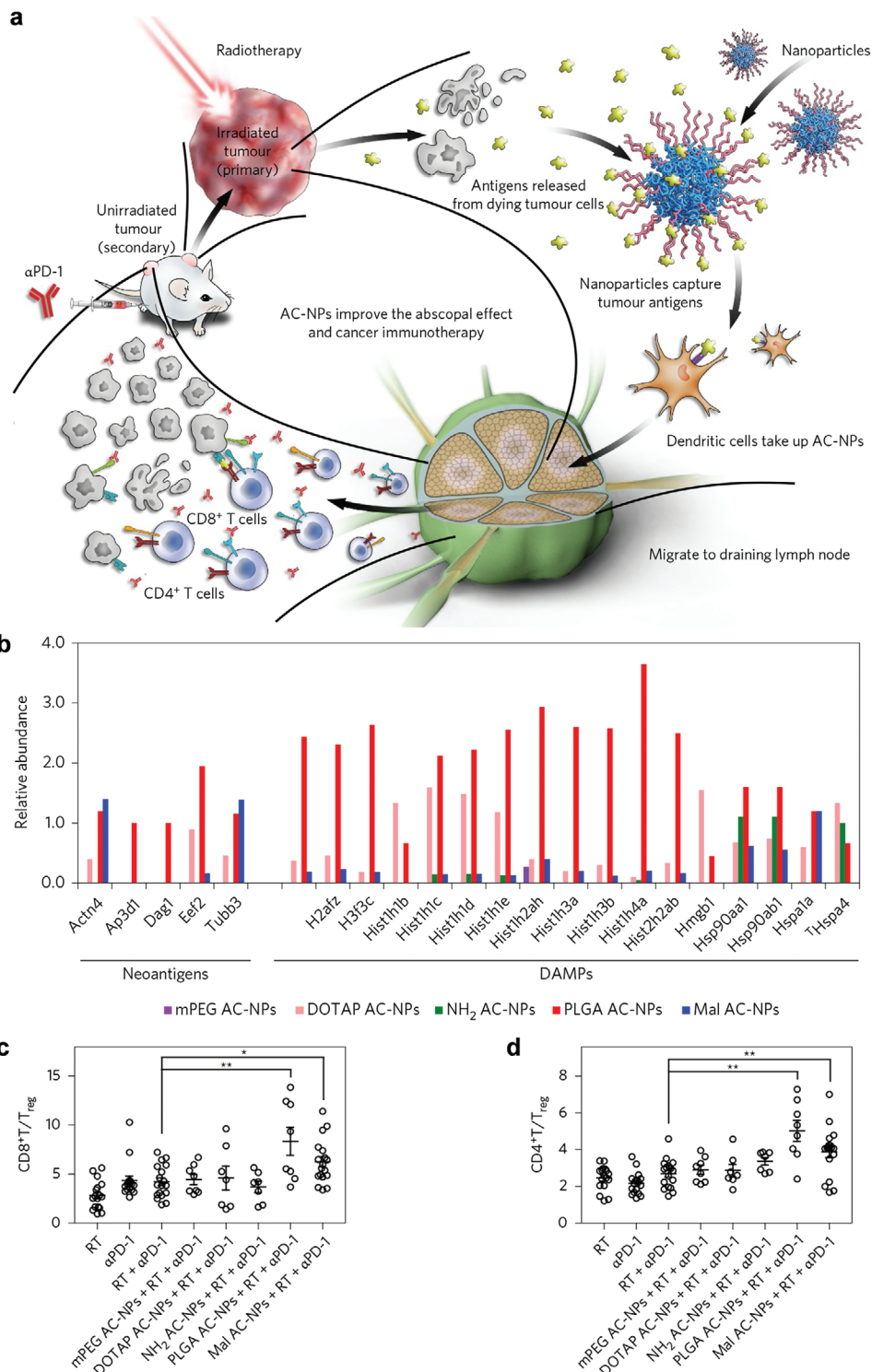


**Figure 8.** a) Mechanism of Ag-capturing NPs mediated the abscopal effect and efficient cancer immunotherapy. b) In silico analysis of the relative abundance of proteins (neoantigens and DAMPs) captured by AC-NP after incubation of lethally irradiated B16F10 tumor cell lysates. Flow cytometric analysis of c)  $CD8^+ T/T_{reg}$  and d)  $CD4^+ T/T_{reg}$  ratio in secondary tumors following different combined treatment. mPEG AC-NPs, DOTAP AC-NPs,  $NH_2$  AC-NPs, Mal AC-NPs refer to AC-NPs coated with PEG, cationic lipid DOTAP, amine PEG, maleimide PEG, respectively; PLGA AC-NPs refer to unmodified PLGA NPs. Reproduced with permission.<sup>[78]</sup> Copyright 2017, Springer Nature.

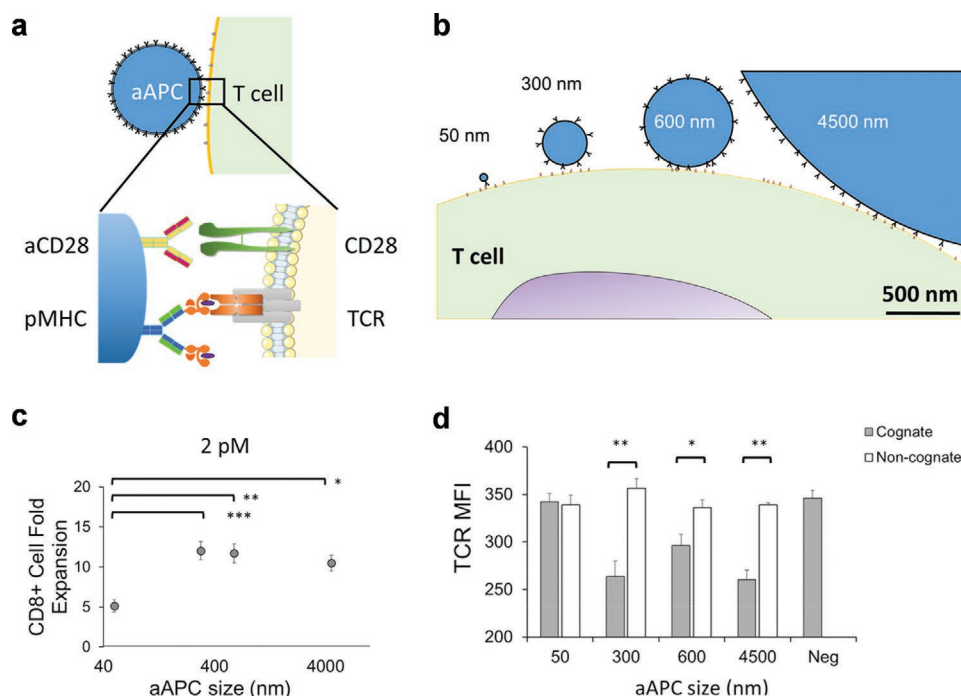


**Figure 9.** a) Schematic of T cell stimulation through the interaction between NP-based aAPC and Ag-specific T cell mediated by two stimulatory signals. Signal 1: pMHC; Signal 2: co-stimulation via anti-CD28 and TCR. b) Schematic illustrating relative sizes, stimulatory ligand densities and concentration of particle aAPCs for the modulation of T cell activation (scale bar = 500 nm). c) Fold proliferation of Ag-specific CD8<sup>+</sup> T cells cultured with aAPCs at the dose of  $2 \times 10^{-12}$  M conjugated pMHC after 7 days. d) Mean fluorescence intensity (MFI) for TCR- $\beta$  of CD8<sup>+</sup> T cells incubated with aAPCs for 5 h. Reproduced with permission.<sup>[81]</sup> Copyright 2017, American Chemical Society.

Chen and co-workers developed a bioinspired albumin/vaccine nanocomplex as an efficient vaccine delivery system for robust cancer immunotherapy (Figure 10a,b).<sup>[86]</sup> By conjugating molecular vaccines with EB into albumin-binding vaccines (AlbiVax), self-assembly of AlbiVax and endogenous albumin occurred *in vivo* to form albumin/AlbiVax nanocomplexes. This nanocomplex was efficiently transported to LNs via lymphatic drainage and extended retention in LNs. Fluorescence imaging showed that considerable albumin/AlbiCpG nanocomplexes were situated within or near the subcapsular region and surrounding B cell follicles post subcutaneous injection. Albumin/AlbiVax nanocomplexes boosted both innate and adaptive immunity, resulting in an obvious expansion of Ag-specific CD8<sup>+</sup> CTLs (Figure 10c,d) and T cell memory (Figure 10e). Apart from *in vivo* assembly with endogenous serum albumin, exogenous formulation involved drug encapsulation into an exogenous albumin-based nanosystem. Cai and co-workers presented a bioinspired hybrid protein oxygen carrier NP without incorporation of extra Ags or adjuvants for oxygen-augmented PDT.<sup>[87]</sup> Human serum albumin was hybridized with oxygen-carrying hemoglobin via intermolecular disulfide bonds to develop a hybrid protein oxygen nanocarrier with Ce6 encapsulated (C@HPOC). Upon laser exposure, C@HPOC increased the production of ROS and induced effective ICD, with the release of DAMPs to activate DCs, T cells and natural killer cells *in vivo*. Thus, C@HPOC-boosted PDT improved

therapeutic efficacy by evoking systemic antitumor immune responses.

#### 4.1.2. Lipoproteins

Lipoproteins are naturally occurring NPs composed of apolipoproteins and lipids, involved in the metabolic transport of fats and biomolecules. Due to their unique targeting capabilities, hydrophobic core and natural functions beyond cholesterol transport, these endogenous lipoprotein-based systems, especially HDLs, are becoming increasingly appreciated as ideal nanoplatforams for the delivery of various imaging or therapeutic agents.<sup>[88]</sup> sHDL-mimicking nanodiscs for cancer immunotherapy have recently been reported as vaccine delivery platforms.<sup>[89]</sup>

Inspired by the function of HDL as an endogenous carrier for cholesterol transport, Moon's group developed a sHDL-mimicking nanodisc vaccine platform for neoantigen peptides and adjuvants delivery (Figure 11a).<sup>[90]</sup> sHDL nanodiscs encompassed phospholipids and apolipoprotein-1 mimetic peptides with Ag peptides and adjuvants loaded. These nanodiscs greatly improved Ag/adjuvant transport to LN (Figure 11b,c). C57BL/6 mice immunized with sHDL-Adpgk (a neoantigen in MC-38 colorectal tumor)/CpG induced 47-fold higher ratios of neoantigen-specific CTLs than free vaccines and 31-fold higher than



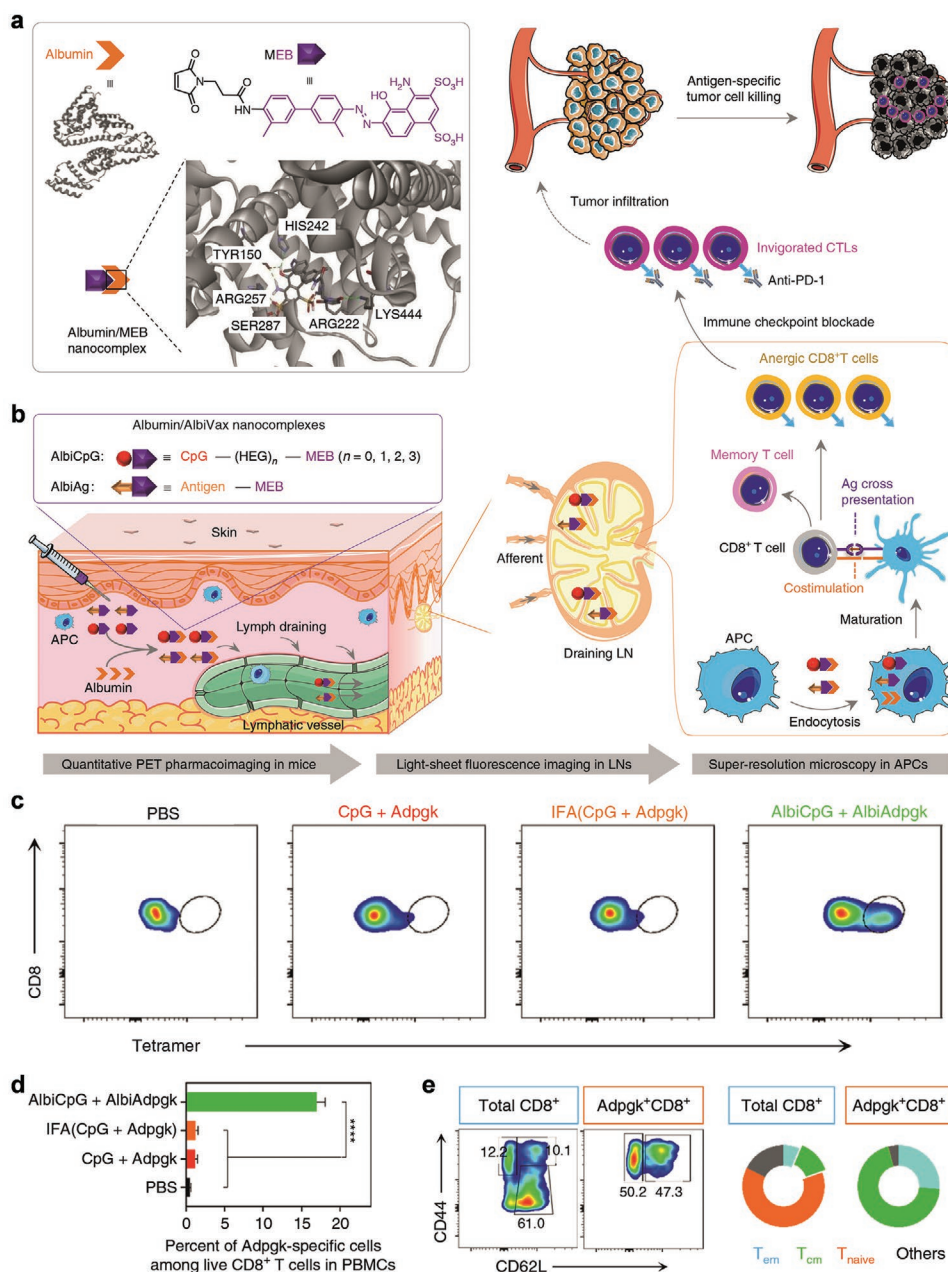


**Figure 10.** a) Schematic structure of albumin, MEB (maleimide derivative of EB dye) and albumin/MEB nanocomplexes. b) Working mechanism of albumin/AlbiVax nanocomplexes as efficient vaccine platform for potent cancer immunotherapy; AlbiCpG and AlbiAg were engineered by conjugating MEB with thiol-modified CpG and cysteine-modified Ags (e.g., Adpgk), respectively. c) Flow cytometric analysis of Adpgk-specific CD8<sup>+</sup> T cells in peripheral blood from C57BL/6 mice vaccinated with AlbiVax (AlbiCpG + AlbiAdpgk) on day 0 and day 14; IFA refers to incomplete Freund's adjuvant. d) Frequency of Adpgk-specific CD8<sup>+</sup> T cells in (c). e) Flow cytometric analysis of effector memory (T<sub>em</sub>), central memory (T<sub>cm</sub>) and naïve (T<sub>naive</sub>) T cells among CD8<sup>+</sup> T population after vaccination on day 50. Reproduced under terms of the CC-BY license.<sup>[86]</sup> Copyright 2017, The Authors, published by Springer Nature.

potentially the strongest adjuvant system CpG emulsified in oil/surfactant-based adjuvant Montanide (Figure 11d,e). Established MC-38 and B16F10 tumors were eradicated with the combination treatment of anti-PD-1 and anti-CTLA-4 checkpoint blockade immunotherapy. In their subsequent work, they further utilized sHDL nanodiscs to deliver chemotherapeutic ICD inducers, doxorubicin (DOX), as in situ vaccination to elicit effective antitumor immune responses.<sup>[91]</sup>

In addition to delivering tumor-specific neoantigens for personalized cancer immunotherapy, Moon's group was the first to present a novel nanodisc carrying cancer stem cells (CSCs) neoantigens for eliminating CSCs.<sup>[92]</sup> They identified two aldehyde dehydrogenase (ALDH) epitopes from CSCs and developed sHDL nanodiscs carrying these ALDH epitope peptides and CpG adjuvant to elicit ALDH-specific T cell responses. This nanodisc vaccination strategy improved Ag trafficking to LNs after subcutaneous injection and decreased

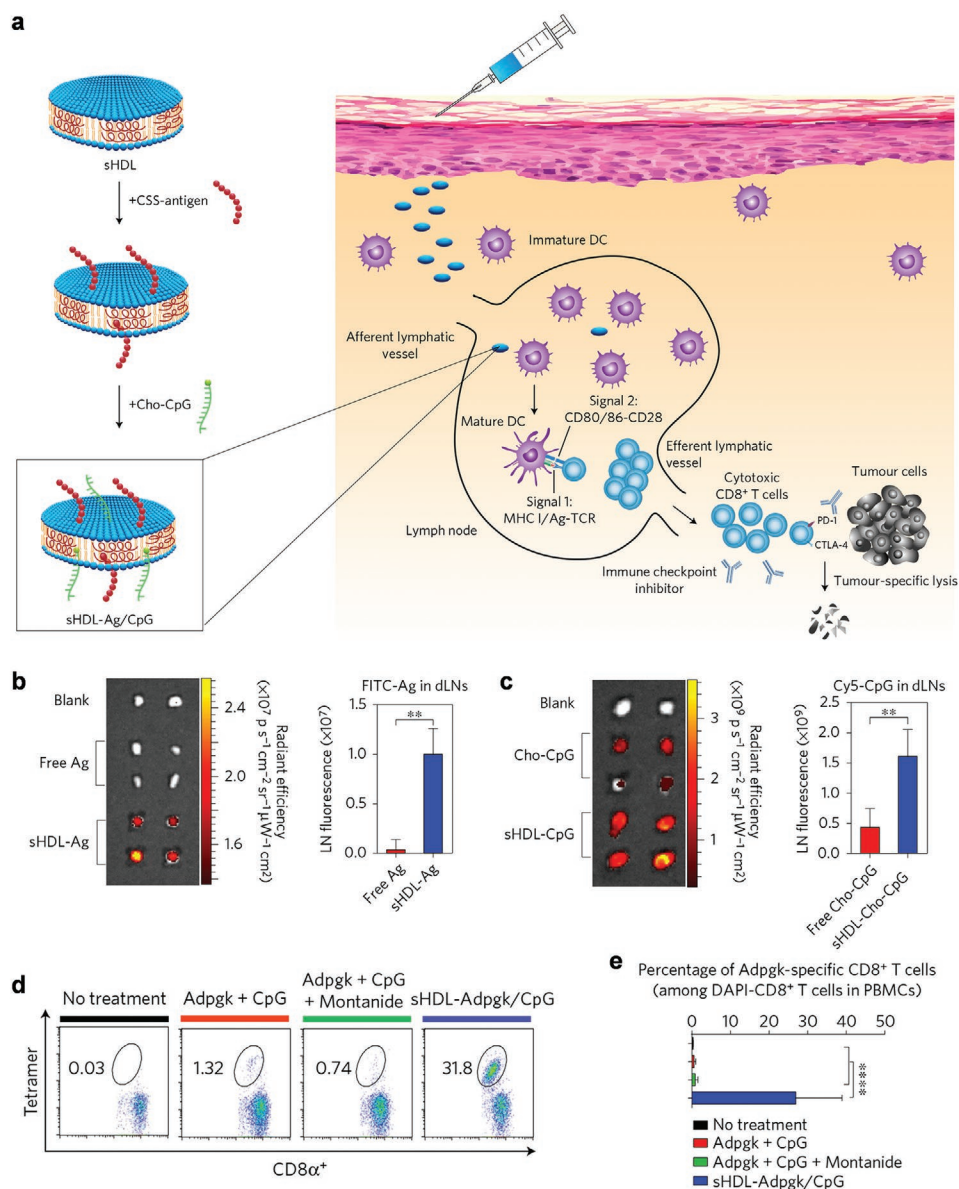


**Figure 11.** a) Scheme of HDL-mimicking nanodisc platform as vaccine delivery system for personalized cancer immunotherapy. sHDL nanodiscs were co-loaded with cysteine-serine-serine (CSS) linker modified Ags (CSS-Ag) and cholesterol-modified CpG adjuvant (Cho-CpG) to form sHDL-Ag/CpG vaccine. Ex vivo fluorescence imaging and quantitative analysis of b) FITC-tagged Ag and c) Cy5-labeled Cho-CpG in draining inguinal LNs from C57BL/6 mice after 24 h vaccination. d) Flow cytometric analysis of Adpgk-specific CD8 $\alpha^+$  T cells in peripheral blood from C57BL/6 mice on day 35 after three doses of different vaccines. e) Quantitative analysis of the percentage of Adpgk-specific CD8<sup>+</sup> T cells in (d). Reproduced with permission.<sup>[90]</sup> Copyright 2016, Springer Nature.

the proportion of ALDH<sup>high</sup> CSCs in tumor tissues, thus exerting robust antitumor efficacy against various tumors harboring CSCs.

#### 4.1.3. Nucleic Acids

Nucleic acids are versatile materials useful for the fabrication of nanostructures. With well-defined architectures and specific functions, nucleic acids offer tremendous potential for use in molecular imaging, biosensing and drug delivery.<sup>[93]</sup> Tapping

on their intrinsic programmable self-assembly ability, multiple strategies such as DNA origami, DNA tile, and ss DNA/RNA origami have been adapted in the design and construction of nanomaterials.<sup>[94]</sup> Given their facile structural programmability and ideal biocompatibility, DNA/RNA nanostructures have also been utilized as an alternative approach to deliver cancer vaccine components.

Ding and co-workers engineered a bioinspired DNA-based nanodevice vaccine for enhanced cancer immunotherapy.<sup>[95]</sup> This DNA nanoplatform was generated by the precise assembly of two TLR agonist adjuvants (double-stranded RNA and CpG

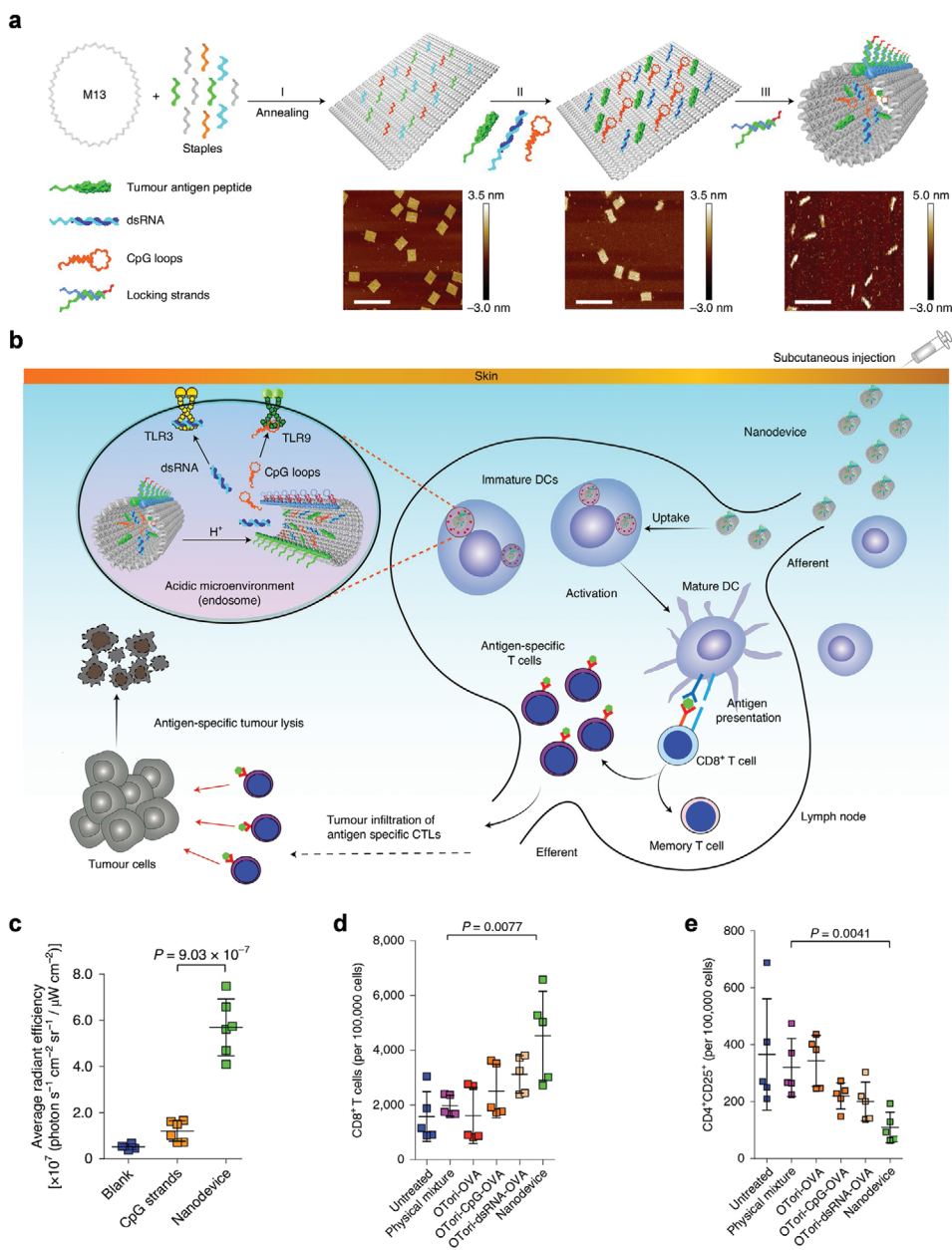


**Figure 12.** a) Schematic of the preparation and characterization of DNA nanodevice-based vaccine. A rectangular DNA origami was constructed from the assembly of an M13 bacteriophage DNA strand and staple strands, while the addition of locking strands enabled the loading of tumor Ag peptide, dsRNA and CpG loop to form Ag/adjuvant-loaded DNA nanodevice vaccine. b) Mechanism of the utilization of DNA nanodevice-based vaccine platform for potent cancer immunotherapy. c) Fluorescence quantitative analysis of Cy5-labeled CpG loops or nanodevice in inguinal dLNs after subcutaneous administration. Flow cytometric analysis of d) CD8<sup>+</sup> T cell and e) CD4<sup>+</sup>CD25<sup>+</sup> Tregs in tumors from B16-OVA tumor-bearing mice on day 14 following various treatments. Reproduced with permission.<sup>[95]</sup> Copyright 2020, Springer Nature.

DNA) and an Ag peptide within a rectangular DNA origami (Figure 12a,b). The nanodevice offered the Ag/adjuvant payload protection from extracellular ribonucleases and mediated their efficient transport to dLNs (Figure 12c). When localized inside dLN APCs, the nanodevice displayed increased delivery to APCs, and released its active payloads in response to the acidic endosomal condition, leading to DC activation and Ag presentation. Upon in vivo administration, this DNA nanodevice vaccination

increased the amount of CD8<sup>+</sup> tumor-infiltrating T lymphocytes (Figure 12d) while decreasing the amount of CD4<sup>+</sup>CD25<sup>+</sup> Tregs (Figure 12e). Some nucleic acids serve as natural ligand of specific pattern recognition receptor, which play an essential role in initiating the innate immune response. Chang and co-workers reported a replicable ss RNA origami (RNA-OG) nanostructure as potent TLR3 agonists for safe and effective cancer immunotherapy.<sup>[96]</sup> This ssRNA origami was assembled by

folding a long RNA molecule in a programmable manner and successfully stimulated a potent innate response through TLR3 pathway. After intraperitoneal injection, the RNA-OG treatment induced potent local antitumor activity without apparent systemic toxicity.

## 4.2. Cell-Inspired Systems

In natural living systems, cells can communicate with each other and respond to changes in the environment, rendering it possible to orchestrate sophisticated cell behavior such as self-recognition, migration, and recruitment of specific cells in response to chemokines. Inspired by these biological processes, considerable effort has been devoted to leverage natural mammalian cells for use as delivery platforms.<sup>[97]</sup> Synthetic delivery systems or artificial nanocarriers may cause adverse effects arising from issues of biocompatibility.<sup>[98]</sup> In contrast, cell-derived systems originate from nature, and as such display good biocompatibility and favorable safety profiles.<sup>[99]</sup> The emergence of biomimetic design has brought a paradigm shift in the design strategies of cell-derived delivery systems for cancer vaccines.<sup>[100]</sup> Cell membrane vesicles, cell membrane cloaking vesicles or extracellular vesicles have been established as delivery platforms for cancer vaccine components.

### 4.2.1. Cytomembrane Nanovesicles

Biological membranes consist of phospholipid bilayers which provide cellular protection and regulate the transport of substances entering and exiting cells. They also comprise various membrane biomolecules with functionalities such as molecular recognition, cell targeting, cellular adhesion and production of cytokines.<sup>[101]</sup> Cell membrane-derived nanovesicles can be generated by breaking down living cells into membrane-enclosed compartments. This approach has attracted much attention for vaccine delivery owing to advantages such as intrinsic tropism, presence of surface Ags and ease of genetic modification.

Kim et al. presented an immunostimulatory lipocomplex coated with cancer cell membrane (CCM) to improve liposome-based cancer therapy (Figure 13a).<sup>[102]</sup> This lipocomplex (Lp-KR-CCM-A) was formed by incorporating a photosensitizer (KillerRed, KR)-embedded CCM and a lipid adjuvant MPLA. This lipocomplex prevented undesired leakage of photosensitizer and immune adjuvant. Due to the homotypic affinity of CCM to their source cells, Lp-KR-CCM-A exhibited an outstanding in vivo tumor-targeting efficiency in homotypic 4T1-firefly luciferase (Fluc) tumor-bearing mice (Figure 13b). Upon laser irradiation, Lp-KR-CCM-A-based PDT generated cytotoxic ROS and induced ICD. Furthermore, the release of MPLA adjuvant after PDT activated DC maturation and promoted the production of CTLs (Figure 13c–e), leading to effective tumor eradication and metastasis prevention. Moreover, Moon's group reported PEGylated tumor cell membrane vesicles incorporated with cholesterol linked CpG ODNs via lipid insertion, which efficiently drained to local LNs and elicited strong CTL responses with potent antitumor efficacy.<sup>[103]</sup>

### 4.2.2. Cytomembrane-Cloaked Nanovesicles

Cell membrane-coating technology represents a biomimetic approach that integrates the merits of natural and synthetic system together.<sup>[104]</sup> These biohybrid platforms enable synthetic systems to overcome the major obstacle of being eliminated rapidly by the immune system. Cloaking NPs with cell membranes enable the NPs to inherit intrinsic biological functions of their source cells (e.g., RBCs, tumor cells and immune cells). At the same time, the synthetic core can be loaded with therapeutic cargos. In view of these advantages, a multitude of strategies based on cell membrane cloaking nanovesicles have been adopted for cancer vaccine delivery.<sup>[105]</sup>

**Cancer Cell Membranes:** Cancer cell membranes carry plenty of tumor-specific Ags. As such, using cancer cell membrane for NP preparation can be a unique biomimetic approach to fully replicate surface antigenic materials of the source cancer cells. Zhang's group first proposed and confirmed that cancer cell membrane coating on NPs can deliver both syngeneic tumor Ags, together with a potent immune adjuvant, to stimulate the immune system to recognize and eliminate cancer, providing a promising way to deliver cancer vaccine.<sup>[106]</sup>

Liu's group developed a cancer cell membrane-coated nanovaccine with mannose modification for enhanced antitumor vaccination (Figure 14a).<sup>[107]</sup> This biomimetic nanovaccine (NP-R@M-M) was constructed by PLGA NP loaded with adjuvant R837 and then coated with mannose-functionalized cancer cell membrane. Both transmission electron microscopy (TEM) and bicinchoninic acid (BCA) assay demonstrated the structural characterization of PLGA cores coated with cell membrane layer (Figure 14b,c). Due to the modification of mannose as an APC-recognition moiety, NP-R@M-M nanovaccine showed increased DC uptake and triggered stronger DC maturation (Figure 14d,e). After intradermal injection and LN retention, NP-R@M-M effectively increased the cytotoxic activity of CTL in the spleen (Figure 14f) and IFN- $\gamma$  generation in the blood (Figure 14g). Vaccination with NP-R@M-M combined with PD-L1 blockade exhibited excellent therapeutic efficacy for the treatment of established tumors. Moreover, Zhang's group designed a NP-based anticancer vaccine to deliver membrane-derived tumor Ag materials in cooperation with CpG adjuvant for cancer immunotherapy.<sup>[108]</sup> This biomimetic strategy based on cancer cell membrane-coated NP generated strong antitumor responses for enhanced personalized anticancer vaccines.

**Red Blood Cell Membranes:** RBCs have long circulation time, representing a highly desirable property for use in in vivo drug delivery nanosystems as stealth coating materials. RBC membrane-coated NPs exhibited prolonged circulation time as compared to PEGylated counterparts. As such, RBC membrane-coated NPs have been used as novel biomimetic carriers to extend drug circulation time in cancer theragnostic and antibacterial vaccines to deliver toxins to the immune system.<sup>[109]</sup> Furthermore, RBC membrane-coated NPs have also been proposed for antitumor vaccination strategies. Zhang's group developed erythrocyte membrane-enveloped PLGA NPs for the entrapment of antigenic peptide and immune adjuvant MPLA.<sup>[110]</sup> A mannose-inserted membrane structure was fabricated for APC targeting, and redox-sensitive peptide-conjugated PLGA NPs were formed for intracellular stimuli-responsive release. After

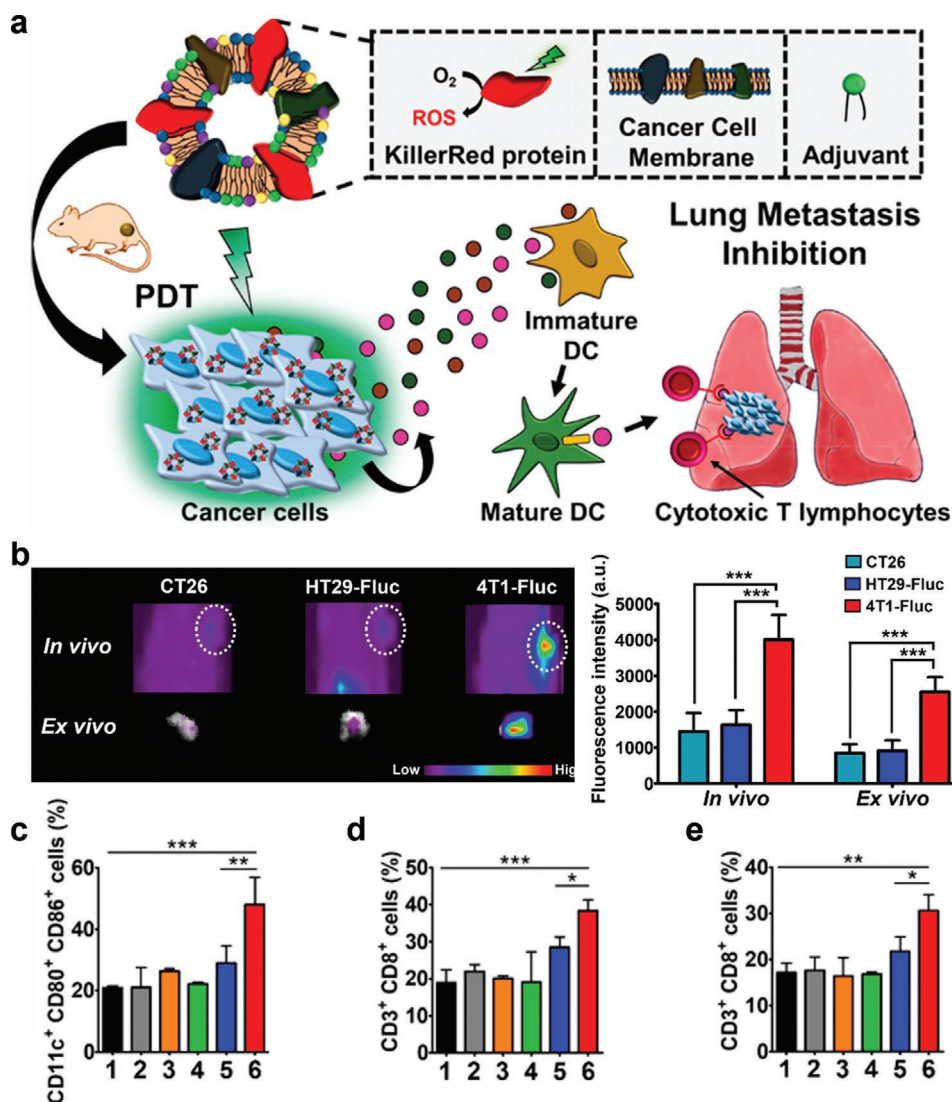


**Figure 13.** a) Scheme of immunomodulatory lipocomplexes with photosensitizer KR-embedded cancer cell membrane (KR-CCM) and MPLA adjuvant for tumor eradication and lung metastasis inhibition. b) In vivo and ex vivo fluorescence imaging and intensity qualification of CT26, HT29-Fluc, and 4T1-Fluc tumor (white dotted circles) 24 h after intravenous injection of lipocomplexes. c) Frequency of mature DC (CD80<sup>+</sup>CD86<sup>+</sup>) in the TdLNs from 4T1-Fluc tumor-bearing mice at 72 h following different treatments. Flow cytometric analysis of CD3<sup>+</sup>CD8<sup>+</sup>T cells in d) the spleen and e) the lungs at 72 h after PDT. 1, PBS + laser; 2, Lp-A (lipocomplex with adjuvant) + laser; 3, Lp-CCM-A (lipocomplex with CCM and adjuvant) + laser; 4, Lp-KR-CCM-A (lipocomplex with KR-CCM and adjuvant); 5, Lp-KR-CCM (lipocomplex with KR-CCM) + laser; 6, Lp-KR-CCM-A + laser. Reproduced with permission.<sup>[102]</sup> Copyright 2019, American Chemical Society.

intradermal injection, this nanovaccine enhanced the accumulation in dLNs and induced DC activation, enabling effective IFN- $\gamma$  and CD8<sup>+</sup> T cell responses for cancer immunotherapy.

**Hybrid Cell Membranes:** Different cell types possess their own unique intrinsic characteristics. As such, they have been exploited as sources of membrane-coating materials. Cell membrane coating technology has been extended to develop fused membrane materials from two types of cells, offering an elaborate method for NP with enhanced functionalities. Zhang and co-workers engineered a biologically derived nanovaccine (NP@FM) by encapsulating the MOF NP with cytomembranes of fused cells acquired from DCs and tumor cells.<sup>[111]</sup> NP@FM inherited the costimulatory molecules of APCs and Ag source of cancer cells for direct T cell stimulation and indirect DC-mediated T cell stimulation. By mimicking both APCs and cancer

cells, this cytomembrane vaccine approach provided powerful antitumor immune responses. Similarly, Xu et al. reported a semiconducting polymer nanoengager comprising a second-near-infrared-window absorbing polymer as the photothermal core coated with DC-tumor fusion cell membrane for synergistic photothermal immunotherapy. The co-delivery of R848 adjuvants further augmented their antitumor immunity.<sup>[112]</sup>

In addition to DC-tumor fusion cell membrane, RBCs and tumor fusion cell membrane have been utilized for vaccine delivery. Inspired by the splenic APC targeting ability of senescent RBCs, Wang and co-workers designed tumor Ag-loaded nanoerythrocytes by fusing damaged RBC membrane and tumor cell membrane to splenic APCs and activated T cell mediated immune responses for enhanced cancer immunotherapy.<sup>[113]</sup>

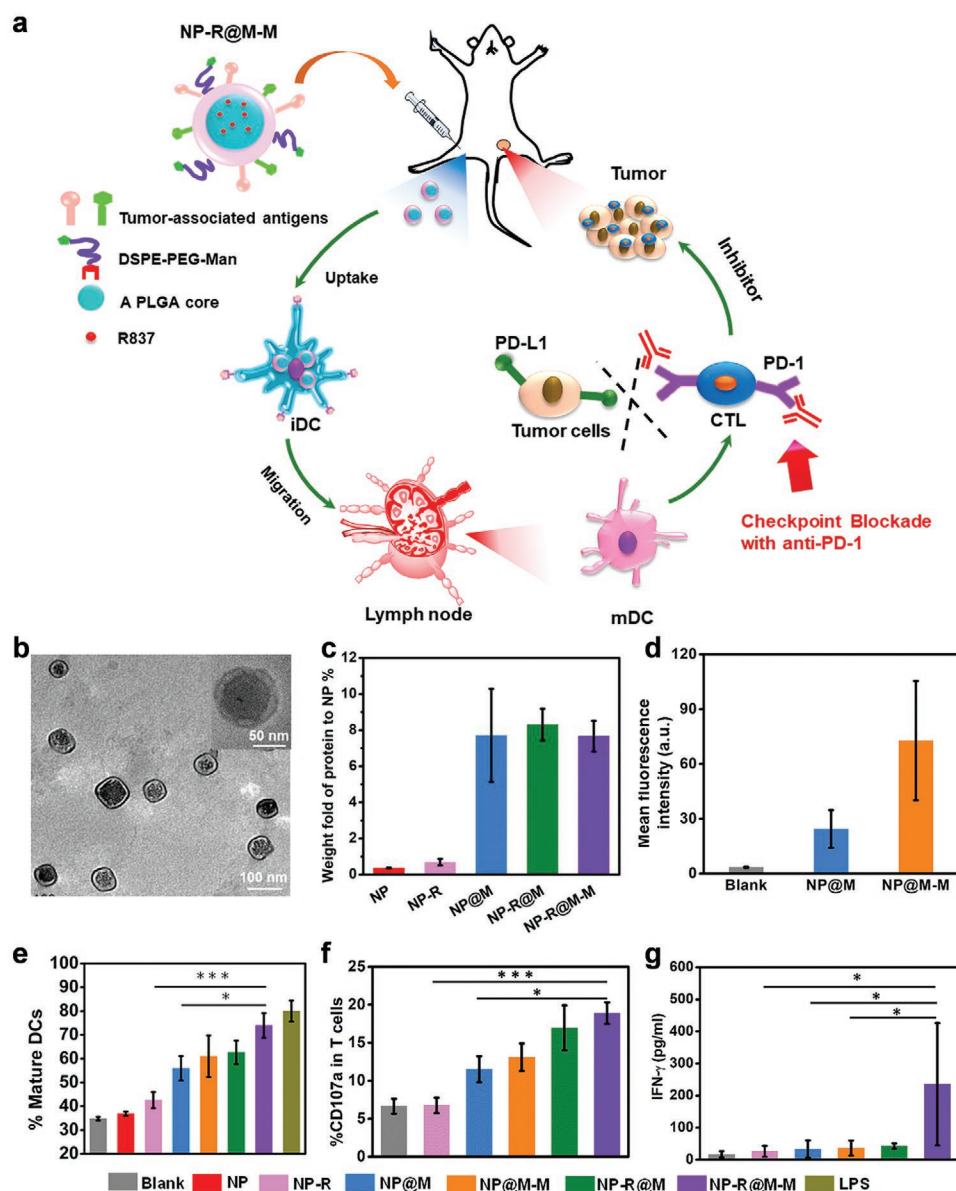


**Figure 14.** a) Schematic of the design of tumor cell membrane-coated adjuvant NPs NP-R@M-M and their functions as cancer nanovaccines to boost antitumor immunity. b) TEM imaging of NP@M NPs. c) Protein contents measured by BCA assay for PLGA NPs, NP-R (PLGA NPs loaded with R837), NP@M (PLGA NPs coated with tumor cell membrane), NP-R@M (NP-R coated with tumor cell membrane), and NP-R@M-M (NP-R@M modified with mannose moiety). d) MFI of in vitro cell uptake of nanovaccine after incubated with BMDCs for 12 h measured by flow cytometry. e) Flow cytometric analysis of in vitro DC maturation activated by different treatments. f) Flow cytometric analysis of CD107a<sup>+</sup> CTLs in spleens and g) IFN- $\gamma$  levels in sera from B16-OVA tumor-bearing mice after immunized with various treatments. Reproduced with permission.<sup>[107]</sup> Copyright 2018, American Chemical Society.

#### 4.2.3. Exosome-Inspired Nanosystems

Exosomes are naturally occurring extracellular vesicles secreted by cells. These nanosized membrane vesicles enable cellular communication by transferring a wide repertoire of bioactive cargos derived from the original cells to the recipient cells.<sup>[114]</sup> Due to their naturally biocompatible characteristics, tumor cell- and immune cell-derived exosomes have emerged as nanoscale drug delivery systems of therapeutic agents or vaccine components for cancer immunotherapy.

Kim's group developed a virus-mimetic fusogenic exosome platform to increase tumor immunogenicity via xenogenization of tumor cells for improved antitumor immunity (Figure 15a).<sup>[115]</sup> The engineered exosomes (mVSVG-Exo) were spherical-shaped nanovesicles adorned with viral fusion-mediated glycoproteins (VSV-G) on their membranes (Figure 15b,c). After intratumoral injection, these fusogenic exosomes loaded with VSV-G delivered viral pathogen-associated molecular patterns to tumor cell surface at tumor extracellular pH, facilitating enhanced Ag presentation and DC

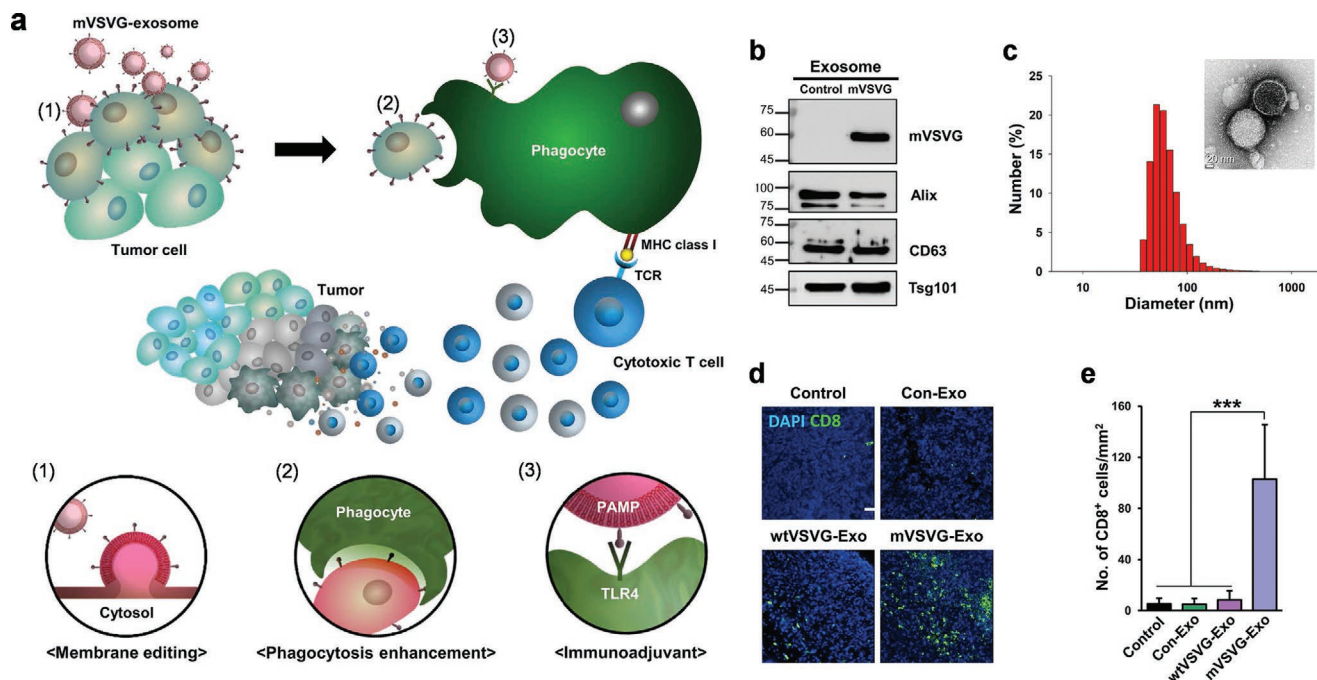


**Figure 15.** a) Mechanism of fusogenic exosome expressing VSV-G on surface (mVSVG-Exo) to mediate the xenogenization of tumor cells for boosting antitumor immunity. b) Western blot analysis of mVSVG-Exo and Con-Exo (exosomes without VSV-G expression) to determine VSV-G and exosomal markers (Alix, CD63, and Tsg101). c) Size distribution detected by dynamic light scattering and TEM imaging of mVSVG-Exo. d) Immunofluorescence imaging of CD8<sup>+</sup> T cell (green) in tumor tissues from EL4-OVA tumor-bearing mice at the end of treatments. e) The amount of CD8<sup>+</sup> T cells in the image of (d) measured by ImageJ. Scale bar = 50  $\mu$ m. Reproduced with permission.<sup>[115]</sup> Copyright 2020, The Authors, some rights reserved; exclusive licensee AAAS. Distributed under a CC BY-NC 4.0 license <http://creativecommons.org/licenses/by-nc/4.0/>.

maturation for CD8<sup>+</sup> T cell cross-priming. Immunofluorescence staining analysis of tumor tissues indicated substantially increased tumor-infiltrating CD8<sup>+</sup> T cells after mVSVG-Exo treatment (Figure 15d,e). This exosome-based tumor xenogenization provided a novel approach for enhancing tumor immunogenicity for cancer immunotherapy. Furthermore, Yin and co-workers employed DC-derived exosomes as a cell-free alternative strategy to DC vaccines for hepatocellular carcinoma (HCC) immunotherapy.<sup>[116]</sup> Exosomes derived from HCC Ag-expressing DCs reshaped the TME and induced a robust Ag-specific immune response in ectopic and orthotopic HCC tumor models.

#### 4.2.4. Bacteria-Inspired Systems

Bacteria-based vectors have emerged as drug delivery systems or are by themselves, therapeutic agents used for cancer therapy. They preferentially colonize in necrotic/hypoxic tumor areas, rendering them ideal candidates for targeted cancer therapy.<sup>[117]</sup> Bacterial membranes possess repetitive surface structure and PAMPs, which can stimulate innate immunity and improve adaptive immunity without the need for adjuvants. To further boost antitumor immunity, bacteria have been engineered via genetic or chemical modifications to deliver tumor Ags or immunomodulatory agents.

Liu's group presented a bacteria-based approach to mediate tumor-specific thrombosis for photoimmunotherapy of cancer (Figure 16a).<sup>[118]</sup> They discovered that attenuated *Salmonella*

*typhimurium* without modification or additional payload could specifically colonize tumors with reduced toxicity. After systemic administration, the tumor-homing bacteria triggered tumor thrombosis and increased the NIR absorbance for PTT. Under laser irradiation, these bacteria-triggered PTT induced DC maturation in TdLNs (Figure 16b,c). In combination with ICB, this bacteria-based therapeutic method demonstrated increased CTL/Treg ratio in tumor tissues (Figure 16d,e) and upregulation of serum TNF- $\alpha$  and IFN- $\gamma$  levels for enhanced antitumor immunity (Figure 16f,g). Thus, such tumor-homing bacteria could act as in situ cancer vaccines to boost systemic antitumor immune responses for photoimmunotherapy. Moreover, Morris and co-workers engineered a multifunctional bacterial membrane-coated NP (BNP) combined with radiotherapy for in situ cancer vaccines.<sup>[119]</sup> The BNP was comprised of an immune activating PC7A/CpG polyplex core coated with bacterial membranes and imide bonds for Ag capture. After intratumoral injection, the BNP captured cancer neoantigens following radiotherapy, enhanced DC uptake and facilitated Ag presentation to potentiate an antitumor T cell response.

#### 4.2.5. Virus-Inspired Systems

Most viruses are naturally immunogenic and can be genetically engineered to express tumor Ags. Viral platforms have gained significant interest in the development of cancer vaccines for inducing Ag-specific immune responses. The repetitive protein structure of viral capsids is capable of

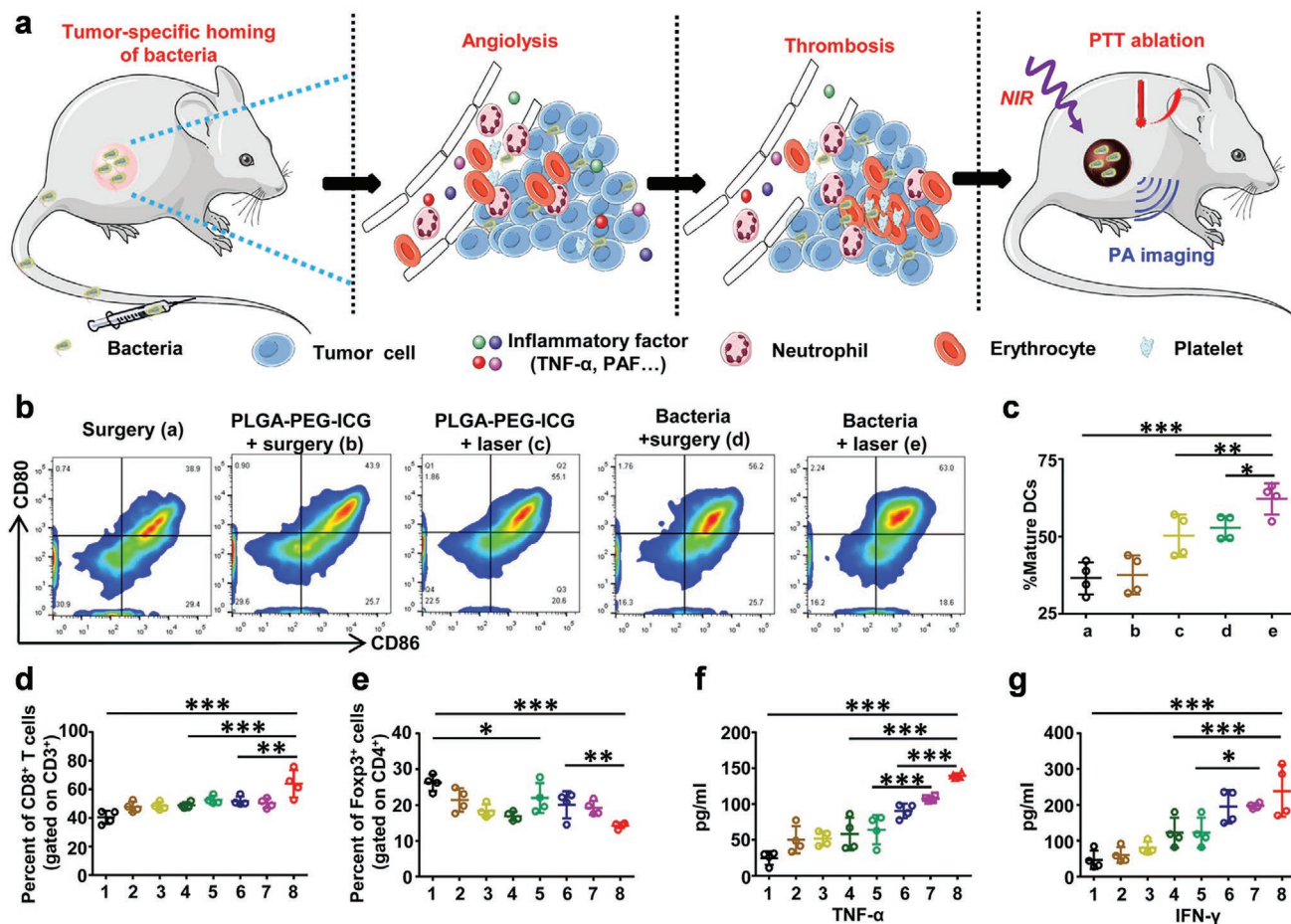


**Figure 16.** a) Scheme of bacteria-triggered tumor-specific thrombosis to mediate increased NIR absorbance for tumor ablation and photoimmunotherapy of cancer. b) Flow cytometry plots of mature DCs (CD80<sup>+</sup>CD86<sup>+</sup>) and c) the frequency of mature DCs induced by bacteria-based PTT in the TdLNs after various treatment. d) Percentages of tumor-infiltrating CD8<sup>+</sup> T cells. e) Percentages of CD4<sup>+</sup>FoxP3<sup>+</sup> Tregs in the distant CT26 tumors at day 10. Serum levels of f) TNF- $\alpha$  and g) IFN- $\gamma$  from CT26 tumor-bearing mice after various treatments at day 10. 1) Surgery. 2) Surgery + anti-CTLA-4. 3) PLGA-PEG-ICG + laser. 4) 3 + anti-CTLA-4. 5) Bacteria + surgery. 6) 5 + anti-CTLA-4. 7) Bacteria + laser, 8) 7 + anti-CTLA-4. Reproduced with permission.<sup>[118]</sup> Copyright 2020, The Authors, some rights reserved; exclusive licensee AAAS. Distributed under a CC BY-NC 4.0 license <http://creativecommons.org/licenses/by-nc/4.0/>.

self-assembly into VLPs, closely resembling the native virus. However, they are replication- and infection-incompetent due to the lack of genetic materials.<sup>[120]</sup> As a result of their envelope, both viruses and VLPs have the advantage of naturally inducing strong immune responses. In addition, oncolytic viruses can selectively replicate in and destroy tumor cells, thereby subsequently inducing systematic antitumor immune responses.

Fu and co-workers designed a viral protein nanocage to deliver Ags for combination cancer immunotherapy (Figure 17a).<sup>[121]</sup> This VLP was self-assembled by a Hepatitis B core protein nanocage (HBc NC) displaying OVA epitope with high density on its surface by genetic modification (Figure 17b,c). After subcutaneous injection, OVA-HBc NCs efficiently deposited in the dLNs (Figure 17d), facilitating DC maturation and Ag presentation for Ag-specific CTL responses. When combined with chemotherapeutic drug paclitaxel, OVA-HBc NC immunization beneficially modulated the TME by reducing Tregs and increasing the CD8<sup>+</sup> T cells with a central

memory phenotype (Figure 17e-h). In addition to Hepatitis B virus, several plant viruses also have been designed as VLPs. For example, Fiering and co-workers first reported self-assembling VLP-based NPs from cowpea mosaic virus as an in situ cancer vaccine that could specifically target and activate neutrophils in the TME to generate potent systemic antitumor immunity against poorly immunogenic tumors.<sup>[122]</sup> Moreover, Steinmetz and co-workers developed a heterologous prime-boost strategy based on three different plant virus particles to deliver the human epidermal growth factor receptor 2 (HER2) epitope for improved systemic antitumor immunity against HER2-overexpressing breast cancer.<sup>[123]</sup>

Aside from VLPs, the utilization of oncolytic virus as an immune adjuvant is an alternative vaccine strategy. Cerullo and co-workers designed an artificially cloaked viral nanovaccine by wrapping the oncolytic virus with tumor cell membranes as antigenic sources.<sup>[124]</sup> Coating the oncolytic virus with tumor cell membrane endowed it with the ability to overcome the coxsackie and adenovirus receptor-mediated uptake and afforded



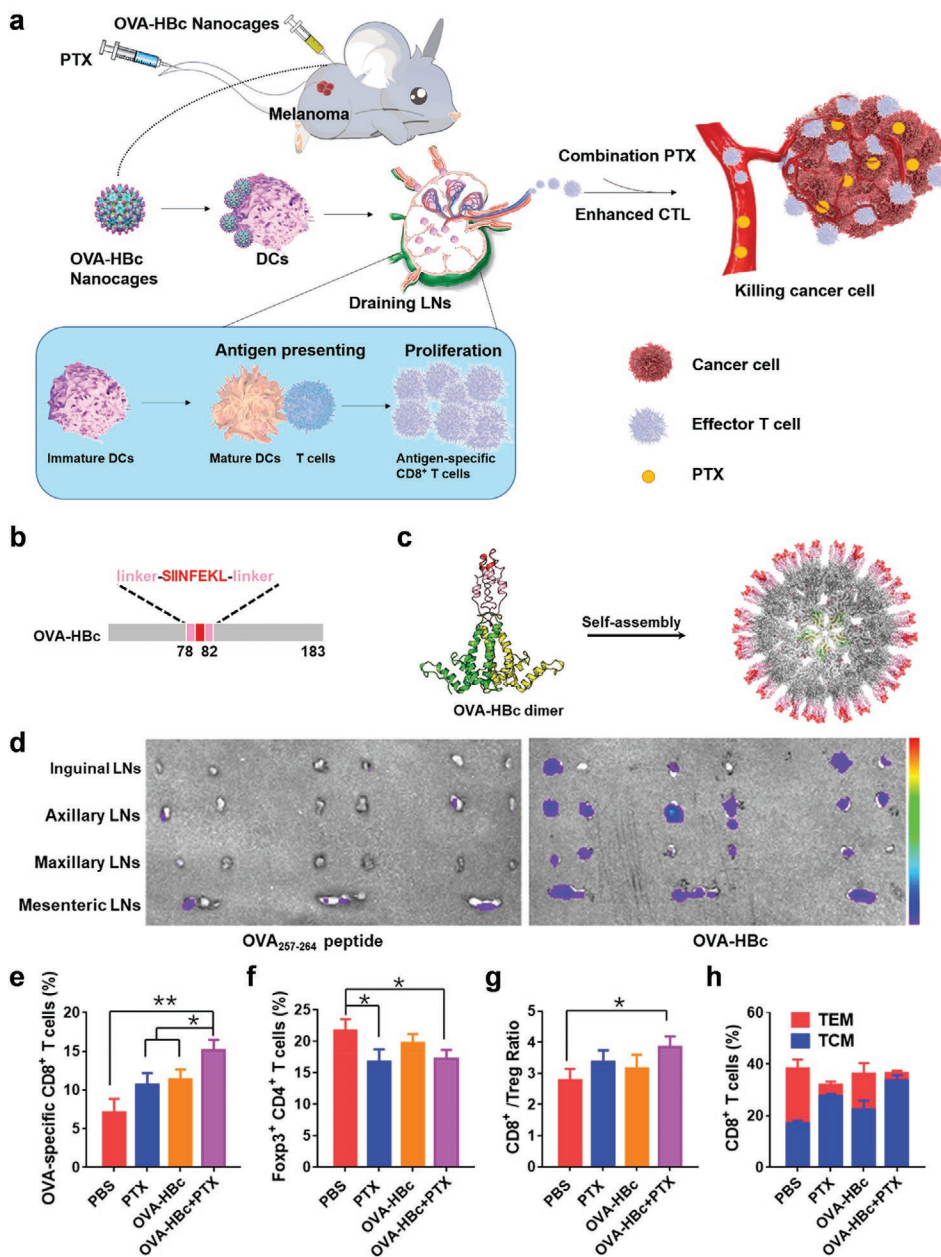


**Figure 17.** a) Schematic illustration of OVA-HBc nanocage-based vaccines to provoke efficient antitumor immunity. b) Schematic of the construction of OVA-HBc chimeric protein. c) 3D reconstruction of dimer of OVA-HBc (left) and self-assembled OVA-HBc nanocage (right). d) Near infrared imaging of Cy5.5-labeled OVA<sub>257-264</sub> peptide and OVA-HBc nanocage deposition in major LNs at 24 h following subcutaneous administration. e) Flow cytometric analysis of the proportion of OVA-specific CD8<sup>+</sup> T cells in lung, f) Foxp3<sup>+</sup> Tregs and g) the CD8<sup>+</sup>/Treg ratio in spleen, h) effector memory (TEM) and central memory (TCM) CD8<sup>+</sup> T cells in spleen at the end of antimetastasis study after various combined treatment. Reproduced with permission.<sup>[121]</sup> Copyright 2019, American Chemical Society.

protective effect from neutralizing antibodies against adenovirus. After intratumoral administration, this nanovaccine provided tumor Ags and immunostimulatory signal to DCs for highly efficient antitumor efficacy in preventive and therapeutic vaccination. This approach potentially offers an alternative application and administration route for oncolytic cancer vaccines, since viral vectors-based gene therapy are plagued by the problem of neutralizing antibodies after systemic administration.<sup>[125]</sup>

### 4.3. Biomaterial Scaffolds for Localized Vaccine Delivery

#### 4.3.1. Microspheres

Microscale carriers have dimensions mimicking that of pathogens, which the immune system has evolved to combat, and as such can be efficiently incorporated by APCs. They are generally made from biocompatible and biodegradable natural or synthetic polymers as drug delivery systems to achieve

controlled release. Owing to the slow release of Ags from the microparticles and superior uptake into APCs of the immune system, a range of microparticulates has been explored to develop ideal platforms for use in vaccine delivery.<sup>[126]</sup> Furthermore, microparticles can also be engineered with APC-like features to promote T cell expansion for enhancing active cancer immunotherapy.

Ma and co-workers engineered a self-healing microcapsule-based platform that can create favorable immunization microenvironments in situ for high-performance potent cancer vaccinations (Figure 18a).<sup>[127]</sup> Ags can be efficiently incorporated into PLA-based microcapsules in a post-diffusion manner. Following which, a mild self-healing process sealed the superficial pores, yielding Ag-loaded microcapsules. Unlike traditional pre-encapsulation methods, this approach featured only a simple mixing process and did not require Ag exposure to organic solvent, thus largely improving Ag stability and loading content. After local injection, the microcapsules accumulated at the vaccinated site. Upon degradation, sustained Ag release from the microcapsules promoted continuously increasing Ag internalization (Figure 18b). Continuous APC recruitment (Figure 18c) also occurred in a spatiotemporal synergistic manner, thereby maximizing Ag utilization. Meanwhile, lactic acid produced from the degradation of PLA-based microcapsules created a favorable acidic surrounding, promoting Ag uptake, cross-presentation, APC recruitment, and activation. Synergistic to Ag cargo release, the microcapsule ameliorated the immunosuppressive TME with increased CD8<sup>+</sup> T cells and decreased Tregs in tumor tissues (Figure 18d). Using this system, efficient Ag loading, sustained cargo released and synergistic creating of TME resulted in potent immune performance even with a single immunization dose. In their subsequent work, the use of PLA microcapsules was employed to co-encapsulate leukemia-associated epitope peptide and PD-1 antibody for anti-leukemia therapy.<sup>[128]</sup> After single administration, sustained release of epitope peptide and PD-1 antibody led to peptide uptake by the recruited APCs and the transportation of anti-PD-1 to LNs for boosting T cell-mediated antitumor immune responses to leukemia.

In another biomaterial-based immunotherapy approach, Schneck's group developed a synthetic aAPC platform to function as effective T cell stimulators.<sup>[129]</sup> The aAPC was made from a PLGA core and further functionalized by the conjugation of the stimulatory signal proteins, including MHC I-IgG fusion protein as signal 1 and anti-CD28 antibody as signal 2. PLGA-based aAPC in combination with anti-PD-1 could activate Ag-specific CD8<sup>+</sup> T cells and enhance antitumor efficacy, providing a potent combination for cancer immunotherapy. As such, biomimetic materials that target the immune system and induce an antitumor response hold great promise in boosting cancer immunotherapy. Synthetic aAPC platforms have potential advantages over cell-based systems in respect of long-term storage and the ability to modulate T cell activation and their biocompatibility.

#### 4.3.2. Implantable Macroporous Scaffolds

Implantable macroporous scaffolds are biomimetic matrices that can function as localized drug delivery systems when

embedded in living hosts, such as tumor resection bed or subcutaneous tissues.<sup>[130]</sup> Implantable biomaterial scaffolds can be made from natural or synthetic materials. Their highly porous 3D matrix facilitates the attachment of biomolecules and cell infiltration. Recently, implantable scaffold-assisted strategies are emerging in the application of localized cancer immunotherapy. These scaffold implants can be designed to create immune niches for the recruitment, homing and programming of host cells in situ by providing sustained release and presentation of Ags or immunomodulatory factors (e.g., immune adjuvant, cytokines and chemokines).<sup>[131]</sup> Immature DCs can be recruited to the implants, become mature and migrate out of the scaffold to the dLNs to initiate antitumor immune responses.

Lim and co-workers designed an implantable synthetic immune niche scaffold (iCD) containing cancer vaccines and gemcitabine (GEM) for improving postoperative immunotherapy (Figure 19a).<sup>[132]</sup> The porous 3D scaffolds were fabricated by crosslinking collagen and hyaluronic acid, which co-delivered GEM and cancer vaccines composed of whole tumor lysates and nanogel loading TLR3 agonist adjuvant. GEM served as a myeloid-derived suppressor cell (MDSC)-depleting agent that could revert the tumor-induced immune suppression, while cancer vaccines could elicit tumor Ag-specific T cell responses. Local and sustained release of GEM could therefore facilitate the local modulation of TME with minimal systemic toxicity. The implanted iCD provided sustained release of nano-adjuvants and tumor cell lysates from scaffolds (Figure 19b), enabling upregulation of costimulatory molecules on DCs (Figure 19c,d). The synergistic action between DC recruitment/activation by cancer vaccines from iCD and inhibition of immunosuppressive MDSCs by releasing GEM enhanced the proportion of CD4<sup>+</sup> and CD8<sup>+</sup> T cells, decreasing MDSC population for enhanced cancer immunotherapy (Figure 19e,f). Moreover, the use of iCD designer scaffolds was extended to co-deliver immune nanoconverters encapsulated with R848 adjuvant and DOX for in situ vaccination.<sup>[133]</sup> The iCD designer scaffold converted nonimmunogenic tumor into immunogenic phenotypes that were less responsive to ICB therapies, thereby contributing to the therapeutic efficacy of ICB treatment for the suppression of postsurgical tumor recurrence and metastasis.

Inspired by bacteria infection, Mooney's group reported infection-mimicking biomaterial-based implantable scaffolds to present inflammatory cytokines along with a danger signal to recruit and program DCs in situ.<sup>[134]</sup> This implantable synthetic matrix was based on macroporous PLGA scaffolds that were loaded with exogenous cytokines (e.g., GM-CSF, danger signals (e.g., CpG-ODN), and tumor Ags. The PLGA scaffolds could release GM-CSF into the surrounding tissue to recruit DC, and subsequently present tumor Ags and CpG ODNs to program DC development and maturation, thus improving cancer vaccination strategies. After that, they further applied this PLGA matrix to present other inflammatory cytokines including GM-CSF, Flt3L, and CCL20 as infection-mimicking vaccine scaffold to achieve DC recruitment and activation for in vivo immunotherapy.<sup>[135]</sup>

Stephan and co-workers designed another implantable porous polysaccharide scaffold that can turn the tumor bed into a self-vaccine site.<sup>[136]</sup> This biopolymer scaffold could deliver

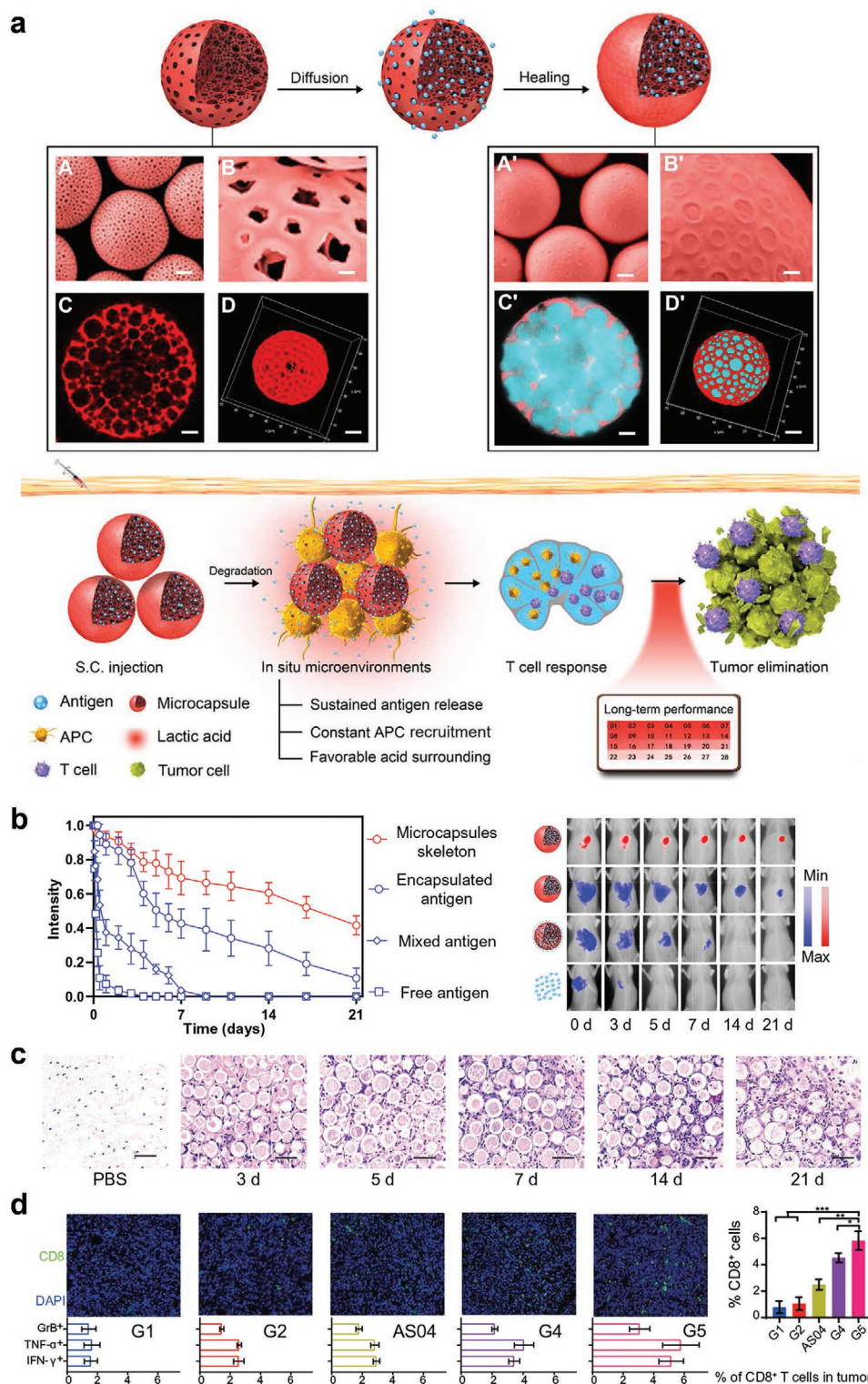


**Figure 18.** a) Schematic of the preparation and characterization of self-healing microcapsules and their functions to modulate immunization microenvironments for potent cancer vaccination. b) Quantitative analysis of fluorescence intensity (left) and relative fluorescence imaging (right) of Cy5-labeled OVA (blue)/Cy7-labeled microcapsules (red) over time. c) Hematoxylin and Eosin staining images of local tissues trapping microcapsules over 21 days. Scale bars = 50  $\mu\text{m}$ . d) Immunofluorescence imaging, corresponding portion and flow cytometric analysis of infiltrated CD8<sup>+</sup> T cells in 4T1 tumor following various treatments. G1, PBS; G2, Ag; AS04, Ag with AS04 adjuvant; G4, microcapsules encapsulated with Ag; G5, microcapsules encapsulated with Ag and MPLA. Reproduced with permission.<sup>[127]</sup> Copyright 2020, The Authors, some rights reserved; exclusive licensee AAAS. Distributed under a CC BY-NC 4.0 license <http://creativecommons.org/licenses/by-nc/4.0/>.

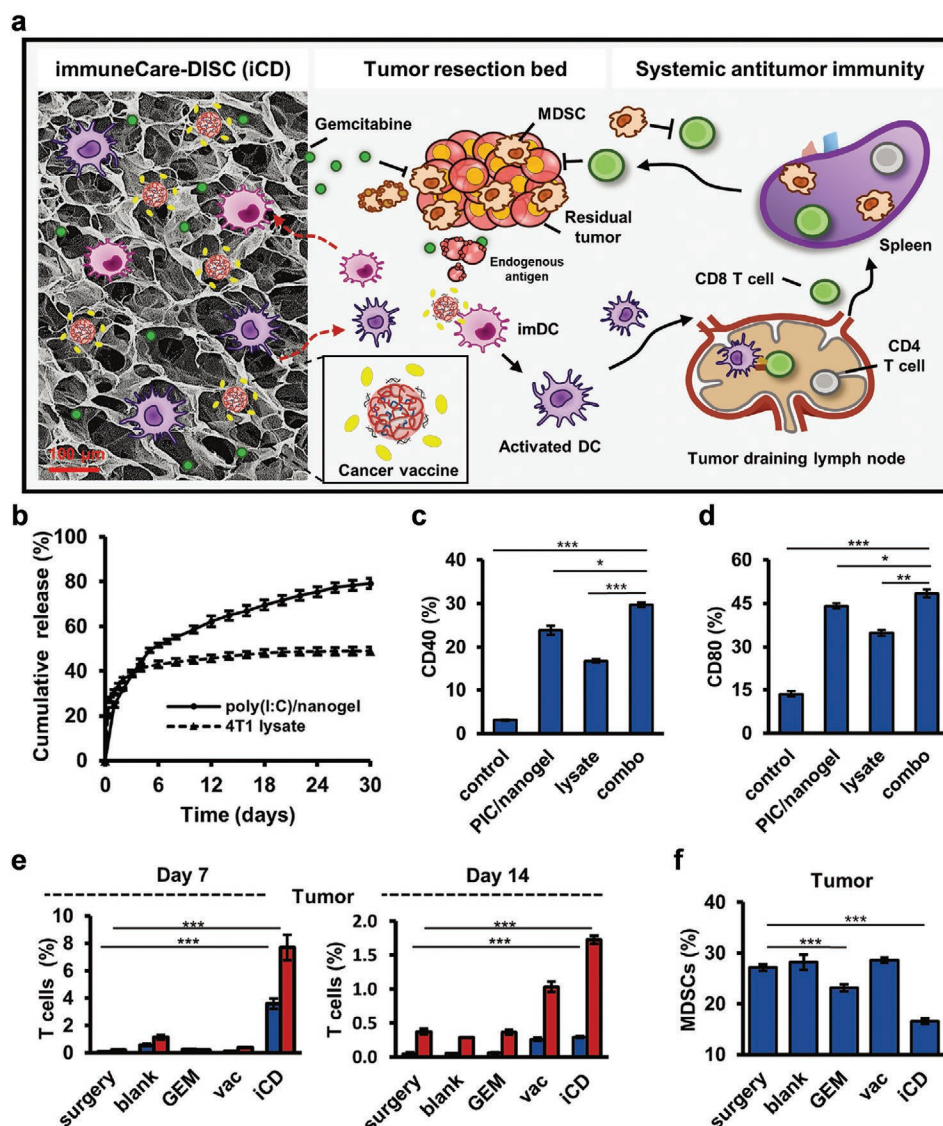


**Figure 19.** a) Schematic depicting of the design of implantable synthetic immune niche (immuneCareDISC, iCD) to modulate the tumor-induced immunosuppression and systemic antitumor immunity for postsurgical immunotherapy. b) Cumulative release profiles of poly(l:C)/nanogel and 4T1 tumor lysate from the iCD scaffold for 30 days. Flow cytometric analysis of c) CD40 and d) CD80 expression on BMDCs treated with poly(l:C)/nanogel (PIC/nanogel), lysate or the two combination (combo). Flow cytometric analysis of the proportion of e) infiltrating CD8<sup>+</sup> and CD4<sup>+</sup> T cells at day 7, 14, and f) CD11b<sup>+</sup>Gr1<sup>+</sup> MDSCs in recurrent tumor at day 7. GEM, vac or iCD indicates scaffolds loaded with gemcitabine, poly(l:C)/nanogel or the combination (combo). Reproduced with permission.<sup>[132]</sup> Copyright 2018, John Wiley and Sons.

CAR T cells directly to and support them at the tumor surface, thus presenting them with high levels of immune cells for a long period of time. CAR T cells migrated from the biopolymer scaffold and eliminated tumor cells capable of serving as Ag sources, thereby inducing tumor inhibition more effectively than systemic administration of CAR T cells. This biopolymer scaffold was also used to co-deliver synergistic combinations of CAR T cells and STING agonists to stimulate immune responses for eliminating tumor variants not recognized by the CAR T cells. Since CAR T treatments do not work well in solid tumors due to the emergence of escape variants that avoid CAR T cell targeting, as well as an immunosuppressive TME that impedes T cell, this approach can be adopted as a complement.

#### 4.3.3. Injectable Macroporous Scaffolds

In addition to implantable scaffolds, injectable scaffolds as biomimetic matrices can be administered without the need for invasive implantation. Due to their viscoelastic properties, injectable biomaterials are able to flow to fill discrete spaces and easily interface with living systems.<sup>[137]</sup> Injectable scaffolds including, MSRs, self-assembling hydrogels and cryogels, have been explored for localized cancer immunotherapy.<sup>[138]</sup> Injectable scaffolds loaded with Ags, immunomodulatory agents, or even cells, can serve as cancer vaccines to create immune priming centers for cell infiltration and immune programming in vivo.

**Injectable Hydrogels:** Injectable hydrogel is a class of in situ forming hydrogel with good fluidity compared to traditional hydrogel. Various types of natural and synthetic materials have been utilized to fabricate injectable hydrogels via physical or chemical crosslinking.<sup>[139]</sup> Injectable hydrogel has shown great potential for tissue engineering and drug delivery, owing to their large water content, similarity to extracellular matrix, porous framework for biological agents loading. In addition, they have been employed as vaccine scaffolds for modulating immune responses or delivering vaccine components for enhanced cancer immunotherapy.<sup>[140]</sup>

Inspired by naturally occurring assembly motifs in protein (e.g.,  $\alpha$ -helix and  $\beta$ -sheet), self-assembling peptide hydrogels with building blocks of amino acids have been developed as promising vaccine scaffolds. For example, Li and co-workers designed a tumor cell-derived cancer vaccine (PVAX) based on self-assembling peptide hydrogel for personalized cancer immunotherapy.<sup>[141]</sup> The vaccine was constructed from JQ1 (a bromodomain and extra-terminal protein inhibitor) for PD-L1 checkpoint blockade, and ICG co-loaded tumor cells within a hydrogel matrix containing tumor-penetrable peptide Fmoc-KCRGDK (FK) (**Figure 20a,b**). Upon NIR laser irradiation, the vaccine released tumor-specific Ags and JQ1 in a controlled manner (**Figure 20c,d**). NIR light-triggered activation of PVAX elicited efficient antitumor immunity and PD-L1 blockade for the prevention of tumor recurrence and metastasis, and established long-lasting immune memory responses for 30 days after vaccination (**Figure 20e**). Moreover, Wang and co-workers reported a vaccine nodule by encapsulating DCs and tumor Ags into a self-assembled peptide nanofibrous hydrogel to improve DC adoptive transfer immunotherapy.<sup>[142]</sup> Yang and co-workers engineered a supramolecular self-assembling hydrogel containing D-tetra-peptide formed by phosphatase as a powerful protein vaccine adjuvant to stimulate cellular and humoral immune responses against tumors.<sup>[143]</sup>

On the other hand, injectable hydrogels based on synthetic polymer also have been utilized for local delivery of vaccine contents to boost cancer immunotherapy. Appel and co-workers designed a polymer–NP hydrogel as a vaccine platform for sustained co-delivery of Ag and adjuvant to enhance the humoral immune response.<sup>[144]</sup> This supramolecular hydrogel was formed by dodecyl-modified hydroxypropylmethylcellulose combined with PEG-*b*-PLA NPs via physical crosslinking. After subcutaneous injection of the hydrogel vaccine, a local inflammatory niche was created within hydrogel to provide sustained release of vaccine cargo for immune activation. More recently, Wang and co-worker reported an injectable hydrogel constructed from polyethylenimine and graphene oxide to encapsulate mRNA and R848 adjuvant via electrostatic interaction and  $\pi$ - $\pi$  stacking.<sup>[145]</sup> This vaccine hydrogel could protect mRNA from degradation and target the LN to stimulate immune cells after injection. The sustained release of nanovaccine further elicits durable and efficient immune responses for cancer immunotherapy.

**Mesoporous Silica MicroRods:** Mesoporous silica materials hold great potential as vaccine delivery platform, due to their adjustable porosity, surface functionality, and excellent biocompatibility.<sup>[146]</sup> Mooney's group reported injectable inorganic scaffolds based on MSRs used for modulating host immune cells in

cancer vaccination.<sup>[147]</sup> Injected MSRs spontaneously assembled in situ to form macroporous structures that provided a 3D cellular microenvironment for housing large numbers of immune cells in vivo. After the incorporation of GM-CSF, CpG ODNs, and OVA proteins, the vaccine MSR scaffold could recruit substantial number of DCs to the structure. The recruitment of DCs and their subsequent homing to LNs were modulated by the sustained release of payload in MSRs. Injection of an MSR-based vaccine formulation induced T helper 1-skewed immune response with higher IgG<sub>2a</sub> serum antibody level, as well as potent CD8<sup>+</sup> CTL immune responses for enhanced antitumor efficacy. Following which, they further utilized cationic polymer polyethyleneimine to present Ags in simple adsorption manner in the MSR vaccine for enhanced Ag immunogenicity, which enabled robust cancer vaccination.<sup>[148]</sup> More recently, Kim and co-workers engineered a MSR-assisted DNA vaccine loaded with plasmid DNA-encoding tumor Ag and GM-CSF to recruit and activate host DCs for effective cancer immunotherapy.<sup>[149]</sup>

#### 4.3.4. Microneedle Patches

Microneedle patches are minimally invasive devices that contain an array of micrometer-sized needles, which enable efficient transdermal delivery of therapeutic payload across the stratum corneum barrier. They have been proposed for use in transdermal immunotherapy as they can directly transport cytokines, antibodies, or other immunomodulatory agents into the immune cell-abundant niche of the dermis layer. This strategy allows controlled release of payloads at the desired site, thereby reducing the required dose and minimizing immune-related adverse effects.<sup>[150]</sup> Furthermore, microneedle patches have recently been applied as promising vaccine platforms to present Ags and immune adjuvants for APC targeting, thus providing a safe and dose-sparing strategy for cancer immunotherapy.<sup>[151]</sup>

Gu' group developed a light-activated transdermal microneedle patch based on hyaluronic acid for enhanced anti-tumor vaccination (**Figure 21a,b**).<sup>[152]</sup> B16F10 melanoma lysate containing natural pigment melanin was encapsulated within the vaccine patch (**Figure 21c**). Upon NIR laser irradiation, melanin as a photosensitizer mediated mild hyperthermia generation to facilitate immune activation and immune cell recruitment (**Figure 21d**). When combined with GM-CSF loaded in the microneedle vaccine patch, increased localization of DCs were observed in the skin after microneedle vaccination (**Figure 21e**). In combined vaccination, microneedles were loaded with tumor lysate and GM-CSF. NIR exposure increased the activation of DC in the dLNs and tumor-infiltrating T cells for enhanced antitumor immune responses (**Figure 21f,g**), thus preventing the growth of primary and distant tumors significantly.

Furthermore, dissolvable and coated microneedle patches have also been exploited for transdermal vaccine delivery. Jeong and co-worker designed a dissolvable microneedle patch based on amphiphilic triblock copolymer for the transdermal delivery of hydrophilic Ag and hydrophobic adjuvants.<sup>[153]</sup> The vaccine patch underwent rapid dissolution in interdermal fluid and generated nanovaccines in situ with suitable size for APC

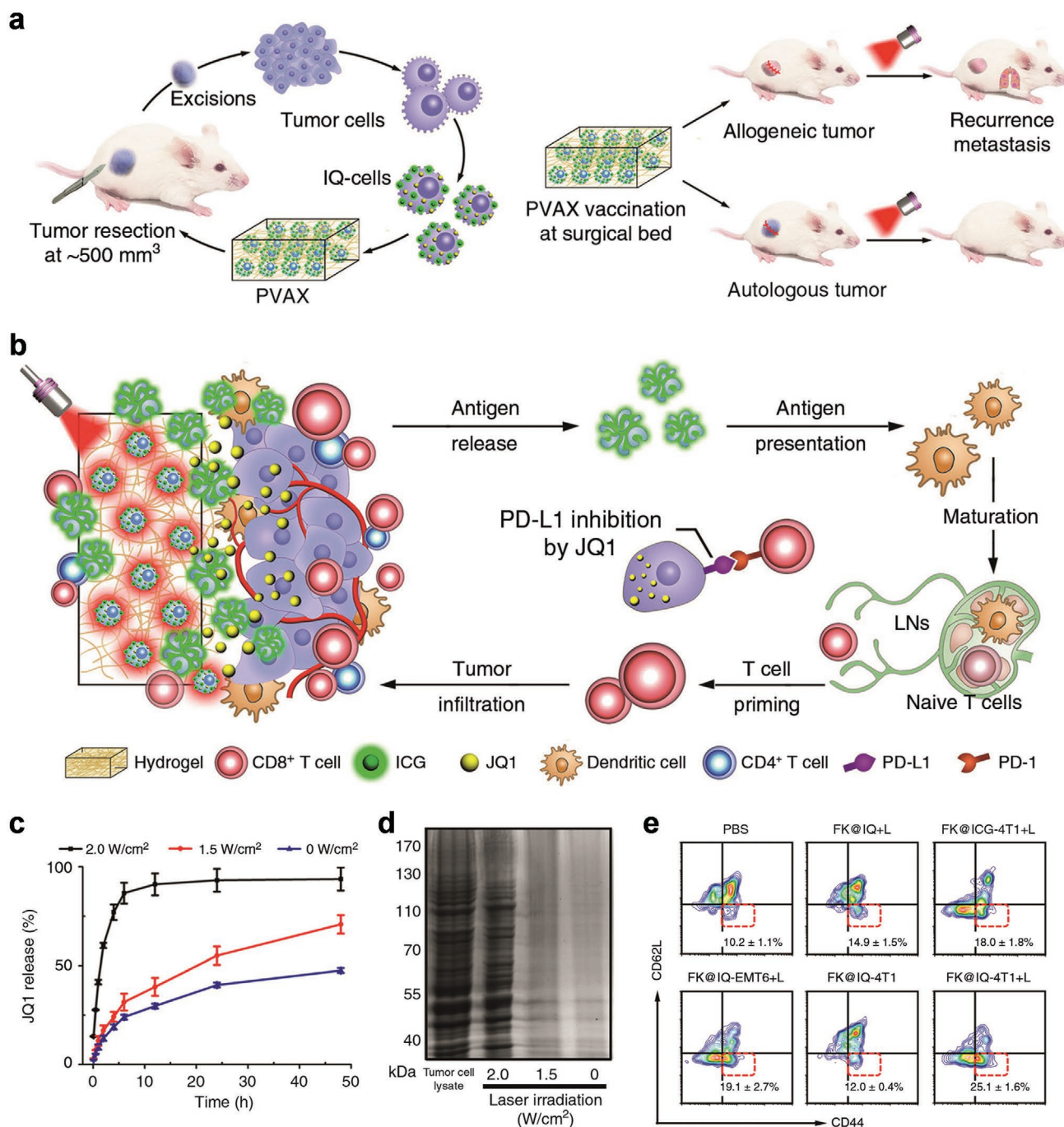


**Figure 20.** a) Scheme of preparation process of PVAX. b) Working mechanism of PVAX as personalized cancer vaccine for postsurgical immunotherapy. c) JQ1 release profile from PVAX activated by NIR light irradiation at different photodensity. d) Gel electrophoresis of NIR light-activated tumor Ag release from PVAX at different photodensity. e) Flow cytometric analysis of effector memory T cells in the spleen on the day for intravenous infusion of 4T1 cells into BALB/c mice 30 days after vaccinations. IQ-4T1 or IQ-EMT6: ICG and JQ1 co-loaded 4T1 tumor cells or EMT6 cells; FK@IQ-4T1: IQ-4T1-loaded FK hydrogels; FK@IQ-EMT6: IQ-EMT6-loaded FK hydrogels. Reproduced under terms of the CC-BY license.<sup>[141]</sup> Copyright 2018, The Authors, published by Springer Nature.

targeting, contributing to increased humoral and cellular immunity for efficient antitumor activity. Hammond and co-workers reported a coated microneedle patch based on pH-responsive charge-invertible synthetic polymer, enabling the formation of cationic NPs at acidic pH and rapid detachment of layer-by-

layer films at physiological pH after merely 1 min skin insertion time.<sup>[154]</sup> The generated layer-by-layer film rapidly transferred Ags from microneedle surface onto dermis and mediated a sustained Ag release, thus eliciting robust immune activation and humoral immunity.

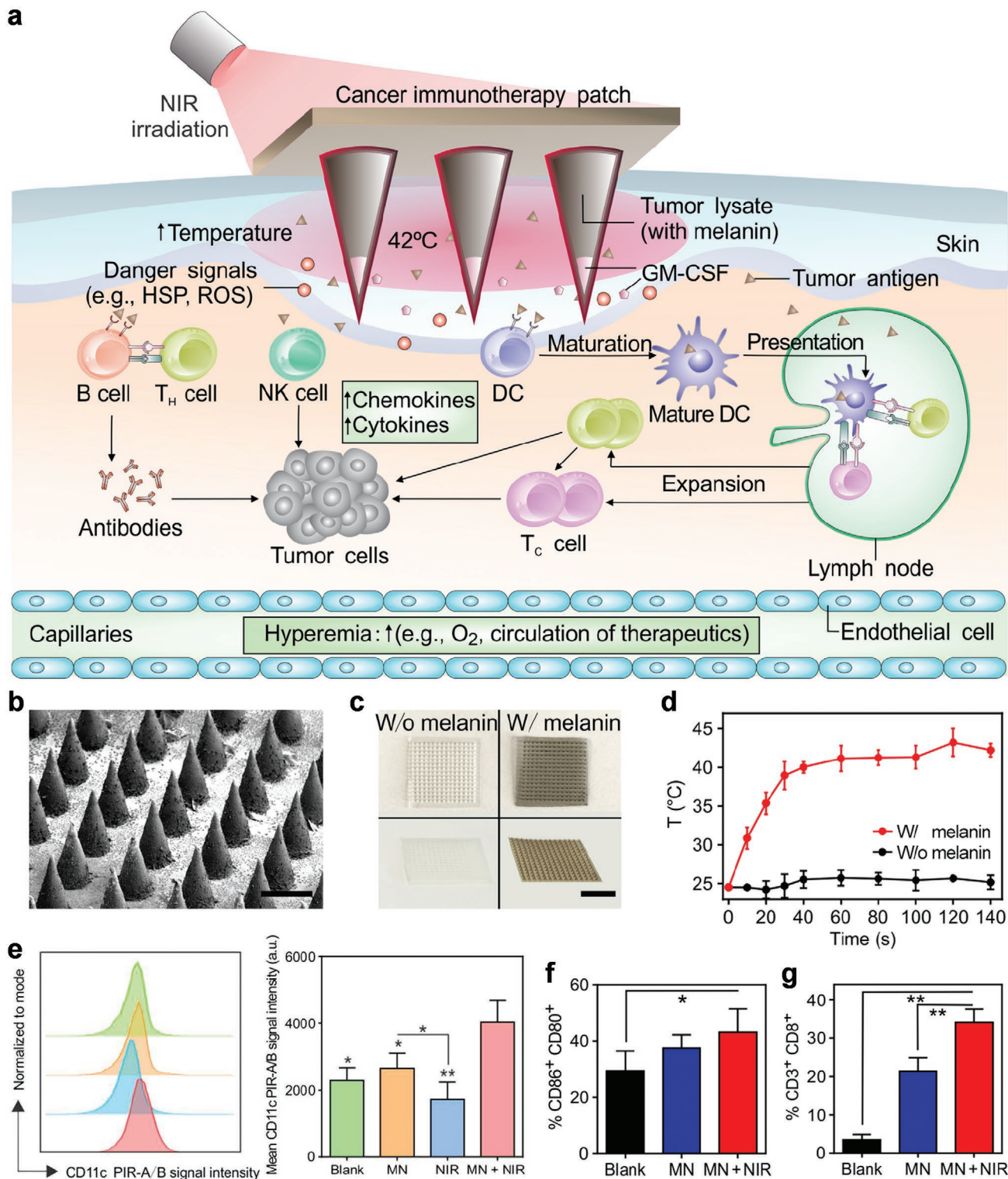


**Figure 21.** a) Schematic illustration of microneedle-based transdermal vaccination. b) Scanning electron microscopy picture of the microneedle patch. Scale bar = 400  $\mu\text{m}$ . c) Images of microneedle patches with or without melanin, scale bar = 200  $\mu\text{m}$ . d) Quantitative analysis of surface temperature of microneedle patch with constant NIR irradiation. e) Flow cytometric analysis of infiltrated DCs in the skin 3 days after various vaccinations. Quantitative analysis of f) activated DCs in the dLNs and g) CD3<sup>+</sup> T cells in vaccinated tumor tissues measured by flow cytometry 15 days after tumor inoculation. Reproduced with permission.<sup>[152]</sup> Copyright 2017, The Authors, published by American Association for the Advancement of Science.

## 5. Summary and Outlook

This review highlighted the progress of utilizing bioinspired and biomimetic strategies for designing delivery platforms in cancer vaccine development. While major roadblocks such as efficacy and safety have hindered the broad implementation of cancer vaccines, bioinspired and biomimetic delivery systems have shown to be useful in surmounting these challenges. With rapid progress and advancement in nanotechnology, biological sciences and immune engineering, a wide spectrum of bioinspired and biomimetic strategies has been adopted in the creative design of cancer vaccines delivery platforms. By looking at and learning from nature, bioinspired delivery systems can be engineered to imitate biological functions and address specific needs.

1. Drawing inspiration from the ways cells communicate with each other in the body, delivery systems responding to endogenous or exogenous stimuli have been explored for vaccine design to achieve spatiotemporal controllability and on-demand immunoactivation. Still, endogenous stimulus-sensitive delivery systems primarily suffer from a lack of well-defined and site-specific response due to tumor heterogeneity and slight differences between target sites and normal or surrounding tissues. On the other side, exogenous stimulus-sensitive delivery systems afford an active spatiotemporal control of payload release to realize more accurate and controllable release of vaccine cargos through the application of noninvasive stimuli. Of these exogenous-stimuli approaches, thermoresponsive delivery system based on mild hyperthermia appears to be a promising bioinspired vaccine delivery system, since this strategy has been investigated extensively and has advanced the closest toward clinical translation (e.g., thermoresponsive liposomal DOX, ThermoDox). Future research should integrate thermoresponsive system with magnetic resonance imaging to deliver cancer vaccine for precise tissue targeting and temperature control. However, the greatest drawback of all these stimuli-responsive systems is the limited responsiveness, especially when compared to natural processes of cell signal transduction.
2. Cell-derived systems, such as cancer cell membrane coated NP, VLPs, and bacteria-based system possess inherent immunogenicity or adjuvanticity for efficient vaccine design. Despite an increasing amount of clinical proof indicating the feasibility and therapeutic efficacy of personalized neoantigen vaccines, they still suffer from the limited prediction accuracy, complexity and high cost. An off-the-shelf alternative is to apply autologous/allogeneic whole-tumor cells or tumor lysates as antigenic materials, which possess multivalent protein Ag arrays and tumor specificity. In this light, cancer cell membrane coating nanotechnology present a novel and promising method for personalized cancer vaccines, which can employ the patient's own cancer cell as membrane sources in future. Furthermore, NP cores allow the incorporation of immune adjuvants to cancer cell membrane-wrapped nanovesicles, thereby surmounting the insufficient immunogenicity of tumor cell-derived Ags. Various challenges need to be carefully considered before moving toward clinical translation, such as simplified preparation processes, reproducible manufacturing, and the preservation of functional membrane Ags.

3. On the macroscale, 3D biomaterial scaffolds closely mimic the immune niches for DC recruitment, vaccine presentation, and TME modulation. Injectable hydrogels and microneedle patches show great potential for localized, controlled delivery of vaccine cargos at lower dosage. Compared to conventional delivery platforms, these strategies have been successful in optimizing host immune cell modulation, amplifying vaccine potency while alleviating undesirable side effects. Notably, injectable hydrogels can serve as extracellular matrix with high affinity for local tissues, cells, and body fluids. They are ideal for entrapment of proteins or nucleic acids via simple and gentle preparation processes without affecting their biological functions. In addition, rational hydrogel design responds to endogenous or exogenous stimuli and tumor-specific biomarkers to achieve more controlled release of vaccines for the management of cancer. On the other hand, microneedles are substantially practical approach for the presentation of vaccine contents as transdermal delivery in comparison to subcutaneous or intramuscular vaccinations, owing to the rich abundance of APCs inside the skin's epidermis and dermis. Up to now, a series of microneedle-based delivery systems have been explored for cosmetics and therapeutic applications in clinical settings. Microneedles offer numerous advantages over conventional administration routes, such as pain relief, reduced infection risks, possibility of self-administration, and improvement of patient compliance, thus presenting microneedles for use in cancer vaccine delivery with great translational potential.

Despite remarkable progress made in this field, the use of bioinspired and biomimetic platforms for cancer vaccine delivery remains in its nascent stages for clinical applications. Key challenges need to be overcome before translation from bench to bedside is possible. First, the ability to scale-up and manufacture at low cost is essential for clinical translation. Unlike small molecule therapeutics, the bioinspired and biomimetic strategies used for designing delivery systems tend to be sophisticated and more complex due to the incorporation of multiple functionalities. Thus, this presents a major hurdle for large scale production and ensuring batch-to-batch consistency. As such, researchers need to fine tune a balance between intricate functionalities and architectural simplicity in vaccine design and formulation. Second, despite Ag-specific immunity responses induced by TAA-based cancer vaccines, issues of limited vaccination efficacy or undesired autoimmune reactivity (against normal tissues that present the same Ag at low levels) is still prevalent. Cancer vaccines developed against neoantigens exclusively expressed by cancer cells are excellent candidates with remarkable safety and potency, but are plagued by the problem of low immunogenicity. Bioinspired delivery systems that respond to endogenous stimulus (e.g., pH, hypoxia, redox, or enzymes) can thus enable enhanced Ag cross-presentation by facilitating cytosolic delivery of neoantigens. Future work could also leverage the inherent immunogenicity of biomaterials for neoantigen-based cancer vaccination in personalized immunotherapy.<sup>[155]</sup> Clinical trials have demonstrated that various cancer vaccines induce tumor-specific T cells, however, these T cells may be insufficient to mediate substantial anti-tumor activity due to immunosuppressive mechanisms within



TME. Further work can thus be carried out to investigate synergistic effects between cancer vaccines and other types of cancer treatments, such as ICB or antiangiogenic therapies.<sup>[156]</sup>

In this review, the current technology commonly used for immune monitoring upon vaccine administration primarily focuses on multiparameter flow cytometry-based assays to measure DC activation and CLT infiltration, in order to predict outcomes for cancer treatment. These methods are invasive and static. With recent advancements made in in vivo imaging technologies to study the immune system, treatment progress and outcomes can be investigated using dynamic imaging modalities for immune responsive biomarkers, e.g., Granzyme B nanoreporters.<sup>[157]</sup> Such theranostic-based cancer immunotherapy allows for image-guided vaccine delivery and real-time monitoring of patient responses, rendering precision therapy and personalized medicine a possibility in the field of immunology. The future of bioinspired and biomimetic delivery platforms for cancer vaccines involves continuous learning and understanding of natural biological systems so as to incorporate desirable architectures and functionalities to leverage their use in addressing longstanding challenges. Given that the field is still in its infancy, many challenges will no doubt be encountered along the way. Therefore, it is essential to further push the boundaries of current research involving bioinspired and biomimetic delivery platforms for cancer vaccines, to realize their potential for clinical application as a class of cancer immunotherapeutics.

## Acknowledgements

K.P. thanks the Ministry of Education Singapore, Academic Research Fund Tier 1 (2019-T1-002-045 RG125/19 and RT05/20), Academic Research Fund Tier 2 (MOE2018-T2-2-042), A\*STAR SERC AME Programmatic Fund (SERC A18A8b0059), the National Key R&D Program of China (2017YFA0205600), the National Natural Science Foundation of China (51633008), the Science and Technology Program of Guangzhou (007306355061), Guangdong Provincial Pearl River Talents Program (2017GC010713), the China Postdoctoral Science Foundation (2019M662933), and the Natural Science Foundation of Guangdong Province, China (No. 2021A1515010592, 2019A1515011926) for the financial support.

## Conflict of Interest

The authors declare no conflict of interest.

## Keywords

biomimetic materials, cancer immunotherapy, cancer vaccines, drug delivery, nanomedicine

Received: May 18, 2021

Revised: June 30, 2021

Published online:

- [1] a) M. F. Sanmamed, L. Chen, *Cell* **2018**, 175, 313; b) S. A. Rosenberg, *J. Immunol.* **2014**, 192, 5451; c) F. S. Hodi, S. J. O'Day, D. F. McDermott, R. W. Weber, J. A. Sosman, J. B. Haanen,

- R. Gonzalez, C. Robert, D. Schadendorf, J. C. Hassel, W. Akerley, A. J. van den Eertwegh, J. Lutzky, P. Lorigan, J. M. Vaubel, G. P. Linette, D. Hogg, C. H. Ottensmeier, C. Lebbe, C. Peschel, I. Quirt, J. I. Clark, J. D. Wolchok, J. S. Weber, J. Tian, M. J. Yellin, G. M. Nichol, A. Hoos, W. J. Urbaniak, *N. Engl. J. Med.* **2010**, 363, 711.
- [2] a) I. Mellman, G. Coukos, G. Dranoff, *Nature* **2011**, 480, 480; b) J. C. Del Paggio, *Nat. Rev. Clin. Oncol.* **2018**, 15, 268; c) A. Finck, S. I. Gill, C. H. June, *Nat. Commun.* **2020**, 11, 3325.
- [3] a) A. Ribas, J. D. Wolchok, *Science* **2018**, 359, 1350; b) C. H. June, M. Sadelain, *N. Engl. J. Med.* **2018**, 379, 64; c) C. J. Melief, T. van Hall, R. Arens, F. Ossendorp, S. H. van der Burg, *J. Clin. Invest.* **2015**, 125, 3401.
- [4] a) M. Yarchoan, A. Hopkins, E. M. Jaffee, *N. Engl. J. Med.* **2017**, 377, 2500; b) S. Rafiq, C. S. Hackett, R. J. Brentjens, *Nat. Rev. Clin. Oncol.* **2020**, 17, 147.
- [5] a) P. C. Tume, C. L. Harview, J. H. Yearley, I. P. Shintaku, E. J. Taylor, L. Robert, B. Chmielowski, M. Spasic, G. Henry, V. Ciobanu, A. N. West, M. Carmona, C. Kivork, E. Seja, G. Cherry, A. J. Gutierrez, T. R. Grogan, C. Mateus, G. Tomicic, J. A. Glaspy, R. O. Emerson, H. Robins, R. H. Pierce, D. A. Elashoff, C. Robert, A. Ribas, *Nature* **2014**, 515, 568; b) P. Sharma, S. Hu-Lieskova, J. A. Wargo, A. Ribas, *Cell* **2017**, 168, 707.
- [6] M. Nishino, N. H. Ramaiya, H. Hatabu, F. S. Hodi, *Nat. Rev. Clin. Oncol.* **2017**, 14, 655.
- [7] a) J. H. Park, I. Riviere, M. Gonen, X. Wang, B. Senechal, K. J. Curran, C. Sauter, Y. Wang, B. Santomasso, E. Mead, M. Roshal, P. Maslak, M. Davila, R. J. Brentjens, M. Sadelain, *N. Engl. J. Med.* **2018**, 378, 449; b) S. J. Schuster, J. Svoboda, E. A. Chong, S. D. Nasta, A. R. Mato, O. Anak, J. L. Brogdon, I. Pruteanu-Malinici, V. Bhoj, D. Landsburg, M. Wasik, B. L. Levine, S. F. Lacey, J. J. Melenhorst, D. L. Porter, C. H. June, *N. Engl. J. Med.* **2017**, 377, 2545; c) Y. Leyfman, *Cancer Cell Int.* **2018**, 18, 182; d) M. M. D'Aloia, I. G. Zizzari, B. Sacchetti, L. Pierelli, M. Alimandi, *Cell Death Dis.* **2018**, 9, 282.
- [8] S. S. Neelapu, S. Tummala, P. Kebriaei, W. Wierda, C. Gutierrez, F. L. Locke, K. V. Komanduri, Y. Lin, N. Jain, N. Daver, J. Westin, A. M. Gulbis, M. E. Loghin, J. F. de Groot, S. Adkins, S. E. Davis, K. Rezvani, P. Hwu, E. J. Shpall, *Nat. Rev. Clin. Oncol.* **2018**, 15, 47.
- [9] a) N. van Rooij, M. M. van Buuren, D. Philips, A. Velds, M. Toebes, B. Heemskerk, L. J. van Dijk, S. Behjati, H. Hilkmann, D. El Atmioui, M. Nieuwland, M. R. Stratton, R. M. Kerkhoven, C. Kesmir, J. B. Haanen, P. Kvistborg, T. N. Schumacher, *J. Clin. Oncol.* **2013**, 31, e439; b) A. Snyder, V. Makarov, T. Merghoub, J. Yuan, J. M. Zaretsky, A. Desrichard, L. A. Walsh, M. A. Postow, P. Wong, T. S. Ho, T. J. Hollmann, C. Bruggeman, K. Kannan, Y. Li, C. Elipenahli, C. Liu, C. T. Harbison, L. Wang, A. Ribas, J. D. Wolchok, T. A. Chan, *N. Engl. J. Med.* **2014**, 371, 2189.
- [10] J. Banchereau, K. Palucka, *Nat. Rev. Clin. Oncol.* **2018**, 15, 9.
- [11] a) C. Nabhan, *N. Engl. J. Med.* **2010**, 363, 1966; b) R. M. Conry, B. Westbrook, S. McKee, T. G. Norwood, *Hum. Vaccines Immunother.* **2018**, 14, 839.
- [12] a) J. Fu, D. B. Kanne, M. Leong, L. H. Glickman, S. M. McWhirter, E. Lemmens, K. Mechette, J. J. Leong, P. Lauer, W. Liu, K. E. Sivick, Q. Zeng, K. C. Soares, L. Zheng, D. A. Portnoy, J. J. Woodward, D. M. Pardoll, T. W. Dubensky, Y. Kim, *Sci. Transl. Med.* **2015**, 7, 283ra52; b) Y. H. Huang, J. P. Yuan, E. Righi, W. S. Kamoun, M. Ancukiewicz, J. Nezivar, M. Santosuosso, J. D. Martin, M. R. Martin, F. Vianello, P. Leblanc, L. L. Munn, P. Huang, D. G. Duda, D. Fukumura, R. K. Jain, M. C. Poznansky, *Proc. Natl. Acad. Sci. USA* **2012**, 109, 17561.
- [13] R. E. Hollingsworth, K. Jansen, *npj Vaccines* **2019**, 4, 7.
- [14] a) O. J. Finn, *Nat. Rev. Immunol.* **2003**, 3, 630; b) G. Zhu, F. Zhang, Q. Ni, G. Niu, X. Chen, *ACS Nano* **2017**, 11, 2387; c) W. H. Li, Y. M. Li, *Chem. Rev.* **2020**, 120, 11420.

- [15] a) Z. Hu, P. A. Ott, C. J. Wu, *Nat. Rev. Immunol.* **2018**, *18*, 168; b) J. Jou, K. J. Harrington, M. B. Zocca, E. Ehrnrooth, E. E. W. Cohen, *Clin. Cancer Res.* **2021**, *27*, 689.
- [16] T. F. Gajewski, H. Schreiber, Y. X. Fu, *Nat. Immunol.* **2013**, *14*, 1014.
- [17] a) C. W. t. Shields, L. L. Wang, M. A. Evans, S. Mitragotri, *Adv. Mater.* **2020**, *32*, 1901633; b) R. Zhang, M. M. Billingsley, M. J. Mitchell, *J. Controlled Release* **2018**, *292*, 256.
- [18] a) R. S. Riley, C. H. June, R. Langer, M. J. Mitchell, *Nat. Rev. Drug Discovery* **2019**, *18*, 175; b) C. Zhang, K. Pu, *Chem. Soc. Rev.* **2020**, *49*, 4234.
- [19] a) Y. Bar-Cohen, *Bioinspir. Biomim.* **2006**, *1*, P1; b) B. Bhushan, *Philos. Trans. R. Soc., A* **2009**, *367*, 1445; c) U. G. Wegst, H. Bai, E. Saiz, A. P. Tomsia, R. O. Ritchie, *Nat. Mater.* **2015**, *14*, 23.
- [20] a) J. W. Yoo, D. J. Irvine, D. E. Discher, S. Mitragotri, *Nat. Rev. Drug Discovery* **2011**, *10*, 521; b) R. A. Meyer, J. C. Sunshine, J. J. Green, *Trends Biotechnol.* **2015**, *33*, 514.
- [21] Y. Xia, T. Song, Y. Hu, G. Ma, *Acc. Chem. Res.* **2020**, *53*, 2068.
- [22] R. S. Tu, M. Tirrell, *Adv. Drug Delivery Rev.* **2004**, *56*, 1537.
- [23] C. Mukai, L. Gao, J. L. Nelson, J. P. Lata, R. Cohen, L. Wu, M. M. Hinchman, M. Bergkvist, R. W. Sherwood, S. Zhang, A. J. Travis, *Angew. Chem., Int. Ed. Engl.* **2017**, *56*, 235.
- [24] S. C. Balmert, S. R. Little, *Adv. Mater.* **2012**, *24*, 3757.
- [25] a) D. E. Discher, A. Eisenberg, *Science* **2002**, *297*, 967; b) P. Schwille, J. Spatz, K. Landfester, E. Bodenschatz, S. Herminghaus, V. Sourjik, T. J. Erb, P. Bastiaens, R. Lipowsky, A. Hyman, P. Dabrock, J. C. Baret, T. Vidakovic-Koch, P. Bieling, R. Dimova, H. Mutschler, T. Robinson, T. D. Tang, S. Wegner, K. Sundmacher, *Angew. Chem., Int. Ed. Engl.* **2018**, *57*, 13382; c) B. S. Kim, D. J. Mooney, *Trends Biotechnol.* **1998**, *16*, 224.
- [26] F. Lussier, O. Staufer, I. Platzman, J. P. Spatz, *Trends Biotechnol.* **2020**, *S0167-7799*, 30210.
- [27] A. B. Cook, P. Decuzzi, *ACS Nano* **2021**, *15*, 2068.
- [28] Z. Chen, Z. Wang, Z. Gu, *Acc. Chem. Res.* **2019**, *52*, 1531.
- [29] G. F. Luo, W. H. Chen, X. Zeng, X. Z. Zhang, *Chem. Soc. Rev.* **2021**, *50*, 945.
- [30] D. Hanahan, R. A. Weinberg, *Cell* **2011**, *144*, 646.
- [31] Y. Zhang, X. Han, G. Nie, *Nat. Protoc.* **2021**, *16*, 405.
- [32] M. Karimi, A. Ghasemi, P. Sahandi Zangabad, R. Rahighi, S. M. Moosavi Basri, H. Mirshekari, M. Amiri, Z. Shafaei Pishabad, A. Aslani, M. Bozorgomid, D. Ghosh, A. Beyzavi, A. Vaseghi, A. R. Aref, L. Haghani, S. Bahrami, M. R. Hamblin, *Chem. Soc. Rev.* **2016**, *45*, 1457.
- [33] J. W. Ivey, M. Bonakdar, A. Kanitkar, R. V. Davalos, S. S. Verbridge, *Cancer Lett.* **2016**, *380*, 330.
- [34] L. E. Gerweck, K. Seetharaman, *Cancer Res.* **1996**, *56*, 1194.
- [35] K. M. Holmstrom, T. Finkel, *Nat. Rev. Mol. Cell Biol.* **2014**, *15*, 411.
- [36] C. Wang, T. Zhao, Y. Li, G. Huang, M. A. White, J. Gao, *Adv. Drug Delivery Rev.* **2017**, *113*, 87.
- [37] a) I. F. Tannock, D. Rotin, *Cancer Res.* **1989**, *49*, 4373; b) Y. Kato, S. Ozawa, C. Miyamoto, Y. Maehata, A. Suzuki, T. Maeda, Y. Baba, *Cancer Cell Int.* **2013**, *13*, 89.
- [38] Y. Yan, H. Ding, *Nanomaterials* **2020**, *10*, 1613.
- [39] A. Rodriguez, A. Regnault, M. Kleijmeer, P. Ricciardi-Castagnoli, S. Amigorena, *Nat. Cell Biol.* **1999**, *1*, 362.
- [40] L. Zhou, B. Hou, D. Wang, F. Sun, R. Song, Q. Shao, H. Wang, H. Yu, Y. Li, *Nano Lett.* **2020**, *20*, 4393.
- [41] J. Liu, H. J. Li, Y. L. Luo, Y. F. Chen, Y. N. Fan, J. Z. Du, J. Wang, *Nano Lett.* **2020**, *20*, 4882.
- [42] M. Luo, H. Wang, Z. Wang, H. Cai, Z. Lu, Y. Li, M. Du, G. Huang, C. Wang, X. Chen, M. R. Porembka, J. Lea, A. E. Frankel, Y. X. Fu, Z. J. Chen, J. Gao, *Nat. Nanotechnol.* **2017**, *12*, 648.
- [43] D. Shae, K. W. Becker, P. Christov, D. S. Yun, A. K. R. Lytton-Jean, S. Sevimli, M. Ascano, M. Kelley, D. B. Johnson, J. M. Balko, J. T. Wilson, *Nat. Nanotechnol.* **2019**, *14*, 269.
- [44] W. Xiao, J. Loscalzo, *Antioxid. Redox Signaling* **2020**, *32*, 1330.
- [45] P. Kuppasamy, H. Li, G. Ilangoan, A. J. Cardounel, J. L. Zweier, K. Yamada, M. C. Krishna, J. B. Mitchell, *Cancer Res.* **2002**, *62*, 307.
- [46] L. Wei, Y. Zhao, X. Hu, L. Tang, *ACS Cent. Sci.* **2020**, *6*, 404.
- [47] C. Xu, J. Nam, H. Hong, Y. Xu, J. J. Moon, *ACS Nano* **2019**, *13*, 12148.
- [48] A. J. Majmundar, W. J. Wong, M. C. Simon, *Mol. Cell* **2010**, *40*, 294.
- [49] T. Thambi, J. H. Park, D. S. Lee, *Chem. Commun.* **2016**, *52*, 8492.
- [50] S. Im, J. Lee, D. Park, A. Park, Y. M. Kim, W. J. Kim, *ACS Nano* **2019**, *13*, 476.
- [51] M. A. Khan, H. Zubair, S. Anand, S. K. Srivastava, S. Singh, A. P. Singh, *Cancer Lett.* **2020**, *473*, 176.
- [52] a) J. Hu, G. Zhang, S. Liu, *Chem. Soc. Rev.* **2012**, *41*, 5933; b) A. C. Clark, *Chem. Rev.* **2016**, *116*, 6666.
- [53] S. R. Bonam, F. J. Wang, S. Muller, *Nat. Rev. Drug Discovery* **2019**, *18*, 923.
- [54] J. J. Moon, H. Suh, A. Bershteyn, M. T. Stephan, H. Liu, B. Huang, M. Sohail, S. Luo, S. H. Um, H. Khant, J. T. Goodwin, J. Ramos, W. Chiu, D. J. Irvine, *Nat. Mater.* **2011**, *10*, 243.
- [55] B. Wang, S. Van Herck, Y. Chen, X. Bai, Z. Zhong, K. Deswarte, B. N. Lambrecht, N. N. Sanders, S. Lienenklaus, H. W. Scheeren, S. A. David, F. Kiessling, T. Lammers, B. G. De Geest, Y. Shi, *J. Am. Chem. Soc.* **2020**, *142*, 12133.
- [56] D. E. J. G. J. Dolmans, D. Fukumura, R. K. Jain, *Nat. Rev. Cancer* **2003**, *3*, 380.
- [57] J. F. Gohy, Y. Zhao, *Chem. Soc. Rev.* **2013**, *42*, 7117.
- [58] Y. Zhang, C. Xu, X. L. Yang, K. Y. Pu, *Adv. Mater.* **2020**, *32*, 2002661.
- [59] A. Y. Rwei, W. Wang, D. S. Kohane, *Nano Today* **2015**, *10*, 451.
- [60] C. W. Ng, J. C. Li, K. Y. Pu, *Adv. Funct. Mater.* **2018**, *28*, 1870327.
- [61] a) C. Bruno, Y. Waeckerle-Men, M. Hakerud, T. M. Kundig, B. Gander, P. Johansen, *J. Immunol.* **2015**, *195*, 166; b) P. Schineis, Z. K. Kotkowska, S. Vogel-Kindgen, M. C. Friess, M. Theisen, D. Schwyter, L. Hausammann, S. Subedi, E. M. Varypataki, Y. Waeckerle-Men, I. Kolm, T. M. Kundig, A. Hogset, B. Gander, C. Halin, P. Johansen, *J. Controlled Release* **2021**, *332*, 96.
- [62] a) D. V. Krysko, A. D. Garg, A. Kaczmarek, O. Krysko, P. Agostinis, P. Vandenabeele, *Nat. Rev. Cancer* **2012**, *12*, 860; b) J. C. Li, Y. Luo, K. Y. Pu, *Angew. Chem., Int. Ed.* **2021**, *60*, 2.
- [63] H. Chu, J. Zhao, Y. Mi, Z. Di, L. Li, *Nat. Commun.* **2019**, *10*, 2839.
- [64] J. Li, D. Cui, J. Huang, S. He, Z. Yang, Y. Zhang, Y. Luo, K. Pu, *Angew. Chem., Int. Ed. Engl.* **2019**, *58*, 12680.
- [65] M. M. Paulides, H. Dobsicek Trefna, S. Curto, D. B. Rodrigues, *Adv. Drug Delivery Rev.* **2020**, *163–164*, 3.
- [66] A. L. B. Seynhaeve, M. Amin, D. Haemmerich, G. C. van Rhoon, T. L. M. Ten Hagen, *Adv. Drug Delivery Rev.* **2020**, *163–164*, 125.
- [67] a) M. B. Yatvin, J. N. Weinstein, W. H. Dennis, R. Blumenthal, *Science* **1978**, *202*, 1290; b) L. Li, T. L. M. ten Hagen, M. Hossann, R. Suss, G. C. van Rhoon, A. M. M. Eggermont, D. Haemmerich, G. A. Koning, *J. Controlled Release* **2013**, *168*, 142.
- [68] Y. Y. Jjiang, J. G. Huang, C. Xu, K. Y. Pu, *Nat. Commun.* **2021**, *12*, 742.
- [69] J. Li, X. Yu, Y. Jjiang, S. He, Y. Zhang, Y. Luo, K. Pu, *Adv. Mater.* **2021**, *33*, 2003458.
- [70] R. Baskar, K. A. Lee, R. Yeo, K. W. Yeoh, *Int. J. Med. Sci.* **2012**, *9*, 193.
- [71] a) L. Apetoh, F. Ghiringhelli, A. Tesniere, M. Obeid, C. Ortiz, A. Criollo, G. Mignot, M. C. Maiuri, E. Ullrich, P. Saulnier, H. Yang, S. Amigorena, B. Ryffel, F. J. Barrat, P. Saftig, F. Levi, R. Lidereau, C. Nogues, J. P. Mira, A. Chompret, V. Joulin, F. Clavel-Chapelon, J. Bourhis, F. Andre, S. Delaloge, T. Tursz, G. Kroemer, L. Zitvogel, *Nat. Med.* **2007**, *13*, 1050; b) M. Z. Dewan, A. E. Galloway, N. Kawashima, J. K. Dewyngaert, J. S. Babb, S. C. Formenti, S. Demaria, *Clin. Cancer Res.* **2009**, *15*, 5379; c) A. A. Lugade, J. P. Moran, S. A. Gerber, R. C. Rose, J. G. Frelinger, E. M. Lord, *J. Immunol.* **2005**, *174*, 7516.
- [72] Q. Chen, J. Chen, Z. Yang, J. Xu, L. Xu, C. Liang, X. Han, Z. Liu, *Adv. Mater.* **2019**, *31*, 1802228.

- [73] K. Ni, G. Lan, C. Chan, B. Quigley, K. Lu, T. Aung, N. Guo, P. La Riviere, R. R. Weichselbaum, W. Lin, *Nat. Commun.* **2018**, *9*, 2351.
- [74] P. Huang, X. Qian, Y. Chen, L. Yu, H. Lin, L. Wang, Y. Zhu, J. Shi, *J. Am. Chem. Soc.* **2017**, *139*, 1275.
- [75] Q. Zhang, C. Bao, X. Cai, L. Jin, L. Sun, Y. Lang, L. Li, *Cancer Sci.* **2018**, *109*, 1330.
- [76] W. Yue, L. Chen, L. Yu, B. Zhou, H. Yin, W. Ren, C. Liu, L. Guo, Y. Zhang, L. Sun, K. Zhang, H. Xu, Y. Chen, *Nat. Commun.* **2019**, *10*, 2025.
- [77] A. Harari, M. Graciotti, M. Bassani-Sternberg, L. E. Kandalaf, *Nat. Rev. Drug Discovery* **2020**, *19*, 635.
- [78] Y. Min, K. C. Roche, S. Tian, M. J. Eblan, K. P. McKinnon, J. M. Caster, S. Chai, L. E. Herring, L. Zhang, T. Zhang, J. M. DeSimone, J. E. Tepper, B. G. Vincent, J. S. Serody, A. Z. Wang, *Nat. Nanotechnol.* **2017**, *12*, 877.
- [79] M. Wang, J. Song, F. Zhou, A. R. Hoover, C. Murray, B. Zhou, L. Wang, J. Qu, W. R. Chen, *Adv. Sci.* **2019**, *6*, 1802157.
- [80] L. J. Eggermont, L. E. Paulis, J. Tel, C. G. Figdor, *Trends Biotechnol.* **2014**, *32*, 456.
- [81] J. W. Hickey, F. P. Vicente, G. P. Howard, H. Q. Mao, J. P. Schneck, *Nano Lett.* **2017**, *17*, 7045.
- [82] A. K. Kosmides, K. Necochea, J. W. Hickey, J. P. Schneck, *Nano Lett.* **2018**, *18*, 1916.
- [83] a) A. Sparreboom, C. D. Scripture, V. Trieu, P. J. Williams, T. De, A. Yang, B. Beals, W. D. Figg, M. Hawkins, N. Desai, *Clin. Cancer Res.* **2005**, *11*, 4136; b) P. Ma, R. J. Mumper, *J. Nanomed. Nanotechnol.* **2013**, *4*, 1000164.
- [84] F. Kratz, *J. Controlled Release* **2008**, *132*, 171.
- [85] F. F. An, X. H. Zhang, *Theranostics* **2017**, *7*, 3667.
- [86] G. Zhu, G. M. Lynn, O. Jacobson, K. Chen, Y. Liu, H. Zhang, Y. Ma, F. Zhang, R. Tian, Q. Ni, S. Cheng, Z. Wang, N. Lu, B. C. Yung, Z. Wang, L. Lang, X. Fu, A. Jin, I. D. Weiss, H. Vishwasrao, G. Niu, H. Shroff, D. M. Klinman, R. A. Seder, X. Chen, *Nat. Commun.* **2017**, *8*, 1954.
- [87] Z. Chen, L. Liu, R. Liang, Z. Luo, H. He, Z. Wu, H. Tian, M. Zheng, Y. Ma, L. Cai, *ACS Nano* **2018**, *12*, 8633.
- [88] C. S. Thaxton, J. S. Rink, P. C. Naha, D. P. Cormode, *Adv. Drug Delivery Rev.* **2016**, *106*, 116.
- [89] L. Scheetz, P. Kadiyala, X. Q. Sun, S. J. Son, A. H. Najafabadi, M. Aikins, P. R. Lowenstein, A. Schwendeman, M. G. Castro, J. J. Moon, *Clin. Cancer Res.* **2020**, *26*, 4369.
- [90] R. Kuai, L. J. Ochyl, K. S. Bahjat, A. Schwendeman, J. J. Moon, *Nat. Mater.* **2017**, *16*, 489.
- [91] R. Kuai, W. Yuan, S. Son, J. Nam, Y. Xu, Y. Fan, A. Schwendeman, J. J. Moon, *Sci. Adv.* **2018**, *4*, eaao1736.
- [92] A. Hassani Najafabadi, J. Zhang, M. E. Aikins, Z. I. Najaf Abadi, F. Liao, Y. Qin, E. B. Okeke, L. M. Scheetz, J. Nam, Y. Xu, D. Adams, P. Lester, T. Hetrick, A. Schwendeman, M. S. Wicha, A. E. Chang, Q. Li, J. J. Moon, *Nano Lett.* **2020**, *20*, 7783.
- [93] a) D. Jiang, C. G. England, W. Cai, *J. Controlled Release* **2016**, *239*, 27; b) A. V. Pinheiro, D. Han, W. M. Shih, H. Yan, *Nat. Nanotechnol.* **2011**, *6*, 763.
- [94] a) P. W. Rothmund, *Nature* **2006**, *440*, 297; b) B. Wei, M. Dai, P. Yin, *Nature* **2012**, *485*, 623; c) D. Han, X. Qi, C. Myhrvold, B. Wang, M. Dai, S. Jiang, M. Bates, Y. Liu, B. An, F. Zhang, H. Yan, P. Yin, *Science* **2017**, *358*, 206.
- [95] S. Liu, Q. Jiang, X. Zhao, R. Zhao, Y. Wang, Y. Wang, J. Liu, Y. Shang, S. Zhao, T. Wu, Y. Zhang, G. Nie, B. Ding, *Nat. Mater.* **2020**, *20*, 421.
- [96] X. Qi, X. Liu, L. Matiski, R. Rodriguez Del Villar, T. Yip, F. Zhang, S. Sokalingam, S. Jiang, L. Liu, H. Yan, Y. Chang, *ACS Nano* **2020**, *14*, 4727.
- [97] Z. T. Li, Y. X. Wang, Y. Y. Ding, L. Repp, G. S. Kwon, Q. Y. Hu, *Adv. Funct. Mater.* **2021**, *31*, 2100088.
- [98] Y. Liu, J. Hardie, X. Zhang, V. M. Rotello, *Semin. Immunol.* **2017**, *34*, 25.
- [99] R. A. Meyer, J. C. Sunshine, J. J. Green, *Trends Biotechnol.* **2015**, *33*, 514.
- [100] S. Tan, T. Wu, D. Zhang, Z. Zhang, *Theranostics* **2015**, *5*, 863.
- [101] C. T. Saeui, M. P. Mathew, L. Liu, E. Urias, K. J. Yarema, *J. Funct. Biomater.* **2015**, *6*, 454.
- [102] H. Y. Kim, M. Kang, Y. W. Choo, S. H. Go, S. P. Kwon, S. Y. Song, H. S. Sohn, J. Hong, B. S. Kim, *Nano Lett.* **2019**, *19*, 5185.
- [103] L. J. Ochyl, J. D. Bazzill, C. Park, Y. Xu, R. Kuai, J. J. Moon, *Biomaterials* **2018**, *182*, 157.
- [104] R. H. Fang, A. V. Kroll, W. Gao, L. Zhang, *Adv. Mater.* **2018**, *30*, 1706759.
- [105] Z. L. Zeng, K. Y. Pu, *Adv. Funct. Mater.* **2020**, *30*, 202004397.
- [106] R. H. Fang, C. M. Hu, B. T. Luk, W. Gao, J. A. Copp, Y. Tai, D. E. O'Connor, L. Zhang, *Nano Lett.* **2014**, *14*, 2181.
- [107] R. Yang, J. Xu, L. Xu, X. Sun, Q. Chen, Y. Zhao, R. Peng, Z. Liu, *ACS Nano* **2018**, *12*, 5121.
- [108] A. V. Kroll, R. H. Fang, Y. Jiang, J. Zhou, X. Wei, C. L. Yu, J. Gao, B. T. Luk, D. Dehaini, W. Gao, L. Zhang, *Adv. Mater.* **2017**, *29*, 1703969.
- [109] a) C. H. Villa, A. C. Anselmo, S. Mitragotri, V. Muzykantov, *Adv. Drug Delivery Rev.* **2016**, *106*, 88; b) C. M. J. Hu, R. H. Fang, J. Copp, B. T. Luk, L. F. Zhang, *Nat. Nanotechnol.* **2013**, *8*, 336.
- [110] Y. Guo, D. Wang, Q. Song, T. Wu, X. Zhuang, Y. Bao, M. Kong, Y. Qi, S. Tan, Z. Zhang, *ACS Nano* **2015**, *9*, 6918.
- [111] W. L. Liu, M. Z. Zou, T. Liu, J. Y. Zeng, X. Li, W. Y. Yu, C. X. Li, J. J. Ye, W. Song, J. Feng, X. Z. Zhang, *Nat. Commun.* **2019**, *10*, 3199.
- [112] C. Xu, Y. Jiang, Y. Han, K. Pu, R. Zhang, *Adv. Mater.* **2021**, *33*, 2008061.
- [113] X. Han, S. Shen, Q. Fan, G. Chen, E. Archibong, G. Dotti, Z. Liu, Z. Gu, C. Wang, *Sci. Adv.* **2019**, *5*, eaaw6870.
- [114] C. Thery, L. Zitvogel, S. Amigorena, *Nat. Rev. Immunol.* **2002**, *2*, 569.
- [115] G. B. Kim, G. H. Nam, Y. Hong, J. Woo, Y. Cho, I. C. Kwon, Y. Yang, I. S. Kim, *Sci. Adv.* **2020**, *6*, eaaz2083.
- [116] Z. Lu, B. Zuo, R. Jing, X. Gao, Q. Rao, Z. Liu, H. Qi, H. Guo, H. Yin, *J. Hepatol.* **2017**, *67*, 739.
- [117] S. B. Zhou, C. Gravekamp, D. Bermudes, K. Liu, *Nat. Rev. Mater.* **2018**, *18*, 727.
- [118] X. Yi, H. Zhou, Y. Chao, S. Xiong, J. Zhong, Z. Chai, K. Yang, Z. Liu, *Sci. Adv.* **2020**, *6*, eaba3546.
- [119] R. B. Patel, M. Ye, P. M. Carlson, A. Jaquish, L. Zangl, B. Ma, Y. Wang, I. Arthur, R. Xie, R. J. Brown, X. Wang, R. Sriramaneni, K. Kim, S. Gong, Z. S. Morris, *Adv. Mater.* **2019**, *31*, 1902626.
- [120] R. Noad, P. Roy, *Trends Microbiol.* **2003**, *11*, 438.
- [121] W. Shan, H. Zheng, G. Fu, C. Liu, Z. Li, Y. Ye, J. Zhao, D. Xu, L. Sun, X. Wang, X. L. Chen, S. Bi, L. Ren, G. Fu, *Nano Lett.* **2019**, *19*, 1719.
- [122] P. H. Lizotte, A. M. Wen, M. R. Sheen, J. Fields, P. Rojanasopondist, N. F. Steinmetz, S. Fiering, *Nat. Nanotechnol.* **2016**, *11*, 295.
- [123] H. Cai, S. Shukla, C. Wang, H. Masarapu, N. F. Steinmetz, *J. Am. Chem. Soc.* **2019**, *141*, 6509.
- [124] M. Fuscillo, F. Fontana, S. Tahtinen, C. Capasso, S. Feola, B. Martins, J. Chiaro, K. Peltonen, L. Ylosmaki, E. Ylosmaki, F. Hamdan, O. K. Kari, J. Ndika, H. Alenius, A. Urtti, J. T. Hirvonen, H. A. Santos, V. Cerullo, *Nat. Commun.* **2019**, *10*, 5747.
- [125] a) A. G. Zeimet, C. Marth, *Lancet Oncol.* **2003**, *4*, 415; b) J. Chen, M. Liu, Z. Zhou, J. Ke, S. Huang, D. Huang, W. Wu, *Heart* **2015**, *101*, A24.
- [126] Y. Mi, C. T. t. Hagan, B. G. Vincent, A. Z. Wang, *Adv. Sci.* **2019**, *6*, 1801847.
- [127] X. Xi, T. Ye, S. Wang, X. Na, J. Wang, S. Qing, X. Gao, C. Wang, F. Li, W. Wei, G. Ma, *Sci. Adv.* **2020**, *6*, eaay7735.
- [128] X. Xie, Y. Hu, T. Ye, Y. Chen, L. Zhou, F. Li, X. Xi, S. Wang, Y. He, X. Gao, W. Wei, G. Ma, Y. Li, *Nat. Biomed. Eng.* **2021**, *5*, 414.
- [129] A. K. Kosmides, R. A. Meyer, J. W. Hickey, K. Aje, K. N. Cheung, J. J. Green, J. P. Schneck, *Biomaterials* **2017**, *118*, 16.

- [130] S. Talebian, J. Foroughi, S. J. Wade, K. L. Vine, A. Dolatshahi-Pirouz, M. Mehrali, J. Conde, G. G. Wallace, *Adv. Mater.* **2018**, *30*, 1706665.
- [131] M. O. Dellacherie, B. R. Seo, D. J. Mooney, *Nat. Rev. Mater.* **2019**, *4*, 379.
- [132] H. Phuengkham, C. Song, S. H. Um, Y. T. Lim, *Adv. Mater.* **2018**, *30*, 1706719.
- [133] H. Phuengkham, C. Song, Y. T. Lim, *Adv. Mater.* **2019**, *31*, 1903242.
- [134] O. A. Ali, N. Huebsch, L. Cao, G. Dranoff, D. J. Mooney, *Nat. Mater.* **2009**, *8*, 151.
- [135] O. A. Ali, P. Tayalia, D. Shvartsman, S. Lewin, D. J. Mooney, *Adv. Funct. Mater.* **2013**, *23*, 4621.
- [136] T. T. Smith, H. F. Moffett, S. B. Stephan, C. F. Opel, A. G. Dumigan, X. Jiang, V. G. Pillarisetty, S. P. S. Pillai, K. D. Wittrup, M. T. Stephan, *J. Clin. Invest.* **2017**, *127*, 2176.
- [137] a) M. Guvendiren, H. D. Lu, J. A. Burdick, *Soft Matter* **2012**, *8*, 260; b) C. Hu, X. Liu, W. Ran, J. Meng, Y. Zhai, P. Zhang, Q. Yin, H. Yu, Z. Zhang, Y. Li, *Biomaterials* **2017**, *144*, 60.
- [138] D. G. Leach, S. Young, J. D. Hartgerink, *Acta Biomater.* **2019**, *88*, 15.
- [139] M. Sepantafar, R. Maheronnaghsh, H. Mohammadi, F. Radmanesh, M. M. Hasani-Sadradadi, M. Ebrahimi, H. Baharvand, *Trends Biotechnol.* **2017**, *35*, 1074.
- [140] Y. Chao, Q. Chen, Z. Liu, *Adv. Funct. Mater.* **2020**, *30*, 1902785.
- [141] T. Wang, D. Wang, H. Yu, B. Feng, F. Zhou, H. Zhang, L. Zhou, S. Jiao, Y. Li, *Nat. Commun.* **2018**, *9*, 1532.
- [142] P. Yang, H. Song, Y. Qin, P. Huang, C. Zhang, D. Kong, W. Wang, *Nano Lett.* **2018**, *18*, 4377.
- [143] Z. C. Luo, Q. J. Wu, C. B. Yang, H. M. Wang, T. He, Y. Z. Wang, Z. Y. Wang, H. Chen, X. Y. Li, C. Y. Gong, Z. M. Yang, *Adv. Mater.* **2017**, *29*, 1601776.
- [144] G. A. Roth, E. C. Gale, M. Alcantara-Hernandez, W. Luo, E. Axpe, R. Verma, Q. Yin, A. C. Yu, H. Lopez Hernandez, C. L. Maikawa, A. A. A. Smith, M. M. Davis, B. Pulendran, J. Idoyaga, E. A. Appel, *ACS Cent. Sci.* **2020**, *6*, 1800.
- [145] Y. Yin, X. Li, H. Ma, J. Zhang, D. Yu, R. Zhao, S. Yu, G. Nie, H. Wang, *Nano Lett.* **2021**, *21*, 2224.
- [146] T. L. Nguyen, Y. Choi, J. Kim, *Adv. Mater.* **2019**, *31*, 1803953.
- [147] J. Kim, W. A. Li, Y. Choi, S. A. Lewin, C. S. Verbeke, G. Dranoff, D. J. Mooney, *Nat. Biotechnol.* **2015**, *33*, 64.
- [148] A. W. Li, M. C. Sobral, S. Badrinath, Y. Choi, A. Graveline, A. G. Stafford, J. C. Weaver, M. O. Dellacherie, T. Y. Shih, O. A. Ali, J. Kim, K. W. Wucherpfennig, D. J. Mooney, *Nat. Mater.* **2018**, *17*, 528.
- [149] T. L. Nguyen, Y. Yin, Y. Choi, J. H. Jeong, J. Kim, *ACS Nano* **2020**, *14*, 11623.
- [150] Y. C. Kim, J. H. Park, M. R. Prausnitz, *Adv. Drug Delivery Rev.* **2012**, *64*, 1547.
- [151] H. Amani, M. A. Shahbazi, C. D'Amico, F. Fontana, S. Abbaszadeh, H. A. Santos, *J. Controlled Release* **2021**, *330*, 185.
- [152] Y. Ye, C. Wang, X. Zhang, Q. Hu, Y. Zhang, Q. Liu, D. Wen, J. Milligan, A. Bellotti, L. Huang, G. Dotti, Z. Gu, *Sci. Immunol.* **2017**, *2*, eaan5692.
- [153] N. W. Kim, S. Y. Kim, J. E. Lee, Y. Yin, J. H. Lee, S. Y. Lim, E. S. Kim, H. T. T. Duong, H. K. Kim, S. Kim, J. E. Kim, D. S. Lee, J. Kim, M. S. Lee, Y. T. Lim, J. H. Jeong, *ACS Nano* **2018**, *12*, 9702.
- [154] Y. He, C. Hong, J. Li, M. T. Howard, Y. Li, M. E. Turvey, D. Uppu, J. R. Martin, K. Zhang, D. J. Irvine, P. T. Hammond, *ACS Nano* **2018**, *12*, 10272.
- [155] D. Shae, J. J. Baljon, M. Wehbe, P. P. Christov, K. W. Becker, A. Kumar, N. Suryadevara, C. S. Carson, C. R. Palmer, F. C. Knight, S. Joyce, J. T. Wilson, *ACS Nano* **2020**, *14*, 9904.
- [156] a) F. Meric-Bernstam, J. Larkin, J. Tabernero, C. Bonini, *Lancet* **2020**, *397*, 1010; b) D. Fukumura, J. Kloepper, Z. Amoozgar, D. G. Duda, R. K. Jain, *Nat. Rev. Clin. Oncol.* **2018**, *15*, 325.
- [157] a) A. Nguyen, A. Ramesh, S. Kumar, D. Nandi, A. Brouillard, A. Wells, L. Pobeziński, B. Osborne, A. A. Kulkarni, *Sci. Adv.* **2020**, *6*, eabc2777; b) Y. Zhang, S. He, W. Chen, Y. Liu, X. Zhang, Q. Miao, K. Pu, *Angew. Chem., Int. Ed. Engl.* **2020**, *60*, 5921.



**Jing Liu** received her Ph.D. degree in biomaterials from University of Science and Technology of China (USTC), China in 2019. She is currently a postdoc researcher working at South China University of Technology (SCUT), China. Her current research focuses on nanomedicine for cancer treatment, with a focus on biomaterials and cancer therapy.



**Jun Wang** received his Ph.D. degree from Wuhan University in 1999. During the period of 1999–2014, he continued his postdoctoral studies at Johns Hopkins Singapore and the Johns Hopkins University School of Medicine. He joined USTC as a full professor in 2014 and moved to SCUT in 2016. His research interests include biomaterials for drug delivery and immunotherapy.



**Kanyi Pu** received his Ph.D. from the National University of Singapore in 2011 followed by a post-doctoral study at Stanford University School of Medicine. He joined the School of Chemical and Biomedical Engineering at Nanyang Technological University as an associate professor in 2015. His research focuses on the development of molecular optical reporters and semiconducting polymer nanomaterials for in vivo imaging, disease diagnosis, and therapy.